STATENS GEOTEKNISKA INSTITUT
SWEDISH GEOTECHNICAL INSTITUTE

RAPPORT
REPORT No 12

Drained behaviour of Swedish clays

ROLF LARSSON

LINKÖPING 1981

STATENS GEOTEKNISKA INSTITUT
SWEDISH GEOTECHNICAL INSTITUTE

RAPPORT
REPORT No 12

Drained behaviour of Swedish clays

ROLF LARSSON

Detta projekt har finansierats av SGI och Statens vägverk.

LINKÖPING 1981

ISSN 0348-0755

Tryck-Center AB Linkoping 1981

PREFACE

This report deals with drained deformations and drained shear strength in Swedish clays.

The report includes results from a number of inter-related research and development projects at the Laboratory of the Swedish Geotechnical Institute as well as experience gathered from the Laboratory's consulting activities.

The research has been supported by grants from the Swedish National Road Administration and internal research funds at the Swedish Geotechnical Institute.

Valuable assistance has been provided by a number of our colleagues and especially by Chalmers University in Gothenburg, the Norwegian Geotechnical Institute in Oslo and Laval University in Quebec.

Linköping July 1981

Rolf Larsson

CONTENTS

SUMMARY

Compression characteristics of soft clays are generally determined by oedometer tests. The oedometer, which usually contains the soil sample in a confined ring, has been used over a long period of time. In 1918 Virgin explained the consolidation phenomena and the first oedometer in Sweden was constructed in 1922. The fundamentals of the consolidation process were explained by Terzaghi in 1925 and since then the testing procedure proposed by Terzaghi has been widely used.

This procedure involves loading of the sample in increments (duration 24 hours), each increment being equal to the previous consolidation load. In the late 60's this procedure was altered in many laboratories and smaller increments were used to enable a more accurate evaluation of the preconsolidation pressure. At about the same time the first continuous oedometer tests where the sample was deformed by a constant rate of strain were carried out. Since then much research has been done on comparisons between different oedometer tests and between oedometer tests and field observations as regards the preconsolidation pressure. Strain rate effects have been evaluated and theories for evaluation of the tests have been presented. A number of new tests such as the constant rate of strain test (CRS-test), the constant gradient test (CGI-test) and the continuous consolidation test have been developed.

In Sweden a large investigation was carried out in 1971-1975 comparing the constant rate of strain test, the constant gradient test, incremental loading tests and large field tests for determination of the preconsolidation pressure (Sällfors, 1975). This investigation led to the recommendation of the constant rate of strain test as a routine test for soft

clays and recommendations for strain rates and methods for evaluation of preconsolidation pressure and coefficient of consolidation were given.

The constant rate of strain test became a standard test at the Swedish Geotechnical Institute in 1975 and today many Swedish consulting firms use it.

During the five years the CRS-test has been used at SGI much experience has been gathered. Related research concerning permeability, swelling, recompression and secondary deformation has been carried out. A new method for interpretation of the CRS-test and settlement calculation has been introduced. Part of this information has been supplied to the Institute's clients, to the Swedish Universities and to our research colleagues. A paper briefly describing the interpretation and use of the CRS-test results has been published (Larsson & Sällfors, 1981) but this is the first attempt at summarizing all the results.

The oedometer results however represent only the special case of deformations where there are no lateral deformations. Shear strains increase with increasing shear stress level and compression strains are functions of effective pressure and shear stress.

The stress-strain curve in shear testing is highly dependent on the volume change of the soil during the test and stress-dilatancy equations have been formulated to account for this (Rowe, 1964).

The first advanced general model for drained deformations in soils was the concept of "Critical State Soil Mechanics" developed at Cambridge University by Roscoe and the Cambridge group (Scofield & Wroth, 1968). This model however does not consider anisotropy and later research has shown that also the suggested flow rules must be modified.

To obtain a picture of how the boundary conditions affect the compressibility and the shear strains in a Swedish clay tests have been run as triaxial tests using different methods, as plane strain compression tests on vertical and horizontal samples and as direct shear tests.

The results have been compared with results from tests on similar clays available in literature.

The shape of the yield curve is found to be determined by the Mohr-Coulomb failure criteria and the previous stress history of the soil.

The volumetric compressibility of the soil is found to be dependent on the shear stress level. The higher the shear stress level is the more compressible the soil becomes.

The shear strains are governed by the dilatancy equations if the shear stress level is high enough. For more isotropic stresses the shear strains depend more on the variation in compressibility with direction due to stress history.

The drained shear strength in the slightly overconsolidated stress range is governed by the Mohr-Coulomb failure criteria and ϕ_{cv}. In most Swedish clays ϕ_{cv} is about 30^0. The mobilizable angle of friction increases with the overconsolidation ratio. For normally consolidated clays the drained shear strength is seldom equal to the governing strength as the undrained shear strength is lower. To mobilize the drained shear strength in normally consolidated soft clays very large deformations are required. The practical drained problems in this case are therefore problems of deformation rather than strength.

NOTATIONS AND SYMBOLS

a	Pressure defined in Fig. 22
b	Load factor
a_s	Swelling index
C_c	Compression index $\Delta e/\Delta \log \sigma'$
C_α	Secondary compression index $\Delta e/\Delta \log t$
c'	Effective cohesion intercept
c	Correction defined in Fig. 22
c_v	Coefficient of consolidation
CC-test	Oedometer test, constant relation $\dot{u}_b/\dot{\sigma}$
CGT-test	Oedometer test, constant pore pressure gradient
CRS-test	Oedometer test, constant rate of strain
E_v	Modulus of volumetric compression $\Delta\sigma'_y/\Delta v$
e	Void ratio
$\dot{e}$	Rate of void ratio change $\delta e/\delta t$
e_o	Initial void ratio
g	Gravity (9.81 m/s^2)
H	Height
K_o	Coefficient of earth pressure σ'_H/σ'_V
K_{onc}	Coefficient of earth pressure in normally consolidated stage $\sigma'_V = \sigma'_c$
k	Coefficient of permeability
M	Oedometer modulus, Critical state parameter
M_L	Oedometer modulus in linear range defined in Fig. 22
M_o	Initial oedometer modulus
M'	Modulus number
m_j	Modulus number
p	Mean effective normal stress
p_e	Equivalent isotropic consolidation stress
q	Deviatoric stress
S	Swelling, Shear stress in shear box
S_d	Shear stress component due to dilatancy in shear box
T	Time factor
t	Time
$\bar{U}$	Degree of consolidation
u	Pore pressure

u_b	Pore pressure at undrained end in oedometer
$\dot{u}_b$	Rate of pore pressure change at undrained end in oedometer $\delta u_b/\delta t$
V	Volume
v	Volumetric compressive strain
$\dot{v}$	Rate of volumetric compressive strain dv/dt
W_f	Frictional work
w	Water content
w_F	Cone liquid limit
w_L	Percussion liquid limit
w_N	Natural water content
w_P	Plastic limit
w_S	Shrinkage limit
Z	Depth
α	Stress angle defined in Fig. 87
α_S	Coefficient of secondary consolidation
β	Stress exponent, strain angle defined in Fig. 87
ε	Compressive strain
ε_1	Major principal compressive strain
ε_2	Intermediate principal compressive strain
ε_3	Minor principal compressive strain
$\dot{\varepsilon}_1$	Rate of major principal compressive strain $d\varepsilon_1/dt$
ε_a	Axial compressive strain
ε_L	Straight portion of oedometer curve
$\bar{\varepsilon}$	Distortional strain
$\bar{\varepsilon}_e$	Elastic distortional strain
$\bar{\varepsilon}_p$	Plastic distortional strain
γ	Angular deformation
ν	Poissons ratio
ρ_s	Unit weight of solid particles
ρ_w	Unit weight of water
σ	Total stress
σ'	Effective stress
σ'_c	Preconsolidation pressure
σ'_H	Horizontal effective stress
σ'_j	Reference stress
σ'_L	Effective stress defined in Fig. 22
σ'_N	Effective vertical stress in shear box
σ'_o	Initial effective vertical stress

σ'_u	Effective stress to which unloading has been made
σ'_V	Effective vertical stress
σ'_y	Effective stress causing yield
$\dot{\sigma}$	Rate of increase of vertical stress $d\sigma/dt$
τ	Shear stress
φ'	Effective angle of friction
ϕ_{cv}	Effective angle of friction at failure at constant volume
ϕ_f	Corrected angle of friction (Rowe)
ϕ'_{max}	Effective angle of friction at failure
ϕ_p	Corrected angle of friction (Larsson)
ϕ_r	Corrected angle of friction (Bishop)
ϕ_μ	Effective angle of friction between mineral surfaces
θ	Angle between shear stress and sliding direction
SGI	Swedish Geotechnical Institute

1. OEDOMETER TESTS

1.1 Incremental test apparatus

Oedometer tests on natural fine-grained soils are usually performed on "undisturbed" samples fitted into a confining ring. A test procedure with incremental loading, each increment being equal to the previous load and a new increment every 24 hours, was suggested by Terzaghi in 1925 and has been widely used since then. During the test the sample is drained from the ends and readings of the compression are taken in a time sequence enabling a plot of the time-settlement curve for each increment.

Over the years a number of variants of the incremental oedometer and the test procedure have been developed but in essence they remain the same.

The most simple and commonly used oedometer is the fixed ring oedometer with drainage from both ends, Fig. 1a. In this oedometer the piston on top of the sample is loaded and moves into the ring which is fixed in position. If there is friction between the sample and the ring this will cause an uneven stress distribution in the sample. It is therefore very important to minimize this friction, which is done by using a very smooth ring and grease. Swedish investigations (Kallstenius, 1963, Sällfors, 1975) have shown that the ring material is less important than the smoothness of the ring and the most effective grease found so far is silicon grease. As pore water is often highly corrosive other materials than stainless steel, ceramics or plastics should be avoided.

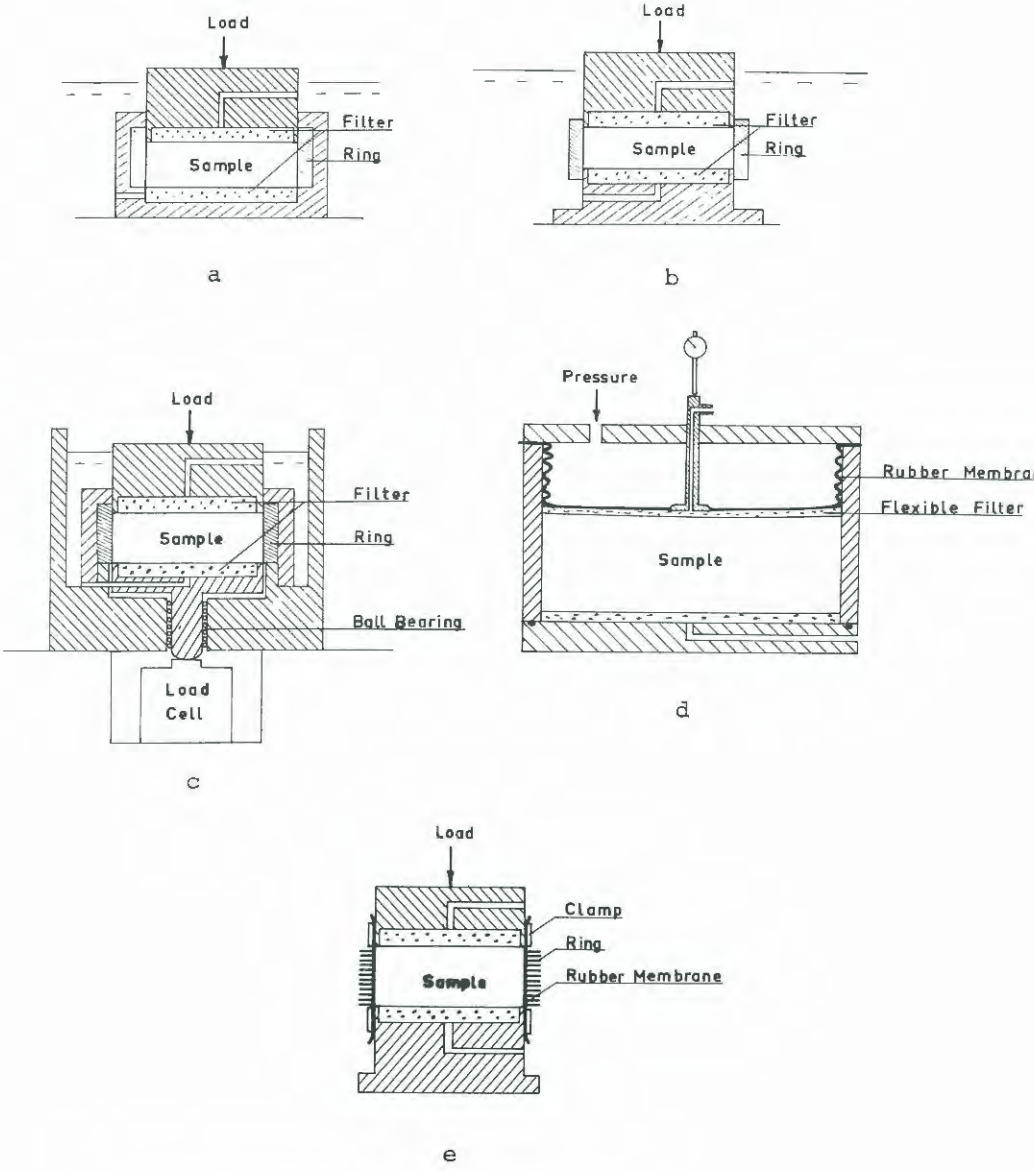

Fig. 1. Different types of oedometers.
a. Oedometer with fixed ring
b. Oedometer with floating ring
c. Oedometer with measurement of ring friction
d. Rowe oedometer
e. Compressiometer

The use of oedometers with floating rings, where both the piston on top of the sample as well as the pedestal on which the sample rests can move into the ring, is one way to reduce friction, Fig. 1b.

For coarser materials side friction cannot be sufficiently reduced to be ignored. In this case the load transmitted through the sample can be measured, Fig. 1c, and the average stress calculated.

A way to obviate side friction is to use a Rowe consolidation cell where the sample is loaded by a pressure acting on a flexible rubber membrane and the settlement is measured in the centre of the membrane, Fig. 1d. This oedometer works excellently with stiff materials such as boulder clays and coarse materials but at least the commercial version has shown to be unsuitable for soft, highly compressible Swedish clays.

In compressiometers, Fig. 1e, the confining ring is replaced by a rubber membrane and lateral deformations are prevented by a number of thin rings spaced so that no vertical load can be transferred between the rings. Compressiometers are often used for measurement of compressibility of sand and gravel.

When simple oedometers are used it is generally assumed that the samples are fully saturated and that full pore pressure dissipation (100% primary consolidation) can be determined from the time-settlement curve from the load step. To check the validity of this assumption the oedometer can be altered so that drainage is allowed from one end only and the pore pressure is measured at the other end, Fig. 2.

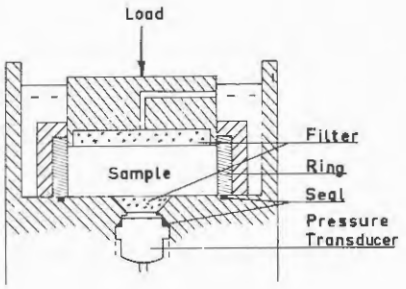

Fig. 2. Oedometer with measurement of pore pressure.

To enable complete saturation of the sample the oedometer can be placed in a triaxial cell where the pore water can be subjected to pressure. Very sophisticated oedometers of this type are now on the market.

The Rowe consolidation cell can very easily be adapted to both back pressure and pore pressure measurement.

Varved and layered soils often have a higher permeability in the horizontal than the vertical direction and time-settlement relations from tests with end drainage may therefore be misleading. In the Rowe consolidation cell the end filters can be replaced by a peripheral filter or by a central drain so that the drainage path is horizontal, Fig. 3.

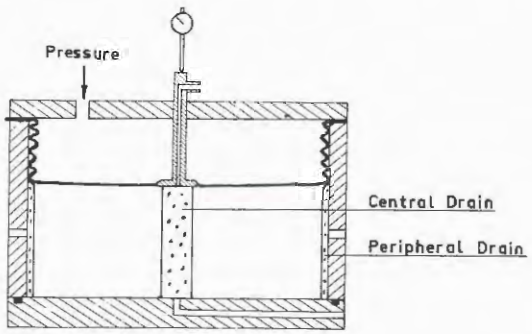

Fig. 3. Oedometer with horizontal drainage.

1.2 Evaluation of the test

The results from incremental oedometer tests are usually presented in a diagram where the strain at the end of each step is plotted against the consolidation pressure. In this plot the vertical effective pressure is in log-scale.

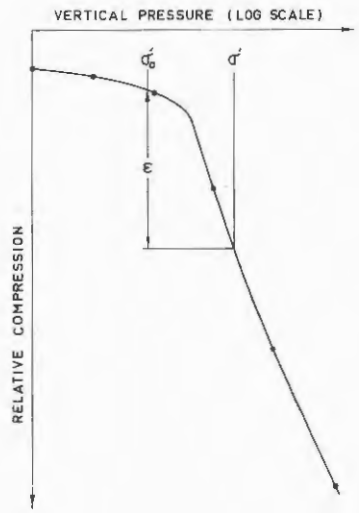

From this diagram settlements may be calculated by reading off the relative compression between the vertical in situ pressure in the ground σ_o' and the calculated final pressure σ' and multiplying by the thickness of the soil layer.

Fig. 4. Typical results from an oedometer test on clay.

For determining the preconsolidation pressure σ_c' the Casagrande method illustrated in Fig. 5 has been widely used (Casagrande, 1936).

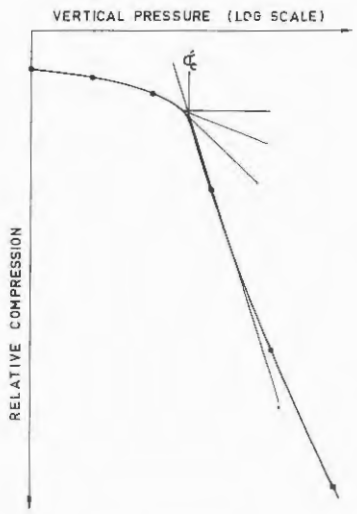

In this method a horizontal line and a tangent to the oedometer curve at the point with the smallest radius of curvature are drawn. The angle between the horizontal line and the tangent is bisected. The straight portion of the oedometer curve is extended and the preconsolidation pressure is evaluated as the pressure at the intersection of this line and the bisectrix.

Fig. 5. The Casagrande method for evaluating the preconsolidation pressure.

As soil samples brought into the laboratory are seldom truly undisturbed the compressions up to and slightly past the preconsolidation pressure are often too large. Methods for evaluation of the preconsolidation pressure taking the disturbance into account have been suggested by Burmeister (1951) and Schmertmann (1953). However, the sampling technique has been improved since then and studies of swelling and reloading have shown that much of this disturbance may occur in the laboratory if the sample is allowed to absorb water during the test set-up.

Provided that the samples are of good quality and are properly handled the correction for disturbance should be small and there is no definite proof that the correction improves the correlation between laboratory and field data.

In many cases though an arithmetic plot should be made in addition to the standard plot to check that there

really is a preconsolidation pressure and that the curvature of the oedometer curve is not due only to the log scale. There is a trend to abandon the log scale and present the oedometer curves in arithmetic plots. In this case the Terzaghi loading sequence is unsuited since the shape of the oedometer curve is difficult to determine as the distance between the points increases.

As will be shown later the evaluated preconsolidation pressure is sensitive to the loading sequence and the duration of each load step.

Apart from the preconsolidation pressure the compression index C_c or ε_2 is also evaluated from the oedometer curve. The presentation of the oedometer curve in a diagram with strain in linear scale and pressure in log scale was chosen as the curve then appeared to be a straight line after the preconsolidation pressure.

The compression index C_c is determined as $\frac{\Delta e}{\log \frac{\sigma' + \Delta\sigma'}{\sigma'}}$ or $\frac{\Delta e}{\Delta \log \sigma'}$, Fig. 6a. To avoid the determination of the void ratio the compression index ε_2 is used in Sweden where ε_2 is the relative compression of the sample at a doubling of the vertical pressure, Fig. 6b.

The relation of these compression indexes is

$$\varepsilon_2 / \log 2 = C_c (1 + e_o)$$

Unfortunately the assumption that the oedometer curve should be a straight line for stresses higher than the preconsolidation pressure in this plot is not valid in soft Swedish clays and this method of describing the compressibility is therefore an approximation valid within a small stress range only.

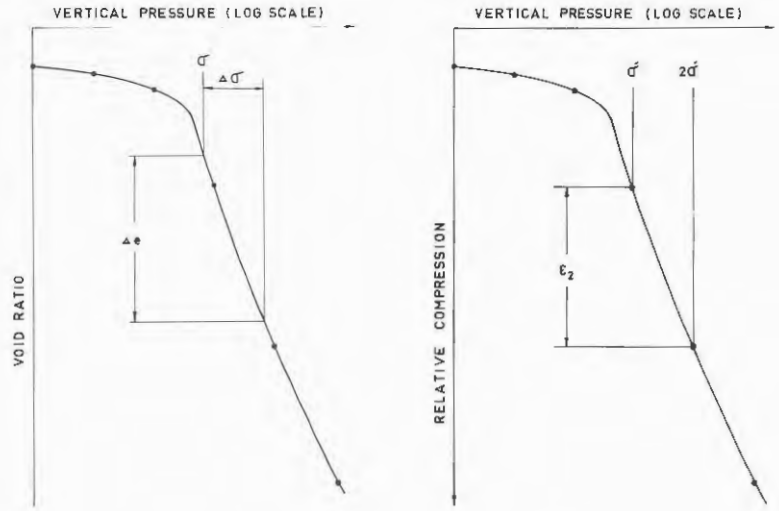

Fig. 6. a. Evaluation of Compression index C_c.
b. Evaluation of Compression index ε_2.

Soil compressibility is therefore often expressed by tangent modulus M Odhe (1951), Janbu (1967), Brinch-Hanssen (1966) and others

$$M = m_j \, \sigma'_j \left(\frac{\sigma'}{\sigma'_j}\right)^{1-\beta}$$

where

m_j = modulus number
β = stress exponent
σ' = effective vertical stress
σ'_j = reference stress (usually 100 kPa)

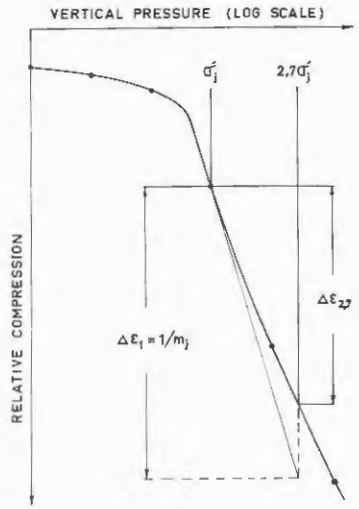

The parameters are evaluated by drawing a tangent to the curve at σ_j' and extending it to $2.7\ \sigma_j'$, Fig. 7. If the oedometer curve had been a straight line the compression between σ_j' and $2.7\ \sigma_j'$ would have been $\Delta\varepsilon_1 = 1/m_j$ and $\beta = 0$. But the real compression is $\Delta\varepsilon_{2,7}$ and β is evaluated from

$$\Delta\varepsilon_{2,7} = \frac{1}{m_j \beta}(2.7^{\beta}-1).$$

Fig. 7. Evaluation of m_j and β.

In all Swedish clays except the dry crusts and boulder clays β has a negative value.

This method of describing compressibility of soft clays is not correct either but the approximation can be used for a larger stress inverval than the compression index.

If readings of the settlements are taken in a time sequence during the load steps the oedometer test will provide information on the time required to reach different stages of consolidation. Terzaghi formulated the equation of the consolidation process

$$\frac{\partial u}{\partial t} = c_v \frac{\partial^2 u}{\partial z^2}$$

where c_v is the coefficient of consolidation.

There are two commonly used methods to determine c_v from incremental oedometer tests. The Casagrande

method involves plotting the deformation versus the logarithm of time, Fig. 8.

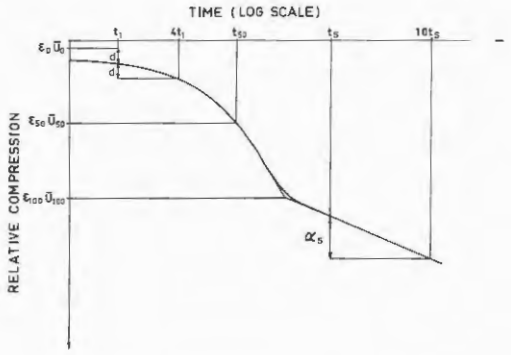

Fig. 8. Casagrande construction of c_v.

$\bar{U} = 0$ is constructed by assuming a parabolic shape of the first part of the curve. $\bar{U} = 100\%$ is constructed as the intersection between the tangent to the curve at its point of inflexion and the extension of the straight end part of the curve. ε_{50} at $\bar{U} = 50\%$ is then calculated, t_{50} is constructed and c_v is calculated from

$$c_v = T_{50} \frac{H^2_{50}}{t_{50}}$$

For oedometers with drainage from both ends $h_{50} = H_o(1-\varepsilon_{50})/2$ where H_o is initial sample height and the time factor $T_{50} = 0.197$.

In the Taylor construction the deformation is plotted versus the square root of time, Fig. 9.

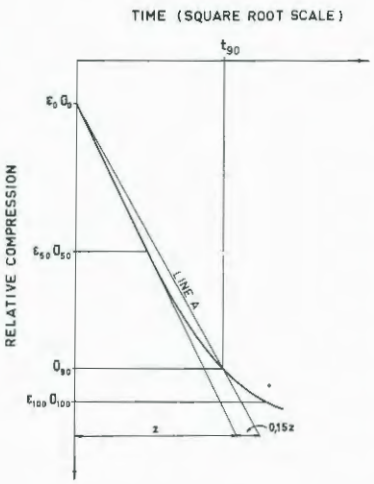

The straight portion of the curve is extended. Line A is then drawn at a distance of 15% "outside" that line (see Fig. 9). $\bar{U} = 90\%$ is taken from the intersection between the curve and line A. ε at $\bar{U} = 50\%$ and $\bar{U} = 100\%$ can now be calculated and t_{90} constructed. c_v is evaluated from $c_v = \frac{T_{90} \cdot H_{50}^2}{t_{90}}$ where the time factor $t_{90} = 0.848$.

Fig. 9. Taylor construction of c_v.

The Casagrande method seems to be used more often and is required if the rate of secondary compression is to be determined.

The coefficient of secondary compression α_s is determined from the slope of the straight part of the time-settlement curve as $\Delta\varepsilon/\Delta log\ t$.

The c_v-value is dependent on permeability which varies with temperature. Ideally, oedometer tests should be performed at ground temperature but as the average ground temperature in Sweden is about 7^0 Centigrade this would be inconvenient. Care should be taken to keep the temperature constant during the tests though and permeability and c_v-values can then be corrected.

1.3 Effect of loading sequence on test results

The time-settlement curve is divided into three parts, Fig. 10.

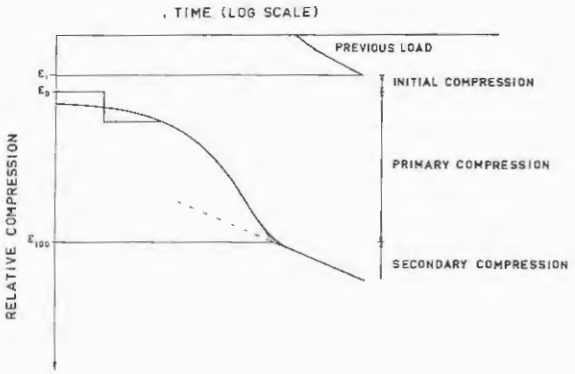

Fig. 10. The three parts of the time-settlement curve.

1. The initial deformation $\varepsilon_i - \varepsilon_o$ which is immediate and not time-dependent.
2. The primary compression $\varepsilon_o - \varepsilon_{100}$ where there is a hydrodynamic delay of the compression as it takes time for the pore water to flow out of the sample.
3. The secondary compression which is due to creep deformations in the soil and is slow enough not to create pore pressures in the soil.

The Terzaghi theory of consolidation assumes among other things that the soil is fully saturated, that pore water and minerals are incompressible and that compression is a function of effective stress only.

If these assumptions were fully valid there would be no initial deformation. The initial deformation for "fully saturated" soils is very small though and consequently the error is small.

A more serious error is caused by secondary compression which ideally should not occur either but in reality can be relatively large. It affects both the final settlement after a certain time and the pore pressure dissipation, since secondary compression

does not start at the end of primary consolidation but already from the start of the test and thus affects the primary consolidation.

This means that the oedometer curve plotted as compression versus effective stress is not unique but is highly dependent on the loading sequence and the duration of each load step and somewhat dependent on temperature.

The traditional loading sequence with doubling of the load for each load step and a duration of the load step of 24 hours has its drawbacks. It takes a long time and the spacing between the points on the stress-strain curve is such that it often gives a high degree of freedom for the individual interpreter in drawing the curve.

Other loading sequences are therefore in use and consequently the results differ somewhat.

To speed up the test the samples are often reloaded at the end of primary consolidation. As the duration of each load step then becomes shorter the settlements become smaller, which will give a somewhat higher preconsolidation pressure, CURVE A Fig. 11. The size of the difference depends on c_v and α_s and also on the height of the oedometer and the drainage conditions. Swedish oedometers for clays have a sample dimension of 20 cm^2 area and 20 mm height with drainage from both ends and most oedometers used for soft clays are of about the same size and type.

To obtain more points on the stress-strain curve smaller load steps are often used. If they are given a duration of 24 hours the strains become larger than in the standard test and the evaluated preconsolidation pressure decreases, CURVE D Fig. 11.

To speed up the test and to find more points on the stress-strain curve Bjerrum (1973) suggested a method where reduced load increments are used until the preconsolidation pressure is reached. These increments have been given a duration long enough to give 100% primary consolidation. After the preconsolidation pressure is reached the test is continued with doubled load increments with 24 hours' duration. Karlsson & Viberg (1978) found that this type of test on the average gives a preconsolidation pressure 15% higher than the preconsolidation pressure evaluated from tests with the standard procedure. On the other hand it gives a higher compression index, CURVE B Fig. 11.

Even for the standard test two curves can be obtained as the strain can be taken as the end of primary compression or as strain at 24 hours. The original standard test uses the strains after 24 hours and this is Swedish practice. Many tests are also performed without any readings after a time sequence or for some load steps only. The 24 hour curve gives somewhat larger strains and lower preconsolidation pressures than the end of the primary compression curve.

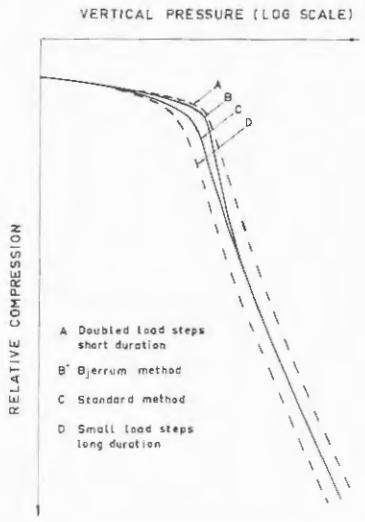

Fig. 11. Oedometer curves with different loading procedures.

The bulk of experience is based on the standard test which has repeatedly shown to give reliable values of the preconsolidation pressure directly comparable to field measurements. If any other test procedure is used the results ought to be corrected to match the standard procedure.

1.4 Oedometer tests with continuous loading

Oedometer tests with continuous loading have been used for the last fifteen years. They have mainly been performed as constant rate of strain tests, CRS-tests, constant gradient tests, CGT-tests, or continuous consolidation tests, CC-tests.

The main advantages of these tests are that they give continuous stress-strain relations as well as continuous ε_v-stress relations and that they can be run automatically.

Most research has been done on the CRS-test and this is the most common automatic test.

In the CRS-test the oedometer is placed in a press which compresses the sample at a constant rate. The sample is drained at the upper end and sealed at the bottom where the pore pressure is measured. During compression the compressive force, the deformation, the pore pressure at the bottom and time are recorded continuously.

Fig. 12 shows a simple set-up for CRS-tests used at SGI.

The average effective stress in the sample during the test is calculated by the simple equation

$$\sigma' = \sigma - 2/3\ u_b \qquad \text{(Smith \& Wahls, 1969)}$$

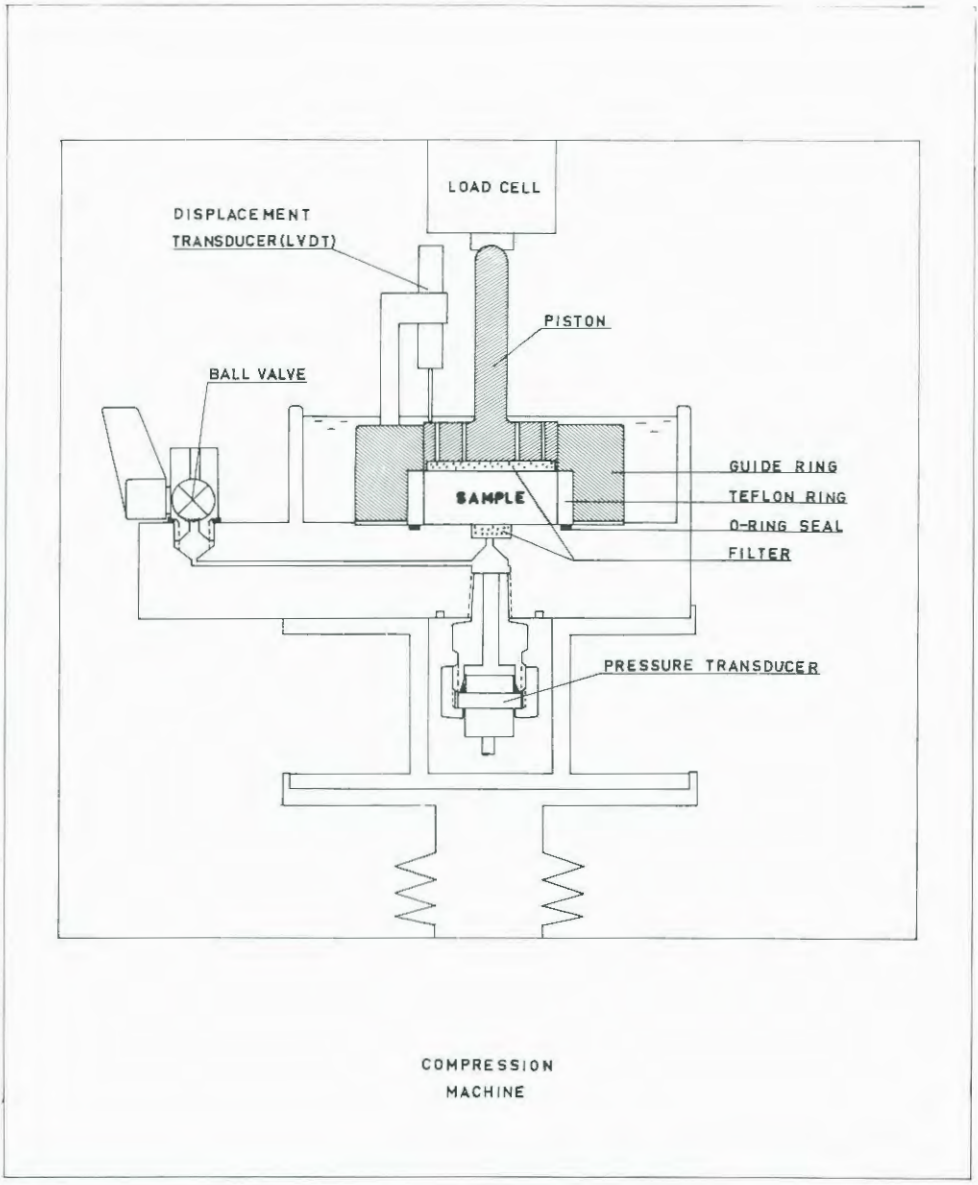

Fig. 12. Oedometer for tests with constant rate of strain.

where σ = total pressure measured by the force transducer

and u_b = pore pressure at the bottom of the sample measured with the pressure transducer.

This equation is not exact but the error is small provided that the pore pressure is low in relation to the vertical pressure. Considering the time dependency of the stress-strain curve the pore pressure should in any case be kept low and thus the formula can normally be used.

Tokheim and Janbu (1976) give the equation

$$\sigma' = \sigma - \frac{4}{5} u_b \frac{5\dot{\sigma} - 4\dot{u}_b}{6\dot{\sigma} - 5\dot{u}_b}$$

where $\dot{\sigma} = d\sigma/dt$

$\dot{u}_b = du_b/dt$

This equation gives the same results at low pore pressures as the simple equation.

c_v is calculated from the simple equation Smith & Wahls (1969), Lowe (1969)

$$c_v = \frac{d\sigma'}{dt} \cdot \frac{H^2}{2u_b}$$

where H is the sample height.

This equation is also valid for low pore pressures only. Sällfors (1975) recommends that the pore pressure should not exceed 15% of the total pressure.

Tokheim and Janbu (1976) give the equation

$$c_v = \frac{M\ H\ \dot{\delta}}{2u_b} \cdot \frac{6\dot{\sigma} - 5\dot{u}_b}{6\dot{\sigma} - 4\dot{u}_b}$$

where M = modulus $(d\sigma/d\varepsilon)$

$\dot{\sigma} = d\sigma/dt$

$\dot{u}_b = du_b/dt$

$\dot{\delta} = dH/dt$

The theory is limited to $\dot{u}_b/\dot{\sigma} < 0.35$.*) The difference between this equation and $c_v = \frac{\Delta\sigma\ H^2}{dt\ 2u_b}$ is negligible for small pore pressures.

From the CRS-test the coefficient of permeability can also be obtained continuously and is calculated by the equation

$$k = \frac{d\varepsilon \cdot H^2 \cdot g \cdot \rho_w}{dt \cdot 2u_b}$$

Evaluations of c_v and k are based on the assumption of a parabolic pore pressure distribution in the sample. Leroueil et al (1980) have shown that this assumption is not valid in a stress interval when the preconsolidation pressure is passed. In this interval the upper part of the sample will have much lower modulus than the bottom part which has not yet reached the preconsolidation pressure and the pore pressure distribution will differ from the assumed. To minimize the stress interval and the error the pore pressure should be kept low.

The stress-strain curves from CRS-tests are dependent on test duration just as any other oedometer test. Thus different results are obtained with different rates of strain. This was first shown by Crawford

*) Tokheim and Janbu have later (1981) given an exact solution and claim that the equations of 1976 are valid for $\dot{u}_b/\dot{\sigma} < 0.7$.

1964 and has been confirmed many times since then, Fig. 13.

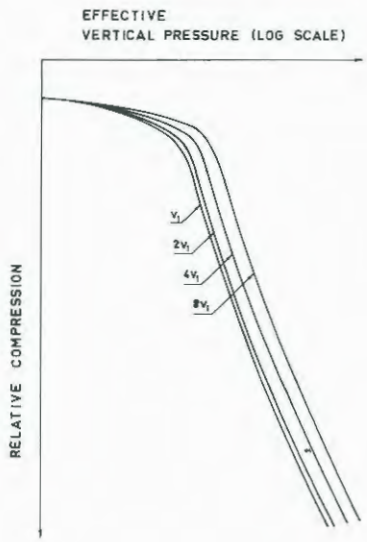

Fig. 13. CRS-tests with different strain rates.

Sällfors (1975) showed that for soft clays the influence of strain rate was considerable down to very low strain rates but with a new method for evaluation of the preconsolidation pressure the curves could be corrected for strain rates up to 0.0024 mm/min equalling 0.012% relative compression per minute on samples with 20 mm height. This rate also normally gives pore pressures lower than 0.15σ and is therefore recommended as a standard rate.

Sällfors also showed how the curve jumps from one stress-strain relation to another when the strain rate is increased during the test, Fig. 14.

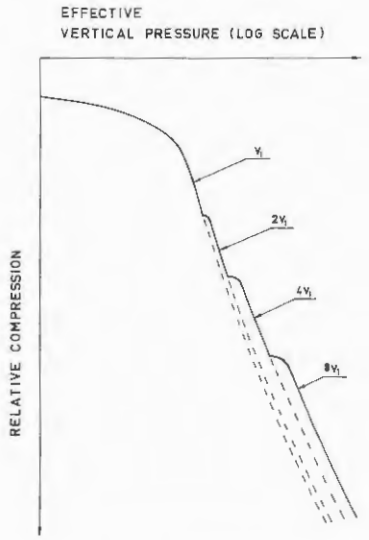

Fig. 14. CRS-test with stepwise increase of strain rate.

In the so called constant gradient test, CGT, the strain rate varies so that the pore pressure in the bottom of the sample is kept constant. This can be accomplished in many ways but always involves a more complicated set-up than the CRS-test. It is also a slower test as the governing pore pressure must be low at the small loads on the sample when the test starts and is then not allowed to increase during the test. The results from this type of test are also rate-dependent. The higher the set pore pressure is the faster the test runs and consequently the higher the preconsolidation pressure seems to be, Fig. 15.

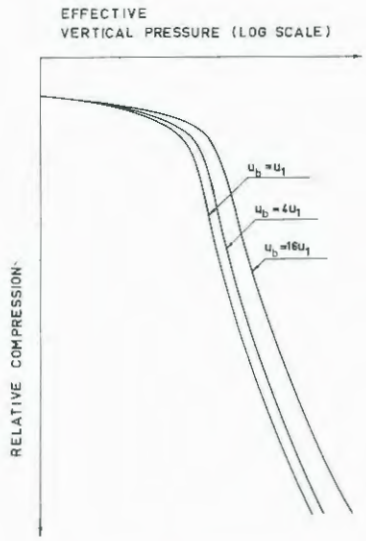

Fig. 15. CGT test with different set pore pressures.

The continuous consolidation test, CC, has mainly been developed at the Norwegian Institute of Technology. In this test the relation between the applied load and the pore pressure in the bottom of the sample is kept constant. It is the most sophisticated type of test and requires the most complicated equipment. However this should not be too great a drawback for the test as electronics development is progressing very rapidly. On the basis of results from tests on low plastic Norwegian clays and mathematical considerations it has been claimed that this test could be performed much faster than the CRS-test. However this is in conflict with experience of rate effects for more plastic clays. The main advantage with the CC-test compared to the CRS-test from a Swedish point of view seems to be that the CC-test automatically adjusts the rate of strain to the tested material. The standard rate of 0.0024 mm/min used in CRS-tests usually gives a pore pressure in the order of 0.1σ for medium to high plastic clays and in these materials the difference between CRS and CC would be very small. For silty clays however this rate is often too slow to give reliable pore pressures and for very soft

and low permeable soils the pore pressures become too high. Today the standard rate in the CRS-test is often adjusted somewhat according to the operator's judgement but this method is far from foolproof. The CC-test can overcome this problem and, in a few years after being adjusted for and tested out for softer soils, will probably be well worth the extra installation cost. The time to complete a test is however likely to increase just as often as decrease.

1.5 Evaluation of oedometer tests with continuous loading

The oedometer curves from continuous loading have clearly shown that the relation between compression and log effective stress is not a constant and have accentuated the time dependency of stress-strain relationships. Already before the continuous tests there was a trend to abandon the semi-log plot and a rational evaluation of the continuous oedometer tests has necessitated this.

From these tests continuous relations between effective stress and strain, modulus and effective stress, coefficient of consolidation and effective stress and permeability and strain are obtained. As the stress-strain relation is time-dependent so are the other relations except the permeability-strain relation. Also this relation can be time-dependent around the preconsolidation pressure if there is a large decrease in modulus when passing σ'_c.

Sällfors (1975) has shown the rate dependency for the different correlations for a soft clay, Figs. 16a, b and c.

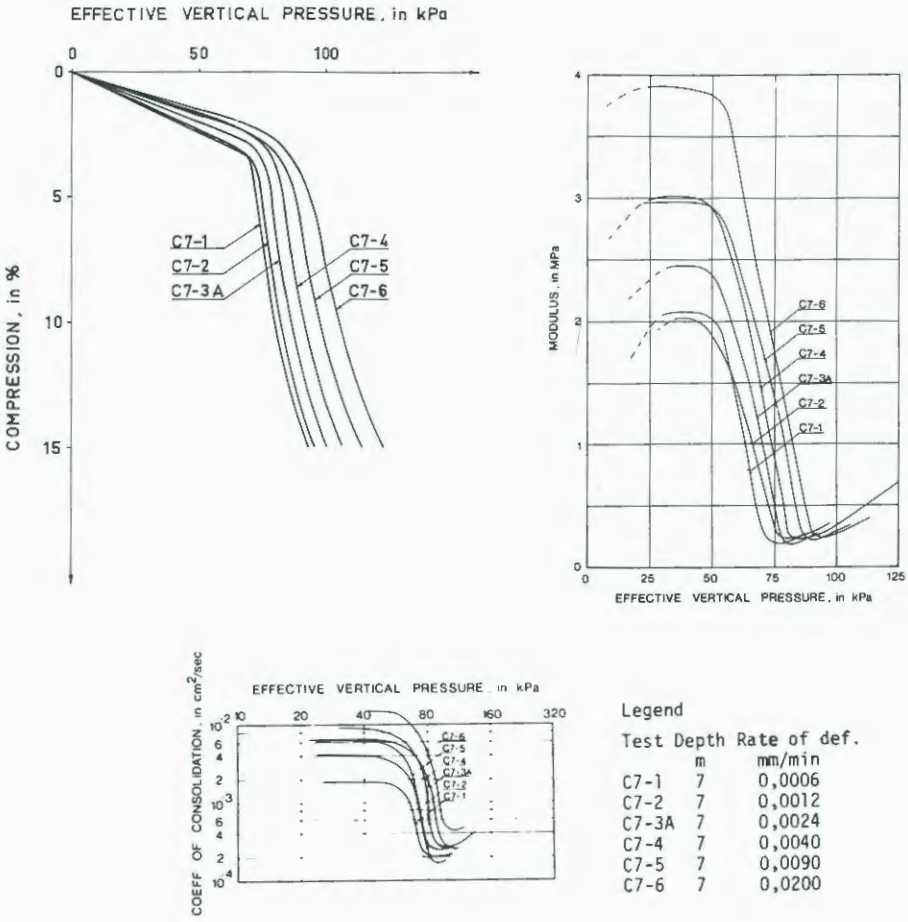

Fig. 16. Rate dependency of consolidation parameters in CRS tests. Bäckebol clay. (From Sällfors (1975).)

From tests on Bäckebol clay (see 7.2), a varved clay and an organic clay Sällfors proposed a method for interpreting the preconsolidation pressure which eliminated most of the rate effects and gave a constant value for rates of deformation of 0.0024 mm per minute and below. This method has been compared with field tests and incremental standard tests and has been found to give a reliable value of the preconsolidation pressure.

The constant rate of strain test has been in use at SGI since 1976 and well over one thousand tests have been run on materials ranging from silt and stiff clays to soft clays and gyttja. The test has become a standard test and a method for interpreting the test has been worked out.

Except for silt, dry crust and boulder clays all stress-strain relations follow the same pattern in arithmetic plots, Fig. 17.

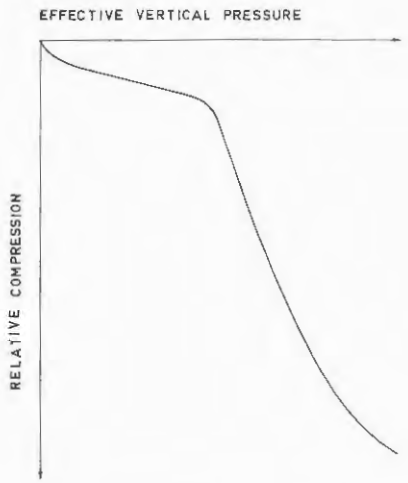

Fig. 17. Stress-strain relation for soft clays.

Initially there is a small irregularity as it is impossible to achieve a perfect fit between the filters and the cut ends of the sample. The stress-strain curve then becomes a straight line, bends downwards, becomes a straight line again and finally slowly bends upwards.

When the modulus $M = d\sigma'/d\varepsilon$ is plotted versus the effective stress the curve becomes as in Fig. 18.

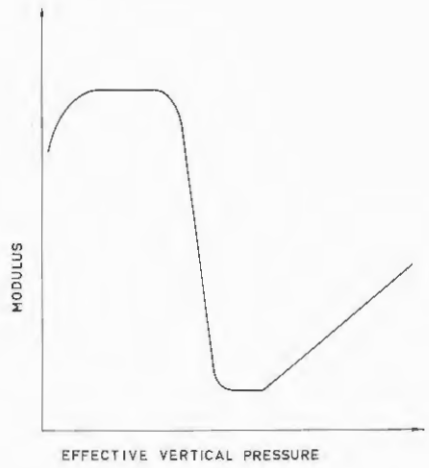

Fig. 18. Modulus-stress relation for a soft clay.

Initially the modulus increases until perfect contact is achieved. The modulus then becomes constant, rapidly drops to a new, almost constant value and then increases linearly with increasing stress.

The curve for the coefficient of consolidation resembles the modulus curve, Fig. 19.

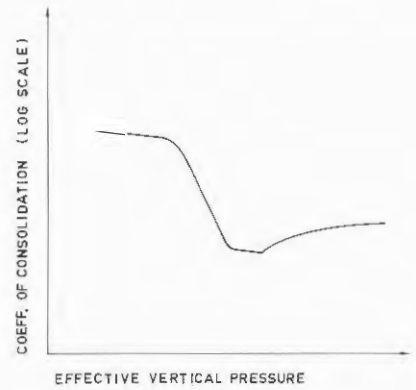

Fig. 19. Coefficient of consolidation versus stress for a soft clay.

After the modulus has become constant the c_v value is fairly high and decreases slowly as the sample is compressed and the permeability decreases. When the modulus drops the c_v value drops too and when the modulus starts to increase the c_v value also increases but very slowly as the relative compression in this stress region is high and the coefficient of permeability is rapidly decreasing.

In all tests the coefficient of permeability versus relative compression becomes, after some initial irregularities, a straight line in a semi-log plot, Fig. 20.

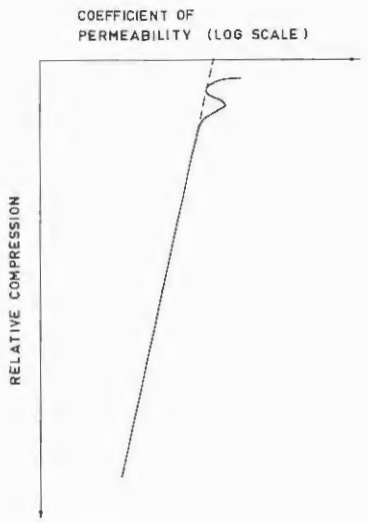

Fig. 20. Coefficient of permeability versus relative compression.

Fig. 21 shows results from an actual test. The modulus-stress curve is more rounded in the plot than in reality as the computer interpolates for several points in the calculation of M.

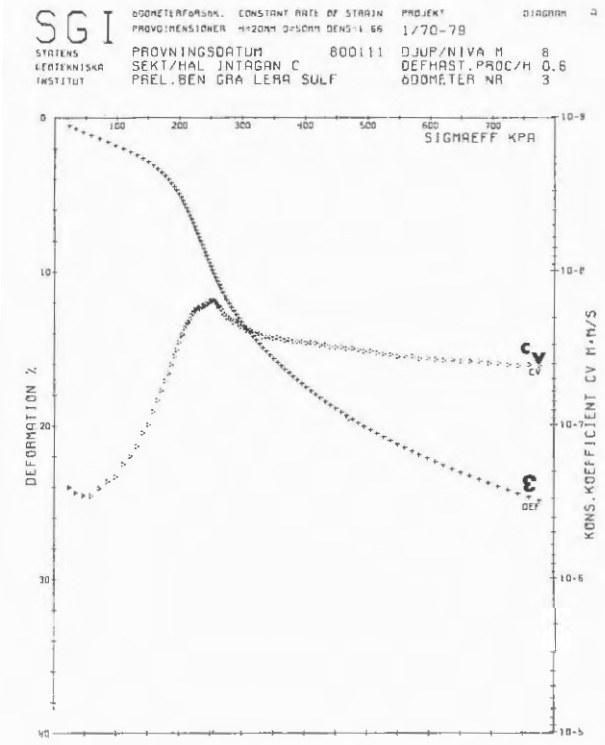

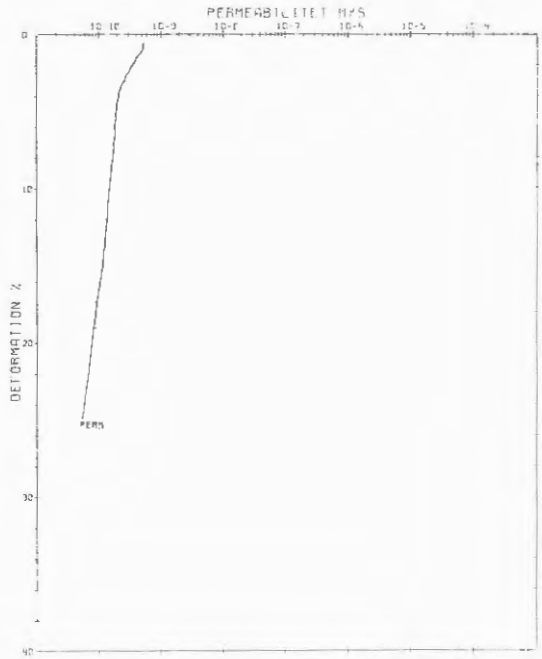

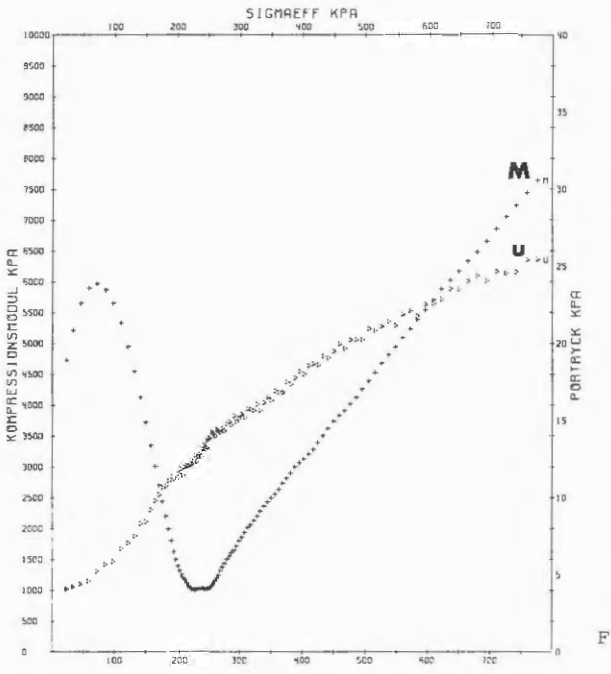

Fig. 21. Results from a CRS-test on a Swedish clay.

The experience gained has led to the following evaluation of the CRS-test, Fig. 22.

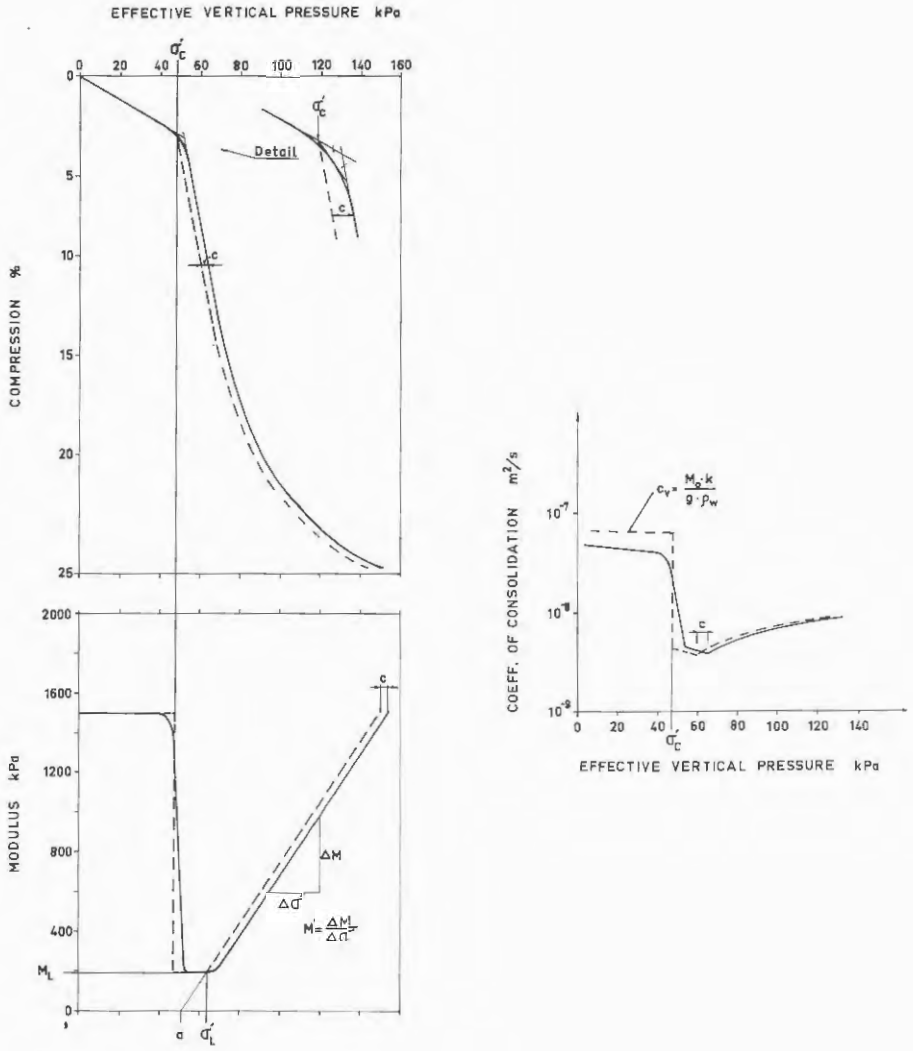

Fig. 22. Evaluation of the CRS-test.

The preconsolidation pressure is evaluated according to Sällfors, 1975. The two straight parts of the stress-strain curve are extended and intersected. An isosceles triangle is inscribed between the lines and the stress-strain curve. The intersection point

between the base of the triangle and the upper line represents the preconsolidation pressure σ_c'. This construction is sensitive to scales and is therefore always made in a plot where 10 mm on the stress axis corresponds to 10 kPa and 10 mm on the strain axis corresponds to 1% relative compression. The stress-strain curve after passing σ_c' is now moved a kPa horizontally to the left to pass through σ_c'. It can be questioned if moving the curve parallel in a linear plot (or any other plot) is quite correct but with the low testing rates used the value of a is small and possible errors can be neglected.

The modulus-stress plot is now modified. The initial constant modulus is extended to σ_c'. At σ_c' the modulus drops vertically to the second constant modulus M_L. The part of the curve where the modulus increases linearly with effective stress is moved a kPa horizontally to the left and extended to the base line where $M = 0$. The intersection with the base line a and the intersection with the constant modulus M_L is evaluated and the modulus number M' is evaluated as $\Delta M/\Delta\sigma'$ for the part of the curve where M increases linearly with effective stress.

The ε_v curve for stresses higher than σ_c' should now be moved a kPa to the left.

Thus the curve is divided into three parts:

1. The part in the stress interval σ_o'-σ_c' where $M = M_o$
2. The part in the stress interval σ_c'-σ_L' where $M = M_L$
3. The part in the stress interval $>\sigma_L'$ where $M = M'(\sigma'-a)$.

M_o from the first loading of soils in the oedometer is never used. It is always too low compared to field

modulus due to sample disturbance, swelling and imperfect fit. In many settlement calculations the settlement for stresses below the preconsolidation pressure is disregarded or some empirical relation such as $M_o \approx 250\ \tau_{fu}$ is used. c_v for this part of the curve is calculated from

$$c_{vo} = \frac{M_o \cdot k}{g \cdot \rho_w}$$

To obtain a useful value of M_o in the laboratory the sample must be unloaded when σ_c' is just exceeded to in situ effective vertical stress σ_o'. It should then be allowed to swell before it is reloaded. M_o is taken from this reloading curve. This procedure is always followed for boulder clays which are first loaded to about 1000 kPa (estimated ice pressure) and then unloaded to in situ vertical stress before the actual test starts.

If it can be estimated that the in situ effective stress has been lower than at present due to unloading and that the soil is in a reloading state the sample should be unloaded to this estimated lowest unloading pressure.

Calculation of compression thus becomes

$$\varepsilon = \frac{\sigma' - \sigma_o'}{M_o} \quad \text{when} \quad \sigma' = \sigma_o' + \Delta\sigma' < \sigma_c'$$

σ_o' = in situ effective vertical stress

$$\varepsilon = \frac{\sigma_c' - \sigma_o'}{M_o} + \frac{\sigma' - \sigma_c'}{M_L} \quad \text{when} \quad \sigma_c' < \sigma' < \sigma_L'$$

and

$$\varepsilon = \frac{\sigma_c' - \sigma_o'}{M_o} + \frac{\sigma_L' - \sigma_c'}{M_L} + \frac{1}{M'} \ln \frac{(\sigma' - a)M'}{M_L}$$

when $\sigma' > \sigma_L'$

Dry crusts can be described with the same parameters but the pattern differs, Fig. 23.

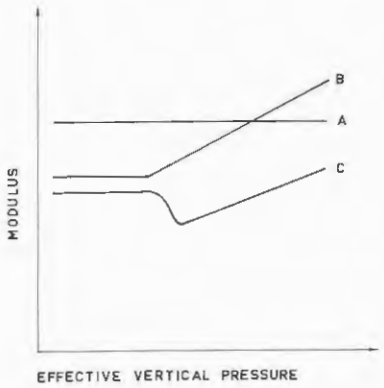

Fig. 23. Modulus-stress relations from dry crusts.

The test can as in curve A yield a constant M value throughout the tested stress range or as in curve B a constant M value for a part of the test and then a slowly increasing M value with increasing stress. None of these curves give a preconsolidation pressure. In curve C a preconsolidation pressure can be evaluated but exceeding the preconsolidation pressure does not involve a dramatic change of the modulus and the increase of the modulus with effective stress in the later stage of the test is moderate.

CRS-tests on dry crusts generally give high modulus low values of modulus number M' (unless the crust contains much silt) and negative values of a.

The general pattern from tests on silt and silty clays is somewhat erratic as the samples are often more or less disturbed. Some of these soils, especially those with a high clay content, follow the pattern from tests on clay, Fig. 24 CURVE A. In some tests it is possible to evaluate a preconsolidation pressure but this is not followed by a constant modulus. Instead, the modulus simply drops and then starts

to increase directly, Fig. 24 CURVE B. The value of a then becomes very small or zero. In very silty soils no preconsolidation pressure can be evaluated but the modulus increases almost from the start of the test and the value of a becomes zero or negative, Fig. 24 CURVE C and D.

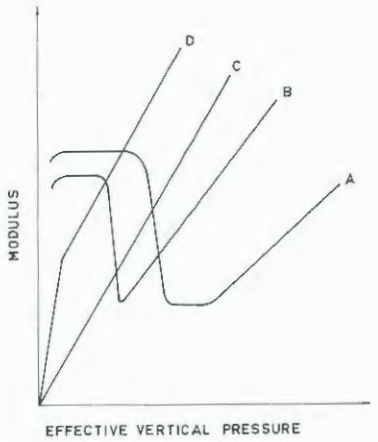

Fig. 24. Modulus versus effective stress for silty soils.

1.6 Factors affecting compressibility and the shape of the pressure-compression curve

Soil is composed of solid particles and voids. As the solid particles are relatively incompressible the total compressibility is governed mainly by the void ratio. For saturated soils the natural water content is a measure of the void ratio.

$$e = w \frac{\rho_s}{\rho_w}$$

For the most common minerals in Swedish clays and silt ρ_s varies very little from the average value of 2.7 t/m^3.

Helenelund, 1951, proposed the empirical relation between compression index C_c and natural water content w_N.

$$C_c = 0.85 \sqrt{w_N^3}$$

Mesri (1974) has compiled data from literature and plotted C_c versus w_N showing that there is a relation even though the spread is considerable, Fig. 25.

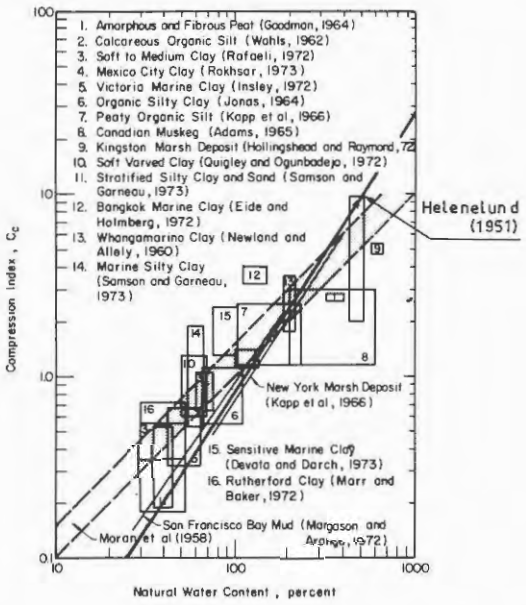

Fig. 25. Compression index for natural soil deposits (from Mesri (1974) with addition of Helenelund (1951) relation).

To study empirical relations for the compressibility factors σ_c', α, σ_L', M_L and M' evaluated from the CRS-tests data from 562 tests was gathered. The test results came from consulting and research projects and represented a very wide range of soils.

The data was subdivided into three groups: 1. organic soils, 2. inorganic clays and 3. silty clays and clays with layers of silt.

Weathered dry crusts were left out of the study.

In Swedish practice the only water contents measured are natural water content and liquid limit.

When studying the total compressibility therefore a number of empirical relations had to be used.

From the very comprehensive collations of consistency limits for Swedish soils made by Rudolf Karlsson at SGI the following empirical relations for plastic limit w_P and shrinkage limit w_S were taken.

Inorganic clay	$w_P = 0.14\ w_L + 0.172$
	$w_S = 0.9\ w_P$
Organic soil	$w_P = 0.3\ w_L + 0.14$
	$w_S = 0.6\ w_P$
Silty clays	$w_P = 0.67\ w_L$
	$w_S = 0.9\ w_P$

A rule of thumb for Swedish engineers is that the capillarity of clays is in the order of 200 m of water. This rule seems to originate from air intrusion tests at the University of Agriculture in Sweden.

When comparing the compressibility factors with each other one definite relation is found. The factor a is almost equal to the preconsolidation pressure σ_c', Fig. 26.

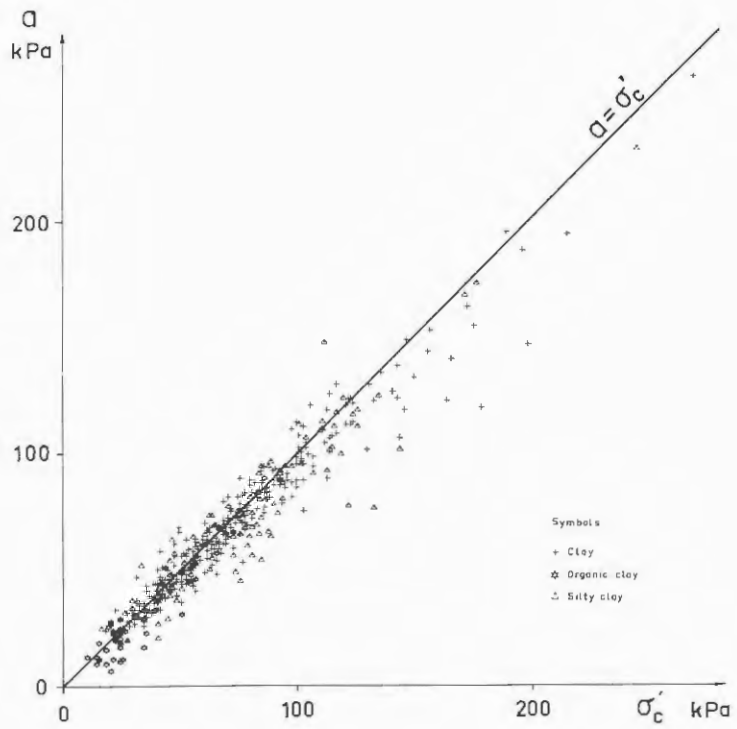

Fig. 26. Parameter a versus preconsolidation pressure σ'_c.

The most marked exceptions are some silty clays where a becomes lower than σ'_c, in some cases zero. Figure 26 shows 542 tests out of 562.

The modulus number M' is related to the natural water content and the best simple relation found was $M' = 4.5 + 6/w_N$, Fig. 27.

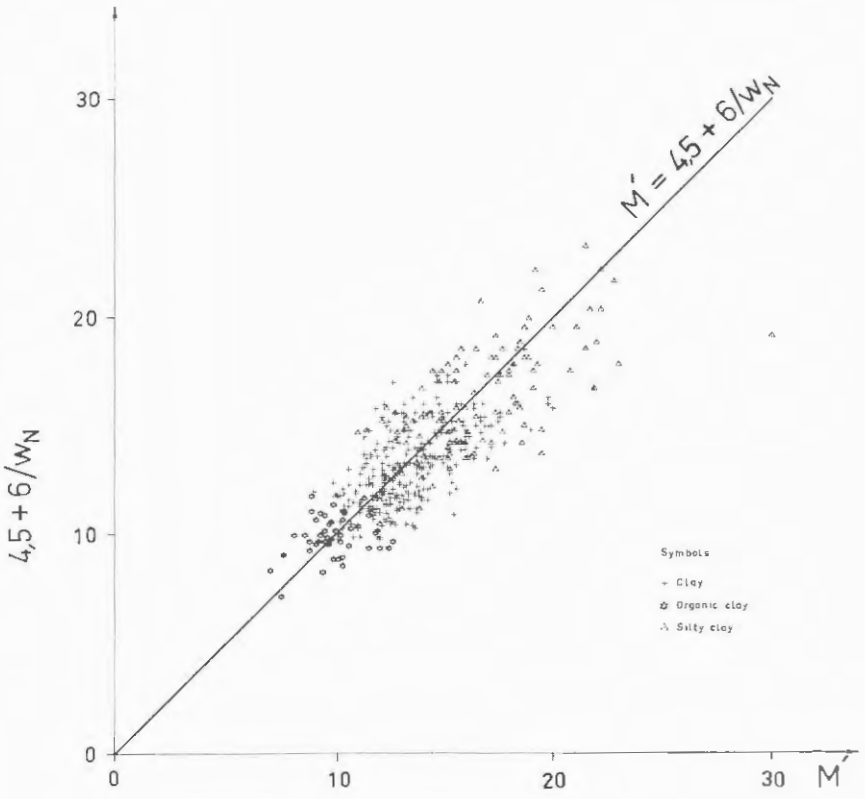

Fig. 27. Simple equation for modulus number versus measured modulus number.

In accordance with these two relations it can be seen that the straight portion of the oedometer curve where $M = M_L$ generally remains straight for a higher amount of compression the higher the water content is.

$$\varepsilon_L = \frac{\sigma'_L - \sigma'_c}{M_L} = \frac{\sigma'_L - \sigma'_c}{M'(\sigma'_L - a)} \quad if \quad a = \sigma'_c \quad \varepsilon_L = \frac{1}{M'}$$

For the two factors M_L and σ'_L however no useful relation has been found except that a combination of them gives the straight portion of the curve ε_L. Of course M_L generally increases with σ'_c but very low values of M_L/σ'_c can be found in soils with high liquidity indexes. Just as a high liquidity index may imply a high sensitivity but does not necessarily

do so, a high liquidity index may imply a relatively low value of M_L but is no rule.

To compare the total compressibility from the oedometer test and other soil properties the following reasoning was made. The soil exists in situ with its preconsolidation pressure and its natural water content. By definition the soil should decrease its water content to the shrinkage limit if it is exposed to an isotropic pressure equal to the capillarity of the soil. In the oedometer the soil is not compressed by isotropic stress but the stress level will be in the same order.

The parameters σ'_c, a, σ'_L, M_L and M' were fed into the computer together with the natural water content w_N. Relative compression up to the preconsolidation pressure was estimated to 3%. The natural water contents ranged between 30 and 230 per cent and the preconsolidation pressures from 10 to 275 kPa. Computed relative compression at σ' = 2000 kPa varied between 13 and 81%. The computed curves for water content versus stress and relative compression versus stress were then drawn, Figs. 28a and b.

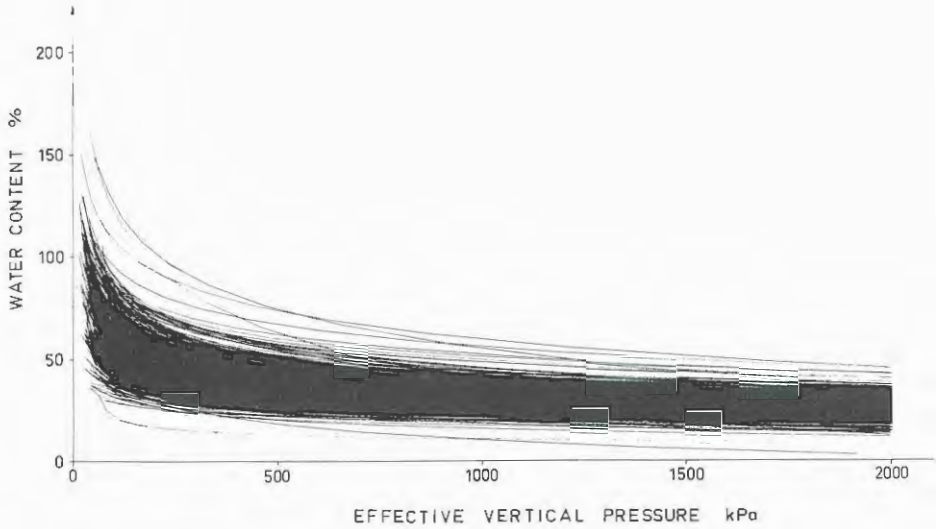

Fig. 28a. Water content versus vertical effective pressure.

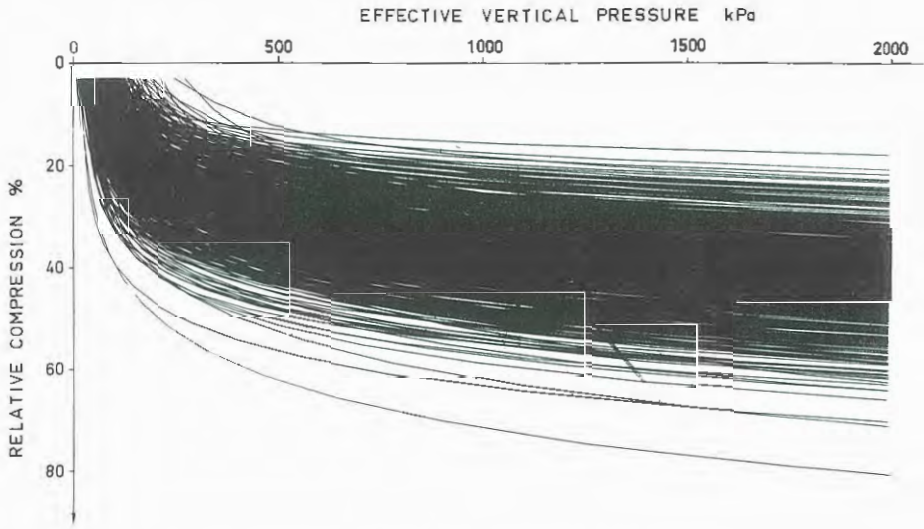

Fig. 28b. Relative compression versus vertical effective pressure.

The empirical relations for shrinkage limits were now used and the curves were normalized with the decrease in water content $(w_N - w)$ divided by $(v_N - w_S)$ and the increase in effective stress $(\sigma' - \sigma'_c)$ divided by $(2000 - \sigma'_c)$.

The normalized curves are shown in Fig. 29.

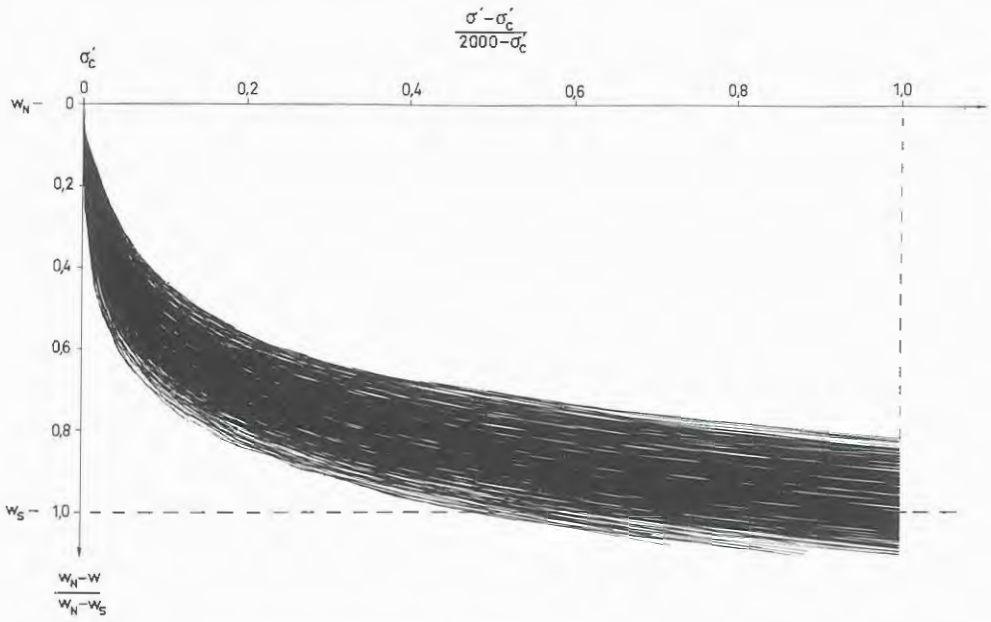

Fig. 29. Normalized stress-strain curves.

The curves in this figure represent 90% of the total. The most uniform picture was obtained for organic clays which is not surprising as the initial water content and total compression were highest for these materials and errors in the empirical relations were not a strong influence. In the same way the curve from silty clays showed the most spread.

At the same time the value of modulus number M' that would give a curve passing through the point $w = w_S$ and $\sigma' = 2000$ kPa was calculated and compared with the actual value of M' from the test, Fig. 30.

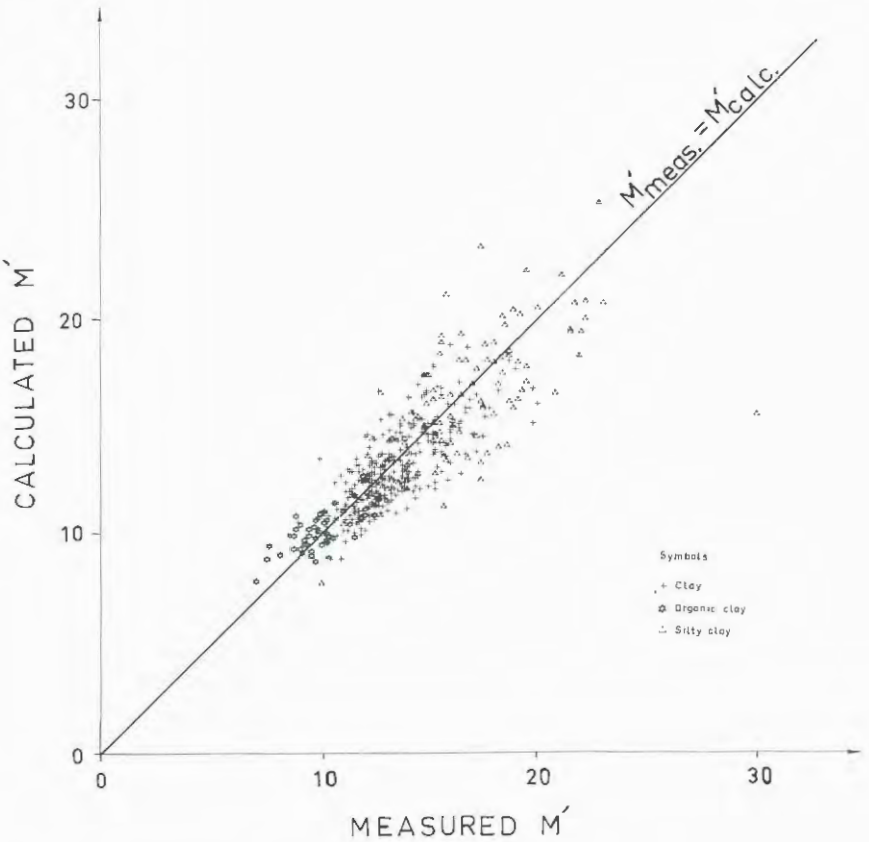

Fig. 30. Calculated versus measured modulus number.

As can be seen the agreement is good except for some silty clays. Trials were made with other capillarities but the equivalent pressure of ~2000 kPa gave the best fit.

The spread in the curves in Fig. 29 is too great for an average to be of any practical use for the engineer beside a general understanding of soil compressibility. It is satisfactory though that different determinations of soil properties match and that the oedometer tests give reasonable results.

1.7 Oedometer tests in different directions

Oedometer tests on samples in different directions are sometimes performed. One reason for these tests is to form a picture of how the preconsolidation pressure varies in different directions and also to see if the soil is more permeable in the horizontal than the vertical direction. Numerous such tests have also been performed lately on samples taken in a natural slope to find the direction of the principal consolidation stresses.

To show the general picture some results from tests on Bäckebol clay[1] are shown. The samples are taken from an area with flat ground and no slopes in the vicinity. As has been found in many other investigations the preconsolidation pressure varies with direction in a sinusoidal relation, Fig. 31.

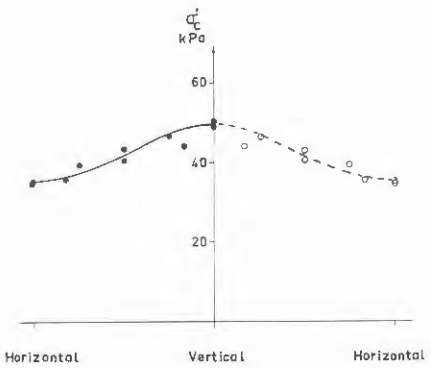

Fig. 31. Variation of σ_c' with orientation of sample.

The preconsolidation pressure here has its maximum in the vertical direction and minimum in the horizontal direction.

The parameter σ_L' does not appear to be much affected by sample orientation.

[1] Data see 7.2.

The constant modulus M_L on the other hand is very much affected by orientation and the relation is sinusoidal with a minimum for vertically oriented samples and a maximum for horizontal samples, Fig. 32.

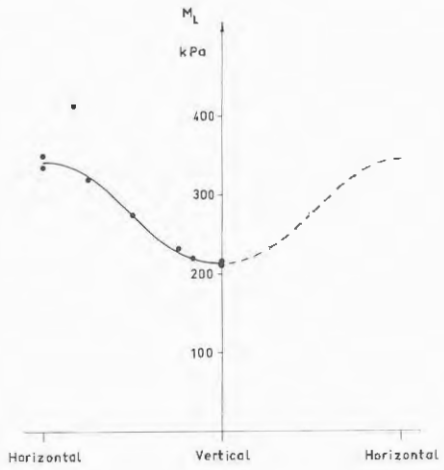

Fig. 32. Variation of M_L with orientation of sample.

The modulus number M' varies very little but a tendency for vertical samples to have a higher M' than horizontal samples can be noted.

If the oedometer curves for samples cut in different directions are plotted together it can thus be seen that samples with a lower preconsolidation pressure than the vertical sample have a higher modulus and approach closer to the curve for vertical samples with increasing deformation. At σ_L' they are very close and by then the sample seems to have lost its "memory" of previous consolidation stresses and the different curves run closely together, Fig. 33.

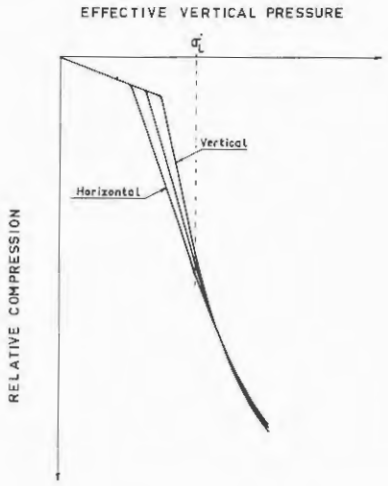

Fig. 33. Oedometer curves for samples with different orientations.

The coefficient of permeability measured in the tests on Bäckebol clay varies a little from test to test but there is no indication that it has anything to do with orientation, Fig. 34.

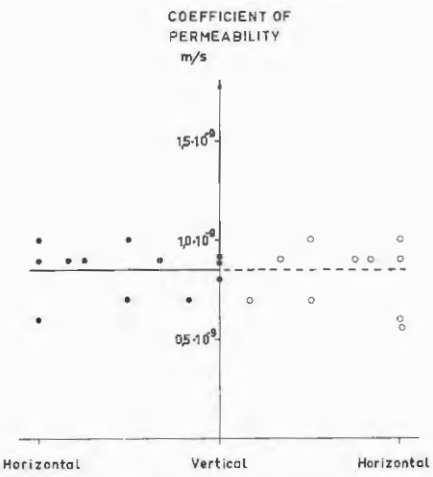

Fig. 34. Initial coefficient of permeability in different directions.

Numerous investigations have been performed on different clays at SGI and there is no indication that

coefficient of permeability should vary with direction in homogeneous Swedish soft clays. That coefficient of permeability can vary with direction in varved and layered soils is obvious. The only "homogeneous" soil where the horizontal coefficient of permeability consistently has been higher than the vertical is peat with a low degree of humification.

1.8 Swelling

If the effective stresses in a soil are decreased enough the soil starts to swell. If a clay has just consolidated for a load increase over the previous preconsolidation pressure secondary compression will proceed at a relatively high rate. A small reduction in load will halt this compression for a while or there may be a small swelling before compression starts again at a reduced rate. If the load reduction is large enough secondary compression stops completely and for even larger load reductions the clay will swell. Like compression, this swelling is time-dependent. At unloading the pore pressure in the clay drops. There is a time lag in the swelling while there is a gradient in the clay and water is absorbed as fast as the permeability and access to the water permits. After the gradient evens out there is secondary swelling at unloading similar to secondary compression at loading.

This is illustrated in Fig. 35 where two oedometer tests with stepwise loading and unloading are shown. The time-swelling curves can be seen to show the same shape as the time-settlement curves. The swelling modulus is high close to the preconsolidation pressure but decreases as the effective stress decreases and is very low at low effective stresses. As the swelling modulus is of the same order as the compression modulus and permeability is not much altered the c_v values are of the same order for swelling and compression.

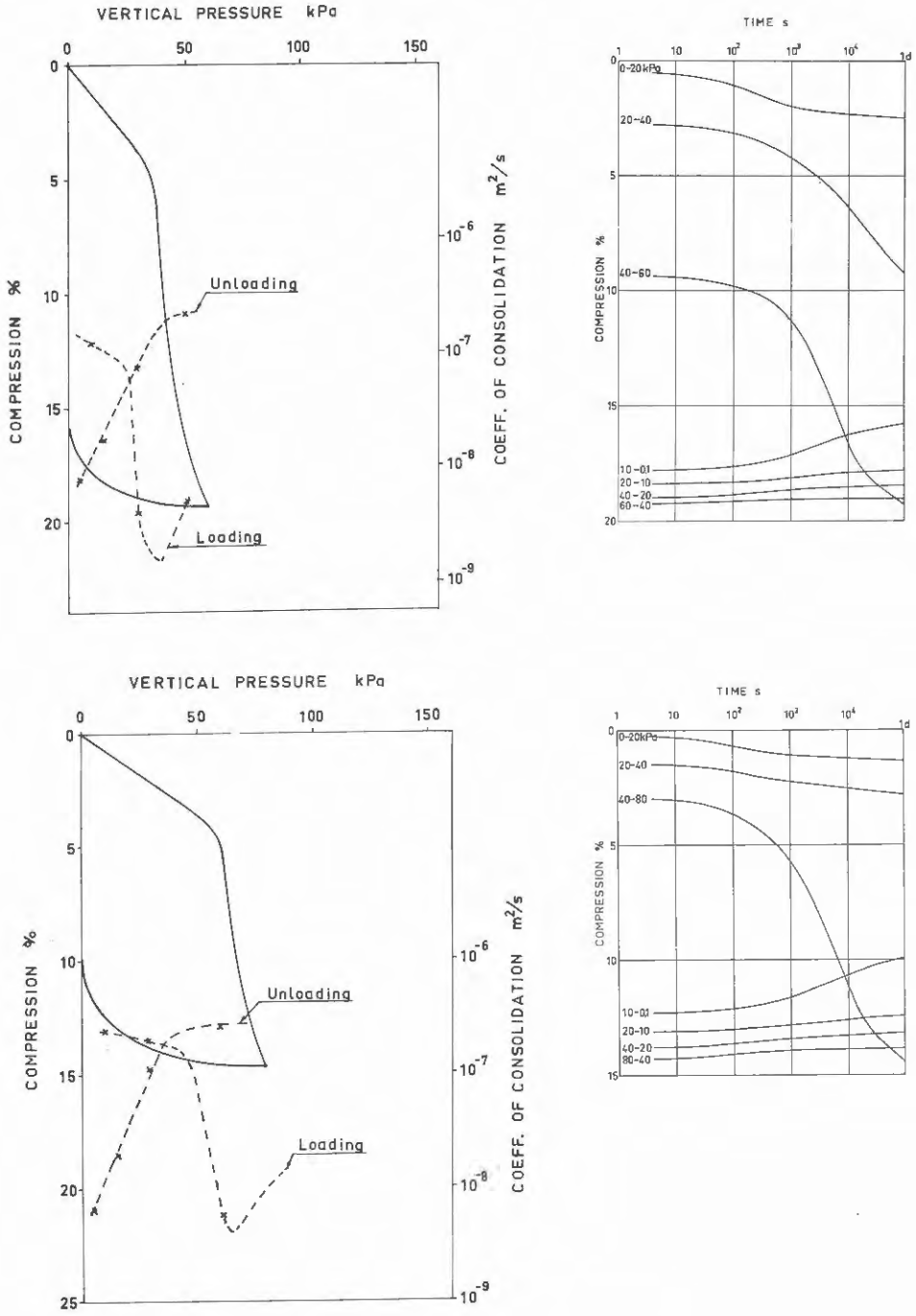

Fig. 35. Oedometer tests with stepwise loading and unloading on Norsholm clay.

The same behaviour is illustrated by CRS-tests in Fig. 36. In these tests the deformation was stopped and the presses were geared down to the lowest possible speed before the direction was reversed and the swelling started. In the test in Fig. 36c swelling was stopped after a time and the sample was then recompressed at the standard rate of strain.

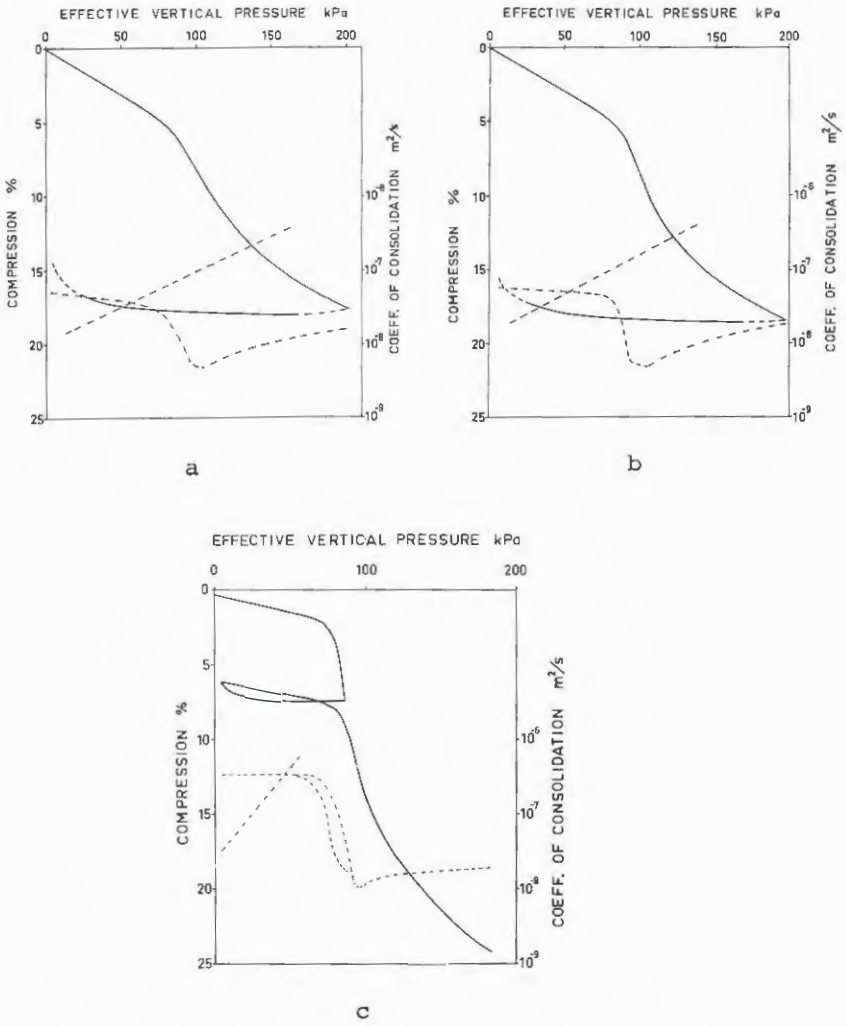

Fig. 36. CRS-tests with loading and unloading on soft clays.

No study of the secondary swelling rates has been performed for Swedish clays but Mesri et al (1978) reports tests indicating that the secondary swelling indexes may be even higher in relation to the swelling index than the index of secondary compression compared to the compression index.

From tests on Swedish soils performed at SGI and Chalmers University a simple equation for swelling can be suggested for the first unloading from $b \cdot \sigma_c'$ to σ'

$$s = a_s \ ln \ \frac{b \cdot \sigma_c'}{\sigma_u'}$$

where

s = total relative increase in sample height
a_s = swelling index
σ_c' = preconsolidation pressure
b = load factor when swelling overcomes secondary compression
σ_u' = effective pressure after pore pressure equalisation

This equation has been used for a variety of soils and found to fit the laboratory test results satisfactory.

For soft clays the swelling index a_s has been found to vary between 0.007-0.012 and the load factor b is about 0.8. a_s decreases with increasing grain size and is about 0.001 for sand and gravel and b increases with increasing grain size to become 1 for gravel.

a_s-values for a number of Swedish soils are plotted against average grain size d_{50} in Fig. 37.

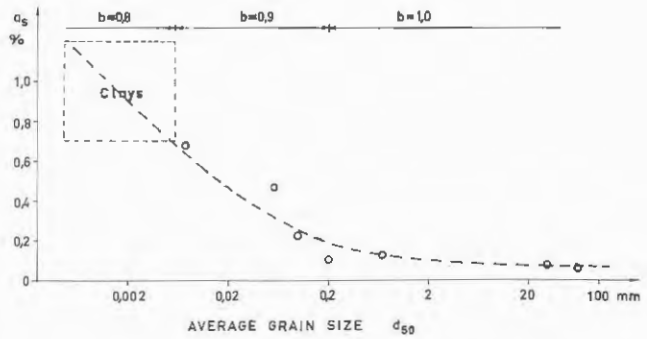

Fig. 37. Swelling index a versus average grain size.

At the top of the figure ranges for approximate b-values are given.

For clays there is probably some correlation between plasticity index, swelling index and the load factor. Possible correlations are sketched in Fig. 38 but as I_p has not been determined in most cases the points obtained so far are too few to give a definite relation.

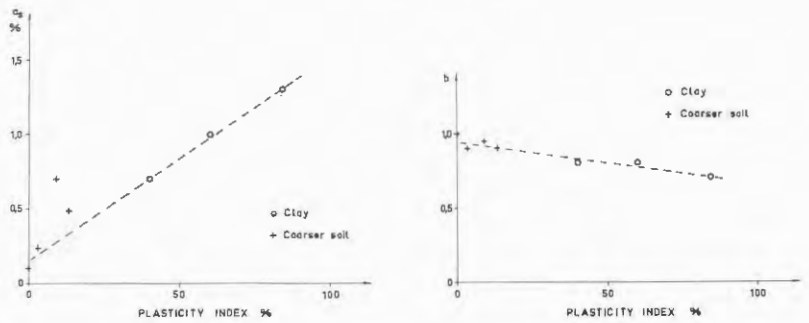

Fig. 38. Swelling parameters versus plasticity index.

1.9 Recompression

The modulus at recompression after swelling is dependent on the magnitude of the swelling. Samples that have only had a small load reduction have not swelled at all and have a relatively high recompression modulus. This modulus is not constant but decreases as the effective stress increases.

A characteristic feature of samples that have undergone swelling is that when they are reloaded they will show a constant compression modulus up to the effective pressure $b \cdot \sigma_c'$ and the compression at this pressure will be equal to the previous maximum compression. b is the same load factor as the factor b that determines at which pressure the sample starts to swell. After passing the pressure $b \cdot \sigma_c'$ the reloading curve bends downwards and the reloading modulus decreases.

This is illustrated in Fig. 39 where a number of tests on the same clay have been preconsolidated for the same effective stress and then unloaded to different loads. After swelling they have been reloaded with small load steps. The curves have been slightly adjusted along the ε-axis to give the same compression at the end of the first loading.

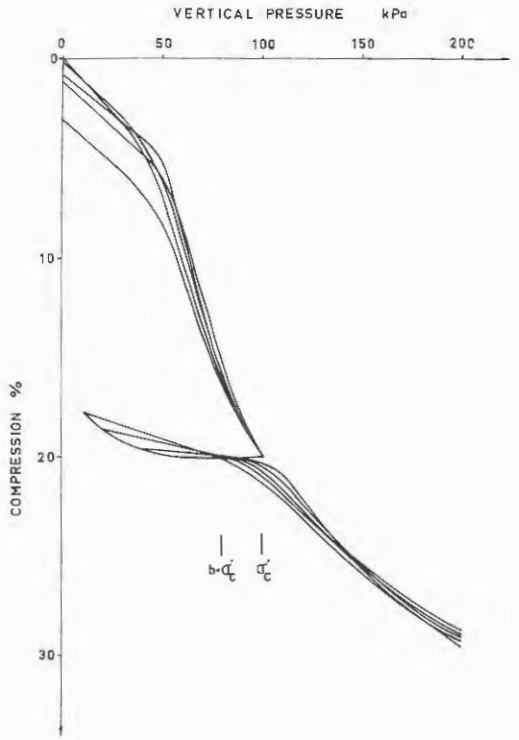

Fig. 39. Effect of swelling on recompression. Curves slightly adjusted in the vertical direction.

Fig. 40 shows results from a number of tests on the same clay where the samples have been consolidated to different effective stresses, unloaded to low stresses and reloaded after swelling. The curves have been slightly adjusted along the ε-axis to fall on the same virgin compression curve. The tests all start to swell at the same b-value and the recompression curves all intersect the swelling curve at $\sigma' = b \cdot \sigma'_c$.

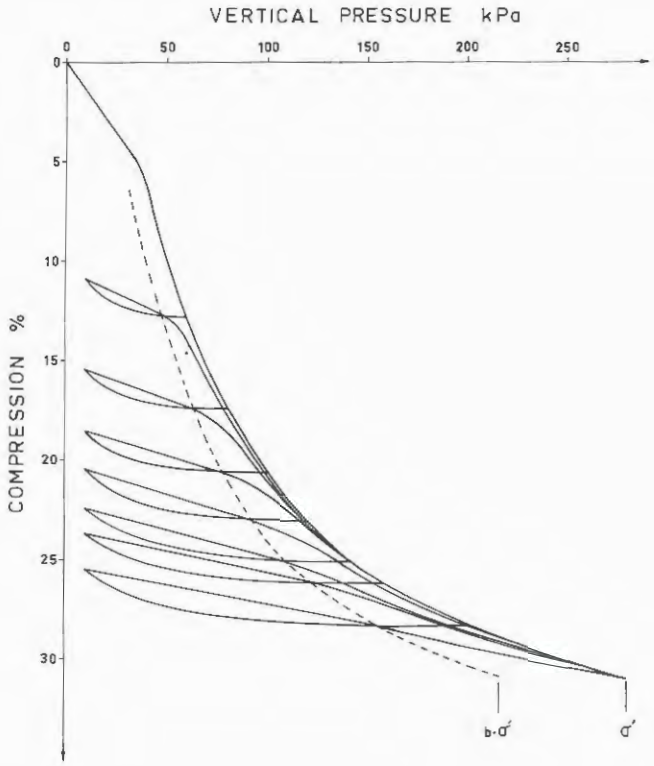

Fig. 40. Swelling and recompression after different preconsolidation. Curves slightly adjusted.

The modulus at recompression M_{rb} in the stress interval σ_u' to $b \cdot \sigma_c'$ thus becomes

$$M_{rb} = \frac{b \cdot \sigma_c' - \sigma_u'}{a_s \ln(\frac{b \cdot \sigma_c'}{\sigma_u'})}$$

where σ_u' is the effective pressure to which the sample was unloaded and a_s and b are the swelling parameters.

In the stress interval $b \cdot \sigma_c'$ to σ_c' the rebound modulus gradually decreases from M_{rb} to a modulus slightly higher than the modulus on the virgin compression line. The curve then asymptotically approaches the virgin compression line.

In Fig. 39 it can be seen how the drop in modulus when passing σ'_c becomes smaller the more the sample has been allowed to swell. If an oedometer curve for a soil which has undergone swelling is plotted with the effective stress in log scale it will appear "disturbed". Before any attempt to correct an oedometer curve for disturbance is made the whole stress history for the soil must be known or the correction may become a distortion.

Any other swelling and recompression than the first unloading and first reloading would be much more complicated to describe and would probably have to be investigated in triaxial apparatus to avoid all influence from side friction.

1.10 Secondary compression and pore pressure dissipation

Except for settlement calculations in peat where secondary compression is of main importance the influence of secondary compression has until lately been much overlooked. Practical problems in estimating settlements for small increases of effective stress close to the preconsolidation pressure where the primary compression is small but the rate of secondary compression high and observation on test fills when settlements occur at a much higher rate than the pore pressure dissipates have initiated closer studies of secondary compression.

More theoretical aspects on the development of a quasi preconsolidation pressure due to secondary compression and the time effects on preconsolidation pressure have also initiated investigations.

Bjerrum (1967, 1972) proposed that stress-deformation curves each valid for a certain duration of sustained load could be drawn, Fig. 41.

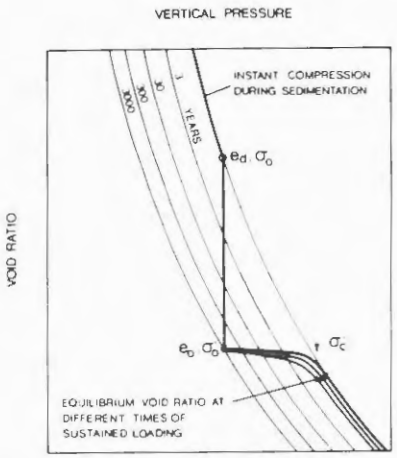

Fig. 41. Effects of secondary compression on void ratio and preconsolidation pressure. (Bjerrum (1967, 1972).)

If a clay is left to consolidate under constant effective stress each curve represents the void ratio versus effective stress for a certain time after primary consolidation. If a clay has been under constant stress for a long time and has a reduced void ratio it can be loaded up to the pressure corresponding to its reduced void ratio on the primary compression line without any significant primary compression. If the clay is loaded further the primary compressions will follow the original primary compression line and if the load is kept constant secondary compression will occur and the void ratio will be adjusted according to pressure and time.

Šuklje (1957) presented this in the way that each void ratio effective pressure relation after primary consolidation corresponded to a certain rate of secondary deformation, Fig. 42.

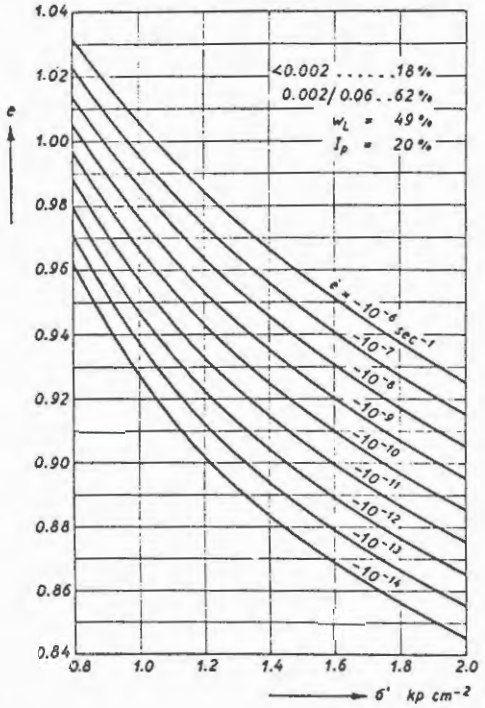

Fig. 42. Equal strain rates versus vertical pressure and void ratio (from Šuklje (1957)). $\dot{e}$ = rate of void ratio change de/dt.

Mesri (1973) collected results from reported tests and showed that the coefficient of secondary compression similar to the compression index is mainly dependent on water content, Fig. 43.

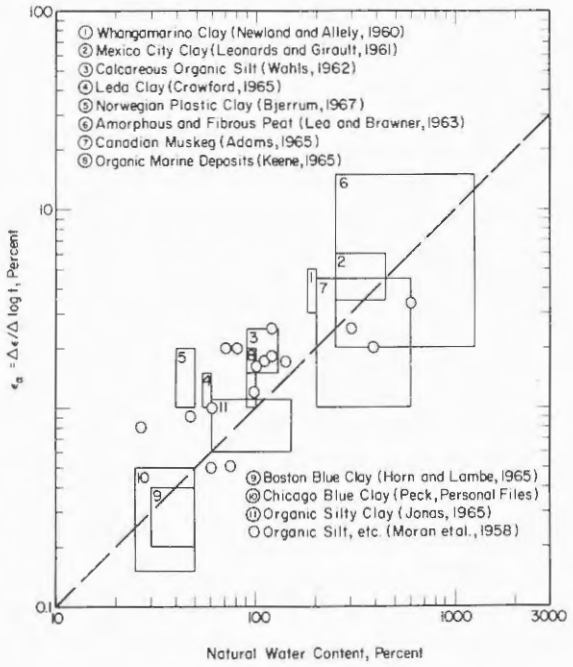

Fig. 43. Coefficient of secondary compression for natural soil deposits (from Mesri (1973)). $\varepsilon_\alpha \approx c_\alpha$

Further comparisons of soil data (Mesri & Godlewski, 1977) gave the average relation between secondary compression index $C_\alpha (\Delta e / \Delta \log t)$ and compression index C_c:

$$C_\alpha / C_c \text{ AVERAGE} \approx 0.05$$

If Mesri & Godlewski data are studied closely the average relation for inorganic clay and silt is $C_\alpha / C_c \approx 0.041$, for organic clays and silt $C_\alpha / C_c \approx 0.053$ and for peat and muskeg $C_\alpha / C_c \approx 0.075$. The relative importance of secondary compression thus increases with increasing content of organic matter.

The time-settlement relation for a load increment is assumed to follow a standard pattern where the curve

in an ε-log t plot becomes a reversed s-shape and then a straight line and where the end of primary consolidation and the coefficient of secondary compression can be evaluated, Fig. 44.

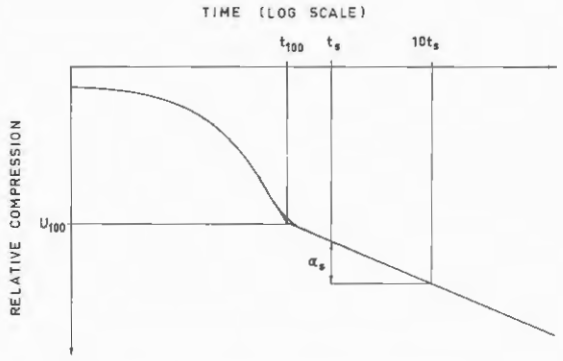

Fig. 44. Ideal time-settlement curve.

This type of curve is not always obtained. To obtain the inverted s-shape the load increment must be of a certain magnitude. Mesri has shown that this magnitude depends on the relation C_α/C_c. It is usually obtained in the standard incremental test with a doubling of the load at each load step but in tests with smaller increments only sometimes. At load increments where the applied stress is slightly below, at or just over the preconsolidation pressure the load-settlement curves will deviate from the standard pattern. The assumption that α_s is a constant is also an oversimplification. In Fig. 45 type curves for time-settlement relations from a standard incremental test on soft clay are shown.

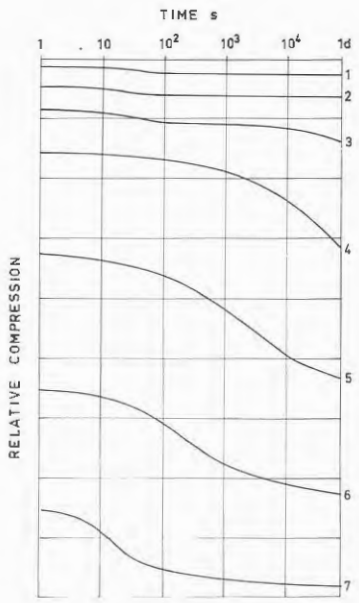

Fig. 45. Types of time-settlement curves from standard incremental test.

In the first two curves the loads are well below the preconsolidation pressure and the curves follow the ideal pattern. The third curve represents a load slightly below the preconsolidation pressure. Here the reversed s-shape comes out but α_s does not remain constant but increases with time. The fourth curve represents a load where the preconsolidation pressure is reached but not much exceeded. In this curve there is no s-shape but the curve bends downwards more and more. This load increment would have to be applied for weeks before the ideal shape came out. With standard increments curves 3 and 4 never appear in the same test and sometimes if the preconsolidation pressure happens to be in the middle between two loads neither of them will occur. The curves representing loads well over the preconsolidation pressure become the reversed s-shape but α_s is not a constant and decreases with time.

The pore pressure dissipation-time curve for a load increment is assumed to correspond to the primary settlement-time curve. This is hardly ever quite true but for load increments not passing the preconsolidation pressure the curves resemble each other. The modulus and coefficient of permeability are not constants during the pore pressure dissipation but the changes partly even out each other. More sophisticated apparatus than standard oedometers and larger samples would often be required to study the differences. If the load increment passes through the preconsolidation pressure though there will be a marked deviation for the pore pressure dissipation-time curve from the settlement-time curve. The coefficient of consolidation and pore pressure equalization is

$$c_v = \frac{M \cdot k}{g \cdot \rho_w}$$

When the preconsolidation pressure is passed there is a sudden decrease in modulus M while the coefficient of permeability k only changes slowly and consequently there is also a sudden change in c_v.

This change in c_v makes the pore pressure dissipation halt for a while before it starts again, Fig. 46.

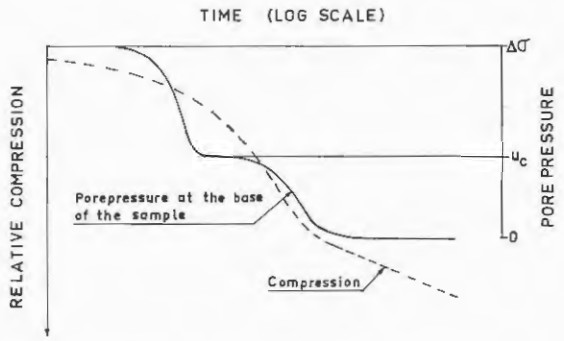

Fig. 46. Pore pressure dissipation and settlement at load increment passing the preconsolidation pressure.

For a load step where the time-settlement curve resembles curve 4 in Fig. 45 the pore pressure in the oedometer will have dissipated far before the time-settlement curve indicates the end of primary consolidation.

This means that measured pore pressures beneath a structure in the field will never give an exact answer as to how much of the final settlement has occurred. If the final load is near the preconsolidation pressure or if the applied load involves bringing an overconsolidated clay into a normally consolidated state the correlation between pore pressure dissipation and settlement may be very poor.

These questions were treated theoretically by Mesri and Rokhsar (1974) and on the basis of the pore pressure dissipation curve in Fig. 46 Leroueil et al (1980) proposed a rapid test for determination of the preconsolidation pressure. In this test a large load step overlapping the preconsolidation pressure is applied on the sample, the pore pressure dissipation curve is studied and the preconsolidation pressure is evaluated from the effective stress at u_c ($\sigma'_c = \sigma'_o + \Delta\sigma - u_c$). Leroueil (1981) has later found that this preconsolidation pressure due to time effects must be divided by about 1.5 to correspond to the standard test.

At SGI a number of tests have been run to study the rate of secondary compression. One series of tests was run on samples from 8 m depth at Bäckebol. In this series the samples were first consolidated for a vertical stress of 60 kPa which is slightly above the preconsolidation pressure and then unloaded to 10 kPa and allowed to swell. The average deformation for the 8 tests at 60 kPa was 3.60% and the settlement gauges were adjusted to this value. After swelling the samples were reloaded with load in-

crements which almost doubled the load but gave a certain spread of the load increment. This enabled an almost continuous study of the way in which the secondary deformation altered with load.

The load-compression curve can be seen in Fig. 47.

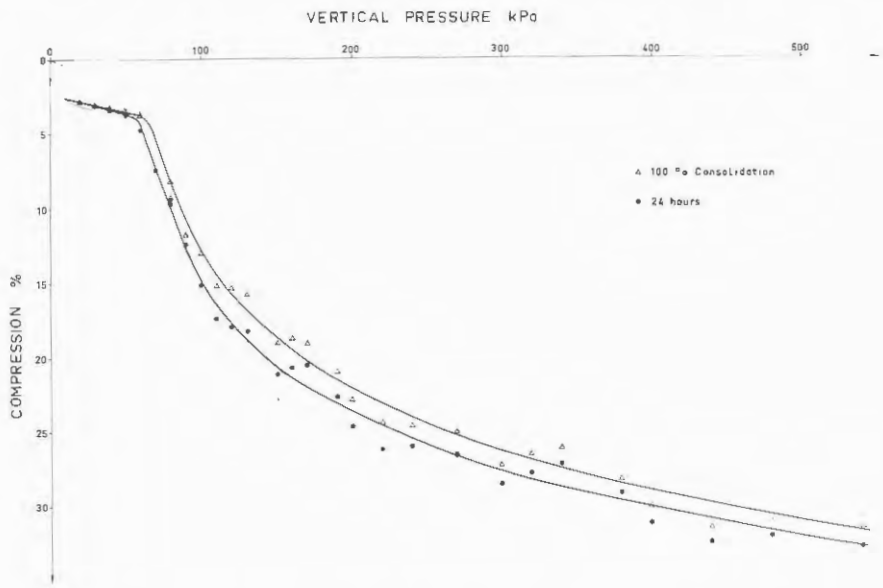

Fig. 47. Load-compression curve for special stepwise tests on Bäckebol clay.

Secondary strain rates have been evaluated according to Šuklje (1957) and are plotted in Figs. 48a and b.

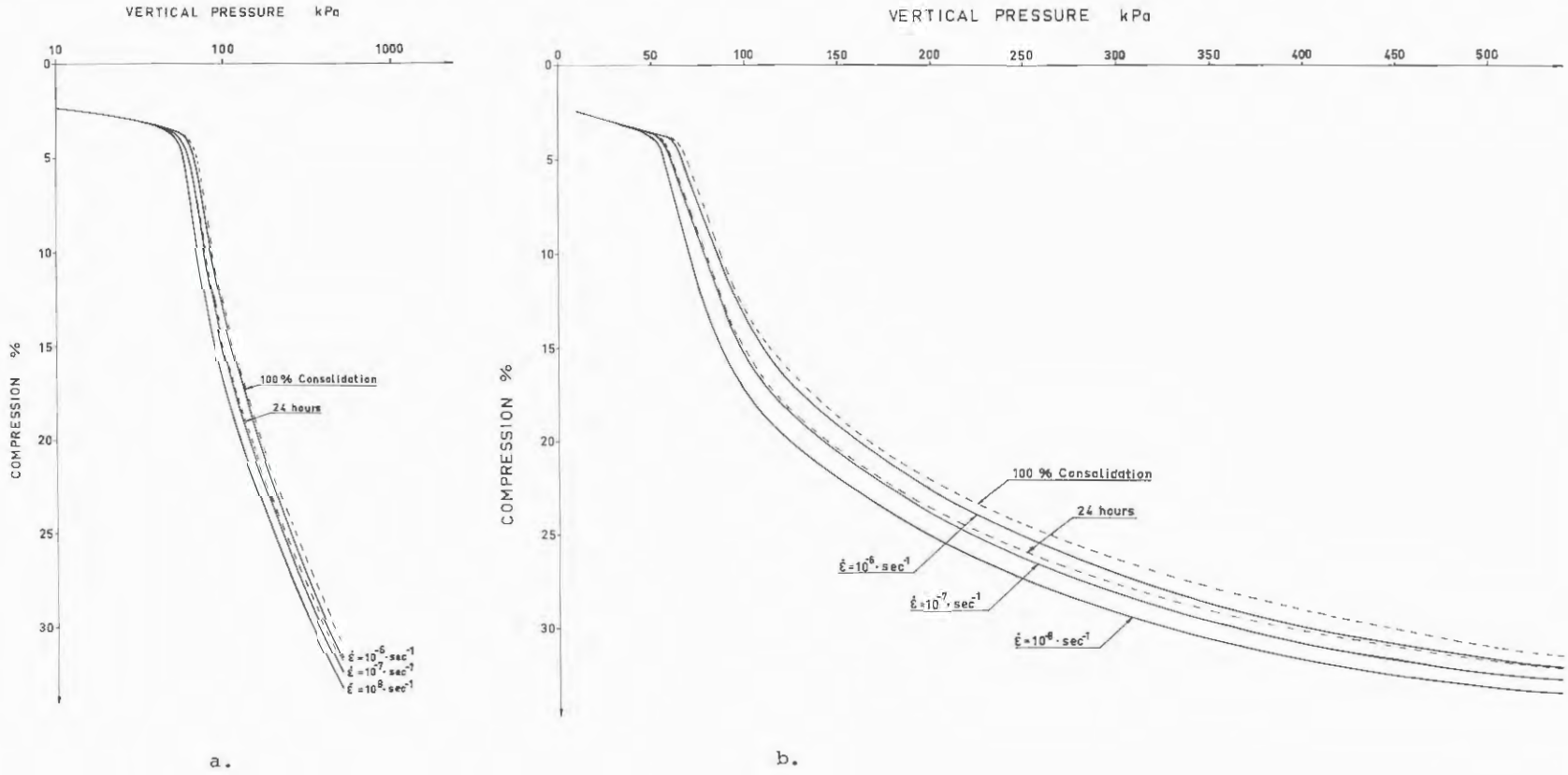

Fig. 48. Secondary strain rate versus vertical pressure and strain. a. vertical pressure in log scale and b. vertical pressure in linear scale.

In Fig. 48 can be seen that the curves for equal strain rate resemble the virgin compression line although they are not quite parallel to it. Neither are the curves for equal strain rate quite parallel to each other. The most pronounced deviation from parallelity is where the curves converge near the preconsolidation pressure. This implies that the preconsolidation pressure is not merely a time effect that will "vanish" at an infinitely low loading rate but a physical property although it becomes highly rate-dependent over a certain strain rate.

The curves for equal strain rate also converge at high stresses.

If the coefficient of secondary compression α_s is evaluated for each load step and plotted versus the effective stress a curve as in Figure 49 is obtained. As α_s is not a constant the relation changes rapidly for stresses just below the preconsolidation pressure where α_s increases and for high effective stresses where α_s decreases with time. The shaded areas in the figure show changes that occurred within 24 hours.

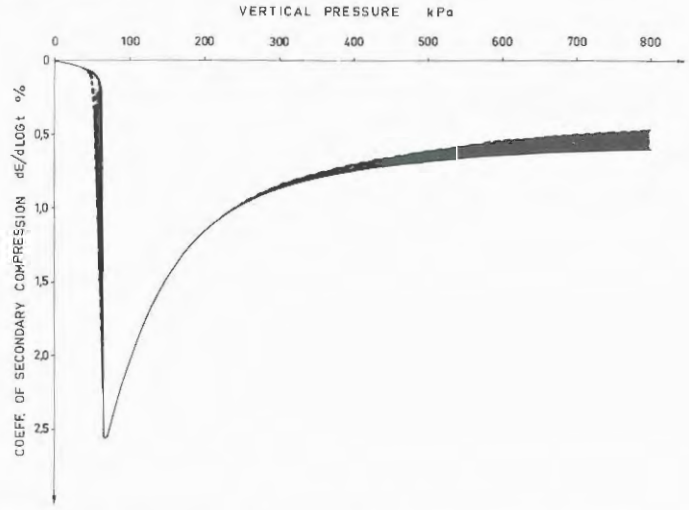

Fig. 49. Coefficient of secondary compression versus vertical pressure.

If the coefficient of secondary compression instead is plotted versus relative compression an almost unique curve is obtained, Fig. 50.

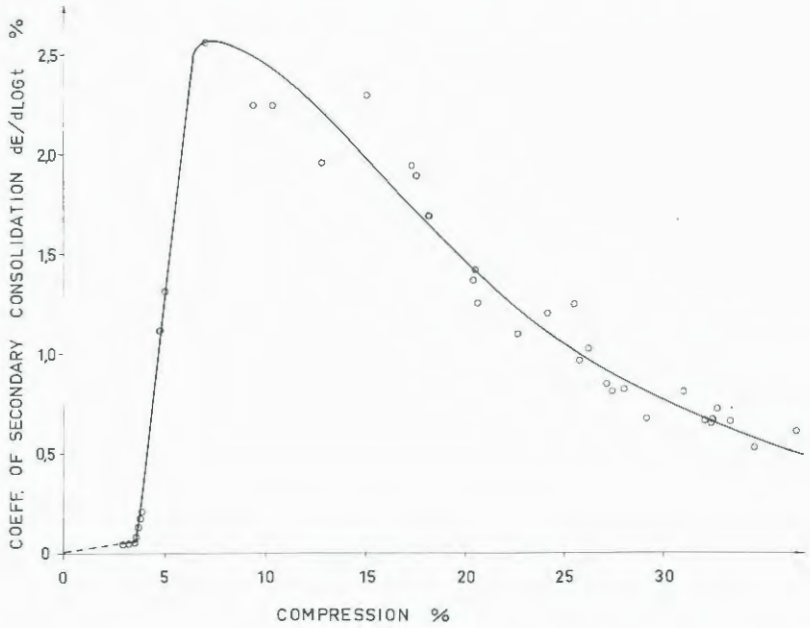

Fig. 50. Coefficient of secondary compression versus relative compression.

The coefficient of secondary compression is very low until a certain compression is reached after which it increases very rapidly up to a maximum value and then slowly decreases with further compression. The critical compression where α_s starts to increase is the same compression as the maximum previous precompression during preloading 3.60%. Other test series run afterwards on other materials give the same result, i.e. the coefficient of secondary compression is low up to the previous precompression and then rapidly increases to a maximum value before decreasing with increasing compression.

The precompression is reached at the load $b \cdot \sigma_c'$. This means that the load $b \cdot \sigma_c'$ can be applied without causing any larger secondary settlement. At higher

loads secondary settlement must be considered. In the SGI laboratory tests the overconsolidation was due to loading and unloading. In the large study of settlement of buildings in Drammen (Bjerrum, 1967) the overconsolidation was attributed to secondary consolidation and ageing. Nevertheless it was concluded that 50% of the difference between σ_o' and σ_c' could be used without causing any larger secondary settlement. In Drammen the overconsolidation ratio was 1.6 and the critical load thus 0.8 σ_c'.

From studies of the time-dependency of the preconsolidation pressure Leonards (1975) stated that preconsolidation seemed to be a predeformation rather than a prestressing and that the change in compressibility occurred at a critical compression. The Swedish investigations on rate effects and secondary compression seem to support this theory.

Mesri (1977) proposed that the relation between the index of secondary compression C_α and the compression index C_c was almost constant. If the results in Figs. 47 and 50 are plotted as C_α versus C_c as in Fig. 51 the relation becomes a loop.

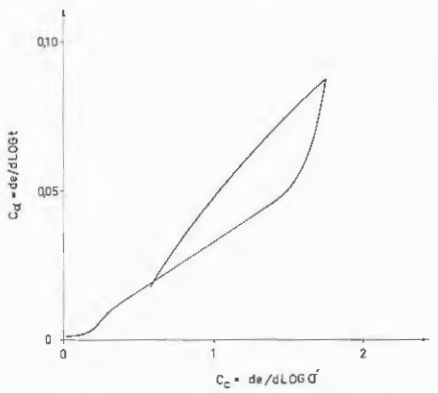

Fig. 51. Index of secondary compression C_α versus compression index C_c.

This curve is typical for relations found in Swedish clays and also the data presented by Mesri showed some variance with stress level. As the influence of secondary compression is greatest at and just above the preconsolidation pressure the maximum coefficient of secondary compression should be the most interesting.

The maximum coefficient of secondary compression $\alpha_{s\ max}$ measured for some Swedish clays is plotted in Fig. 52 together with estimated $\alpha_{s\ max}$ from curves reported by Lo (1963), Crawford (1965) and Bjerrum (1967). The clays (Fornebu clay, Leda clay and Drammen clay) are believed to be of the same type as the Swedish clays.

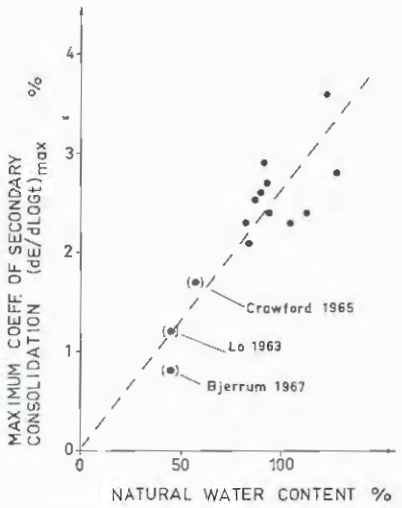

Fig. 52. Maximum coefficient of secondary consolidation versus natural water content.

If the relation from Fig. 52 is drawn in the diagram presented by Mesri (1973) this relation coincides with the maximum reported values of α_s and gives values for the coefficient of secondary compression 2.6 times higher than the average values, Fig. 53.

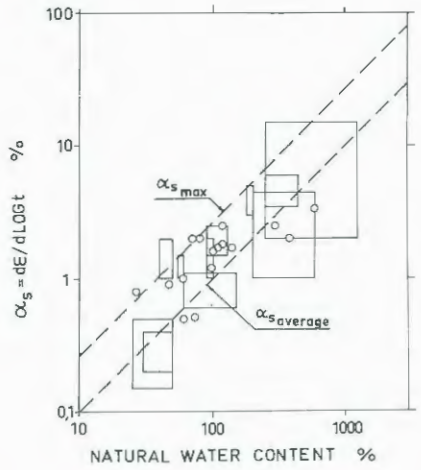

Fig. 53. Comparison between the average and the maximum relation for coefficient of secondary compression against water content (from Mesri (1973) (Fig. 43) with addition of the maximum relation).

In Fig. 54 the maximum coefficient of secondary compression $\alpha_{s\ max}$ is compared to the compression characteristics σ'/M at the corresponding vertical pressure. This is similar to the comparison between C_α and C_c and it can be seen how $\alpha_{s\ max}$ increases relative to σ'/M with increasing natural water content. Further comparsions with data from literature has shown that this is not a unique trend for all clays but may be valid for the types of clay found in Sweden. If consideration is paid to the fact that Drammen clay, as well as normally consolidated Swedish clays with low water content, is rather silty and that Swedish clays with high water contents are usually somewhat organic the relation is in general agreement with Mesri & Godlewski's (1977) findings.

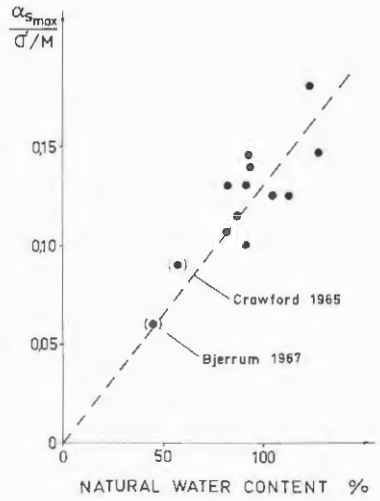

Fig. 54. Relation between the maximum coefficient of secondary consolidation and compression characteristics σ'/M versus natural water content.

Janbu (1970) proposed a new consolidation theory where consideration was paid to the fact that the modulus changes during consolidation. New theories for consolidation of clay taking secondary consolidation and changes in modulus and coefficient of permeability during consolidation into account have been presented e.g. Mesri and Rokhsar (1974), Magnan et al (1979) and Šuklje (1979). Further theories are in development.

Secondary consolidation has considerable influence on pore pressure dissipation, the shape of the time-settlement curve and the "final settlement" in cases where:

1. The final effective stress becomes equal to or just below the preconsolidation pressure.
   $0.80\ \sigma_c' \leq \sigma' \leq \sigma_c'$

2. The final effective stress moderately exceeds the preconsolidation pressure and the value of α_s is high compared to σ'/M.

This conclusion can be drawn from the theoretical studies mentioned and is in agreement with practical field experience.

2. LIMITATIONS OF THE OEDOMETER TEST

The oedometer test is used to determine the compressibility of a soil. The boundary conditions of the test are such that no lateral deformation is allowed. The test corresponds fairly well to engineering cases where an evenly spread vertical load is applied to a large area or the groundwater table is lowered. If the test is examined more closely it is found that in the oedometer test the vertical compression ε_1 for an effective vertical load σ_1' is measured for the special case where there are no lateral deformations. The volumetric strain v is generally given by the equation

$$v = \varepsilon_1 + \varepsilon_2 + \varepsilon_3$$

where ε_1, ε_2 and ε_3 are principal strains and as $\varepsilon_2 = \varepsilon_3 = 0$ in the oedometer

$$v = \varepsilon_1$$

The distortional strains $\bar{\varepsilon}$ are given by

$$\bar{\varepsilon} = \frac{\sqrt{2}}{3} \left[(\varepsilon_1-\varepsilon_2)^2 + (\varepsilon_2-\varepsilon_3)^2 + (\varepsilon_3-\varepsilon_1)^2 \right]^{1/2}$$

which for the oedometer case becomes

$$\bar{\varepsilon} = \frac{2}{3} \varepsilon_1$$

The horizontal stresses are normally not measured and therefore no further evaluation of the test is possible. Research investigations have shown that at effecive vertical stresses well over the preconsolidation pressure the effective horizontal stresses can be

written as $\sigma'_H = K_{onc}\ \sigma'_V$ where K_{onc} is the coefficient of earth pressure in the normally consolidated state.

The mean effective normal stress p is given by

$$p = \frac{1}{3}(\sigma'_1 + \sigma'_2 + \sigma'_3)$$

where σ'_1, σ'_2 and σ'_3 are effective principal stresses and the deviatoric stress q by

$$q = \frac{1}{\sqrt{2}}\left[(\sigma_1-\sigma_2)^2 + (\sigma_2-\sigma_3)^2 + (\sigma_3-\sigma_1)^2\right]^{1/2}$$

which in axisymmetric loading becomes $q = \sigma_1-\sigma_3$.

Thus in the oedometer test the application of the vertical load results in both an increase in mean effective normal stress $\Delta p = \Delta\sigma'_1 \frac{(1+2K_o)}{3}$ and an increase in deviatoric stress $\Delta q = \Delta\sigma'_1(1-K_o)$.

The oedometer test is consequently a combined compression and shear test with the boundary conditions $\sigma'_1 = \sigma'_V$ and $\varepsilon_2 = \varepsilon_3 = 0$ and the results from the tests are directly applicable to cases with these boundary conditions only.

3. INFLUENCE OF DEFORMATION CHARACTERISTICS ON SHEAR STRENGTH. STRESS DILATANCY EQUATIONS.

The drained shear stress which can be mobilized in a granular frictional material depends on the friction between the particles of the material, the stress level in the material and the deformation characteristics of the material. The shear stress is expressed as

$$\tau = \sigma' \tan\phi'$$

in direct shear testing or as

$$\sin\phi' = \frac{\sigma_1' - \sigma_3'}{\sigma_1' + \sigma_3'}$$

in triaxial and plane strain testing according to Mohr-Coulomb.

τ = shear stress
σ' = effective stress normal to the shear plane
σ_1' = effective major principal stress
σ_3' = effective minor principal stress
ϕ' = effective angle of friction

The maximum friction between the particles depends on particle mineral, particle shape and also on whether the material is wet or dry. In clays the friction also depends to some extent on the composition of the pore fluid. (Kenney, 1967)

The deformations can be subdivided into elastic deformations in particles and contact points occurring when the stresses are changed, plastic deformations in terms of rearrangement of the particles as they are displaced in relation to each other and plastic deformations due to crushing of particles. The sum of these deformations determines whether the material will increase or decrease its volume during shear.

The influence of dilatancy (volume increase during shear) has mainly been investigated for relatively dense materials which do increase their volume during shear or where the volume decrease is small. A number of investigators starting with Reynolds 1886 have examined the effect of dilatancy. In soil mechanics the connection between dilatancy and shear strength was observed and demonstrated by A. Casagrande working with Terzaghi and Peck (1948) and by Taylor (1948), Fig. 55.

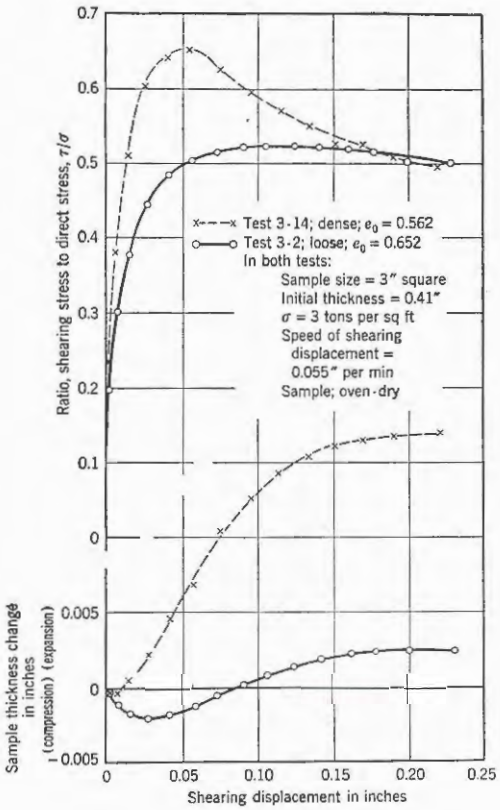

Fig. 55. Plots of direct shear tests on sand in a shear box (from Taylor (1948)).

It was demonstrated that a dense sand had its peak strength (ϕ'_{max}) when the rate of volume increase versus shear strain $dV/d\varepsilon_1$ was at its maximum. ϕ' then gradually decreased until the volume became constant at continued shear $\phi' = \phi_{cv}$. Loose sand has no pronounced peak and a very low rate of volume increase, if any. Very loose sand reaches its maximum ϕ' after very large strains where it becomes equal to ϕ_{cv}.

To separate the shear strength component due to friction from the component due to dilation of the material shear box tests were run on sand by Taylor

(1948) and later by Skempton and Bishop (1950). The work done by increasing the volume δV per unit area against the vertical pressure σ'_N was equated to an equivalent shear stress S_d acting horizontally through a distance $\delta\Delta$ equal to the relative displacements of the halves of the shear box. The residual angle ϕ_r, could thus be calculated from the difference between appliad shear stress S and S_d at maximum shear stress and dilatancy rate $\delta V/\delta\Delta$.

$$tan\ \phi_r = \frac{S-S_d}{\sigma'_N} = tan\ \phi'_{max} - \frac{\delta V}{\delta\Delta}$$

Bishop (1954) introduced a correction for the triaxial compression test in accordance with the same principle where

$$\sigma_1 - \sigma_3 = \frac{dW_f}{d\varepsilon_1} + \sigma'_3 \frac{\dot{v}}{\dot{\varepsilon}_1}$$

where W_f is the work required to overcome friction in the material and $\sigma'_3 \cdot \frac{\dot{v}}{\dot{\varepsilon}_1}$ is the portion of the strength associated with the volume change. $\frac{\dot{v}}{\dot{\varepsilon}_1}$ is the relation between rate of relative volume change and rate of relative axial compression.

Newland and Allely (1957) considered the resultant direction of movement during dilation and proposed the equation for corrected angle of friction ϕ_f

$$\phi'_{max} = \phi_f - \theta$$

where in the shear box

$$tan\ \theta = \frac{\dot{v}}{\dot{\varepsilon}_1}$$

Rowe (1962) and Rowe et al (1964) went into further detail when studying dilatancy. They used ϕ_μ to denote the friction angle obtained at no volume change when an assembly of grains was sheared against a block of the same material and surface roughness.

ϕ_μ is the true angle of friction between mineral surfaces and is smaller than ϕ_f, ϕ_{cv} and ϕ_r.

In addition to the energy to overcome ϕ_μ further energy is required as sliding does not take place with all the particles moving parallel along a plane surface but in a number of directions $(\phi_f - \phi_\mu)$.

Energy is also required as the particles have to climb over each other during dilation before they can fall into the next void $(\phi_r - \phi_f)$.

When the soil dilates the external work is additional to ϕ_r. There is also some stored and recoverable "elastic" energy.

For direct shear tests Rowe et al (1964) give the equations

$$\phi_f = \phi' + \theta$$

corresponding to Newland and Allely (1957) and

$$\tan \phi_r = \frac{\tau}{\sigma'_N} + \frac{dv}{d\gamma}$$

where

τ = horizontal shear stress
σ'_N = vertical effective stress
γ = shear strain.

For triaxial and plane strain tests

in compression

$$\tan^2(45^0+\phi_f/2) = \frac{\sigma_1'}{\sigma_3'(1-dv/d\varepsilon_a)}$$

and extension

$$\tan^2(45^0+\phi_f/2) = \frac{\sigma_1'(1-dv/d\varepsilon_a)}{\sigma_3'}$$

where ε_a is the axial strain.

For triaxial compression the formula

$$\sin\phi_r = \frac{\frac{\sigma_1'}{\sigma_3'} - (1 - \frac{dv}{d\varepsilon_1})}{\frac{\sigma_1'}{\sigma_3'} + (1 + \frac{dv}{d\varepsilon_1})} = \frac{\sigma_1' - \sigma_3'(1 - \frac{dv}{d\varepsilon_1})}{\sigma_1' + \sigma_3'(1 + \frac{dv}{d\varepsilon_1})}$$

is given. Here all strains are considered as non-recoverable slip strains.

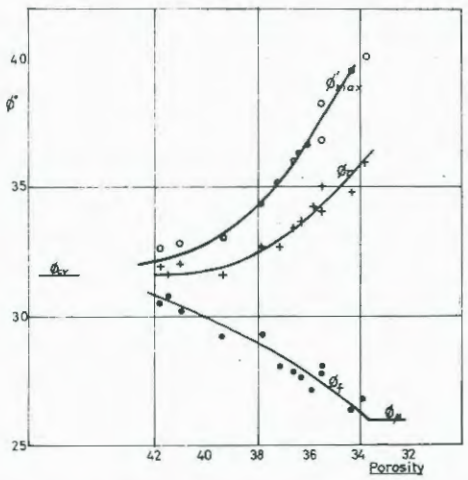

Fig. 56. Variation of ϕ'_{max}, ϕ_f and ϕ_r with porosity (from Rowe et al. (1964)).

Fig. 56 shows how ϕ'_{max}, ϕ_r and ϕ_f vary with porosity. When the porosity is high the dilatancy is small and ϕ'_{max}, ϕ_r and ϕ_f are all very close to ϕ_{cv}. As the porosity decreases dilatancy increases and ϕ'_{max} increases. In a dense material the particles are forced to climb over rather than roll around each other so that ϕ_r increases and ϕ_f decreases.

Rowe (1969) shows differences between different types of tests where ϕ_{cv} for plane strain tests is higher than ϕ_{cv} for direct shear tests. For a material with $\phi_{cv} \approx 30^0$ the difference would be about 3^0-4^0. Test results for triaxial compression tests vary between the two values. For loose materials where $\phi'_{max} \approx \phi_{cv}$ the results from triaxial and plane strain tests are equal but for dense materials the triaxial tests give values close to those from direct shear tests. Skinner (1969) presents data showing that ϕ_μ is not directly related to ϕ'_{max} and ϕ_{cv}. Particle shape seems to have the greatest influence on the behaviour of granular materials.

Studies of dilatancy have mostly aimed at describing and explaining variations in friction angles with density and dilatancy. In most studies ϕ'_{max} has been studied and the strength components ϕ_r or ϕ_f evaluated and possibly compared with ϕ_{cv}.

The studies have been performed on sands, silts and on steel balls, glass balls etc, apart from soils. These materials have all been close to or denser than critical density. The evaluations of dilatancy effects have thus been made on materials which increase their volume during shear. No similar study seems to have been made on materials similar to soft clays which decrease their volume as they consolidate for the stress increase during shear.

In the direct shear tests performed at SGI the angle $\phi_p = \phi' + \theta$ where $\theta = arctan \frac{dv}{d\gamma}$ has been evaluated continuously during the shear tests for the last five years. Later all drained triaxial tests were also evaluated in a similar manner (Larsson, 1977). For triaxial tests with symmetrical deformations in the two horizontal planes

$$\theta = arctan \frac{dv \ tan\beta}{\frac{2d\varepsilon_1}{cos^2\beta} - dv}$$

where $\beta = 45^0 + \phi_p/2$

The aim of this study has been to find a simple "flow rule" for prediction of stresses and strains rather than a correct physical explanation for the relation between shear strength and dilatancy.

A "flow rule" determines the relation between plastic volumetric strains and plastic shear strains.

These studies have shown that with a very good approximation these energy separations are good "flow rules".

In all tests small shear strains are required to mobilize the friction. These strains are essentially elastic and in tests with increasing stresses they are associated with a volume decrease. Once the particles have started to slide in relation to each other stresses and strains are adjusted according to boundary conditions and the flow rule $\phi_p = \phi' + \theta$, Fig. 57. Clay samples do not usually increase their volume but most are so compressible that an ultimate state is not reached during the test. In engineering practice the ultimate drained shear strength is not a design parameter for these clays but the question is rather what strength can be mobilized within a permissible deformation. For stiffer materials ϕ_p can be an important parameter when progressive failure is considered.

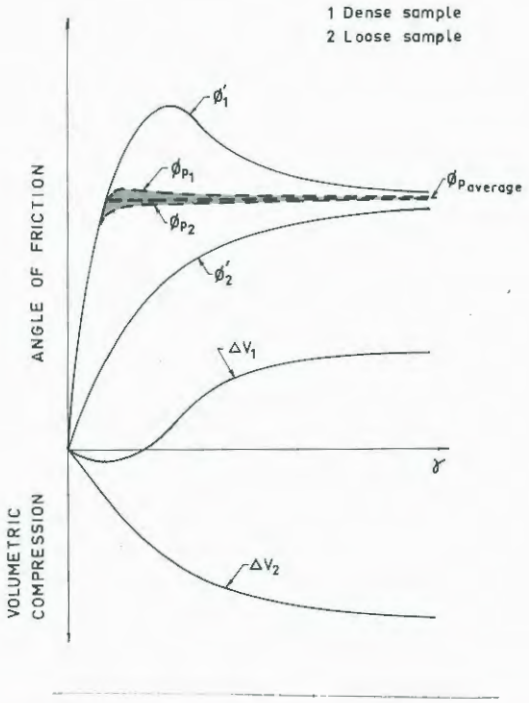

Fig. 57. Variation of ϕ', ϕ_p and volume change during direct shear. Type curves.

4. CRITICAL STATE THEORY

An advanced model for general behaviour of soils linking deformation characteristics and friction angle at constant volume into stress-strain relations was built up by the Cambridge group under Professor Roscoe. The complete model was presented by Scofield and Wroth (1968). The model differentiates between coarser granular materials (Granta gravel model) and clays (Cam clay model) owing to their different deformation characteristics. The Cam clay model has later been somewhat modified (Roscoe and Burland, 1968). The Cam clay model assumes that clay is an ideal elastic/plastic material without anisotropy. If continuously distorted until it flows at constant volume the clay will then have entered its critical

state. In the critical state the deviatoric stress q is a direct function of the mean normal stress p, $q = M \cdot p$. M is calculated from the friction angle at constant volume ϕ_{cv}. The void ratio of the material in critical state is a linear function of the logarithm for p.

The range of stresses for which the material will behave elastically is determined by the yield curve. In the modified Cam clay model the yield curve has the equation $q^2 + M^2 \cdot p^2 = M^2 \cdot p \cdot p_c$ where p_c is the equivalent isotropic consolidation pressure, Fig. 58.

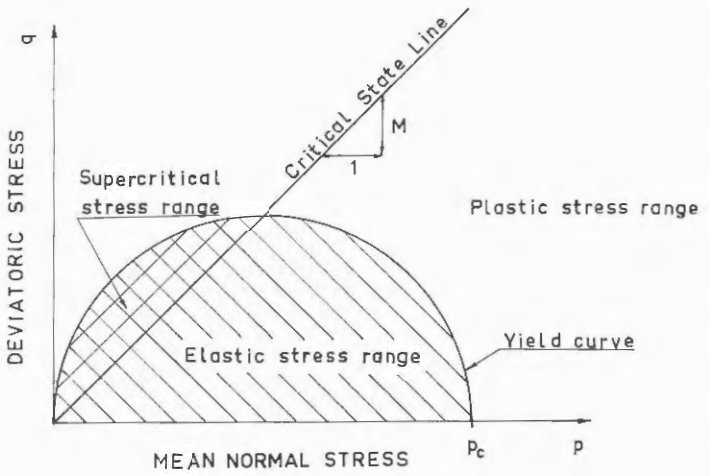

Fig. 58. Stress states in Critical State Theory.

The part of the elastic stress range where the deviatoric stresses are higher than the critical state is called the supercritical stress range. In this stress range the material is strain-softening at yield. In the plastic stress range with deviatoric stresses below the critical state the material is strain-hardening.

When the stresses in the material reach the yield curve the material flows and the deformations become

plastic. The flow rule states that the direction of the strain vector created by plastic distortional strain $\bar{\varepsilon}_p$ and plastic volumetric strain v_p is normal to the yield curve, Fig. 59.

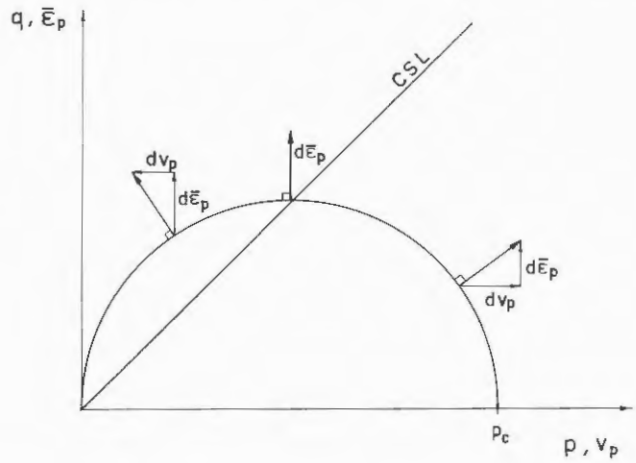

Fig. 59. Plastic flow in the modified Cam clay model.

If the yield curve is reached in the supercritical range dv_p becomes negative. This means that the volume increases and the material becomes looser. At the critical state line the material flows at constant volume and at stresses below the critical state line the material decreases its volume and becomes denser.

The volumetric strains are governed by the mean effective normal stress p. When the isotropic pre-consolidation pressure is changed the void ratio changes according to the virgin isotropic consolidation line, Fig. 60.

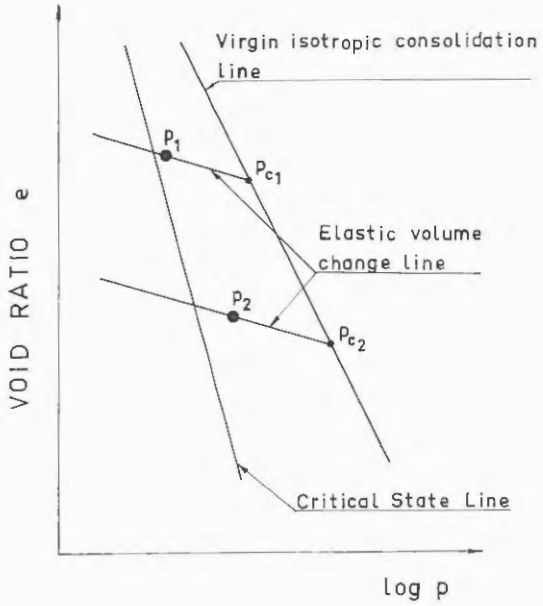

Fig. 60. Void ratio change at stress increase from p_1 to p_2 according to Critical State Theory.

If p is lower than p_c the relation for the void ratio e versus p will be on the line for elastic volume changes during loading and unloading. This line is moved parallel up or down depending on the value for p_c.

The use of the theory to predict stress-strain relations is exemplified for two triaxial tests.

Example A:

A material has been consolidated for the equivalent isotropic preconsolidation pressure p_c. The stresses at starting point D are $q = 0$ and $p = p_c/4$. The test is performed at constant p, Fig. 61.

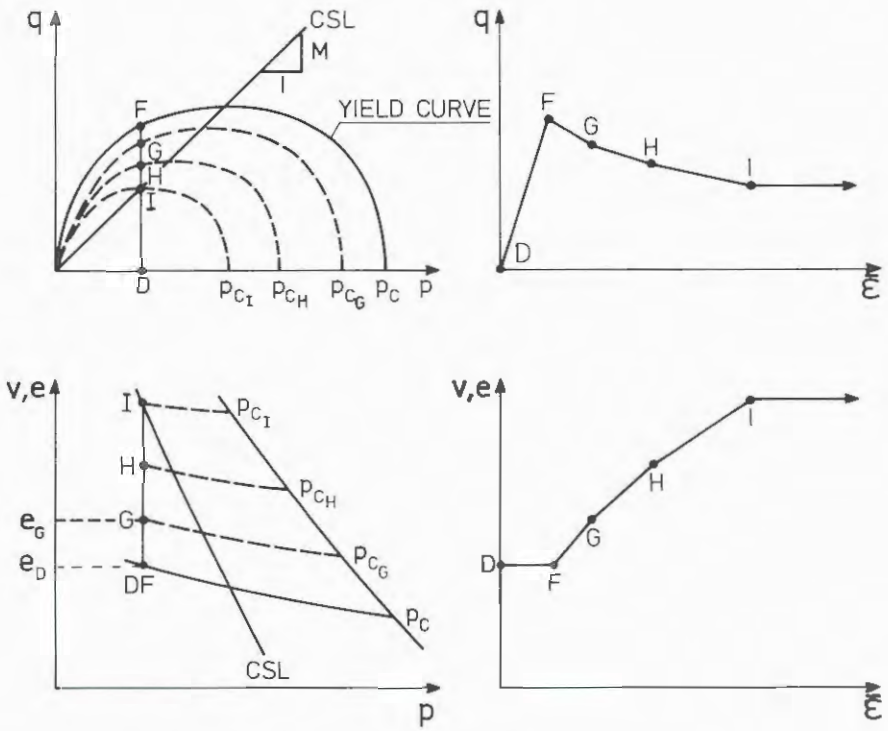

Fig. 61. Predictions of strains according to Critical State Theory. Example A.

Strains are predicted as follows:

The material remains elastic until the stresses reach point *F* which is on the yield curve.

The shear strain $d\bar{\varepsilon}$ becomes $\Delta q_{(D-F)}/3G$ *(for* $\nu = 0.5$*)* and $\Delta e_{(D-F)} = 0$.

At point *F* the material flows and as it is in the supercritical state the void ratio increases and the deviatoric stress decreases until point *I* on the critical state line is reached.

For calculation of the strains during this process points *G* and *H* between *I* and *F* are selected.

At point G the material has increased its void ratio to e_G and the equivalent isotropic consolidation pressure is decreased to p_{eG}.

Using p_{eG} a new yield curve passing through point G is constructed.

The volumetric strain v is obtained from $\frac{\Delta e_{(F-G)}}{1+e_D}$ and $\Delta\bar{\varepsilon}_{p(F-G)}$ is calculated from the normality rule for plastic flow (strain vector normal to the yield curve at point F). $\Delta\bar{\varepsilon}_{(F-G)}$ then becomes $\Delta\bar{\varepsilon}_{p(F-G)}$ minus the elastic deformation $\Delta q_{(F-G)}/3G$ due to the decrease in deviatoric stress between F and G.

In the same way the strains between G and H are calculated followed by the strains between H and I.

At point I the critical state is reached and the material continues to flow at constant volume.

Example B:

A material has been consolidated for the equivalent isotropic consolidation pressure p_e. The stresses are as at point D in Fig. 62 and a conventional triaxial compression test is performed with $\sigma_2' = \sigma_3' = constant$.

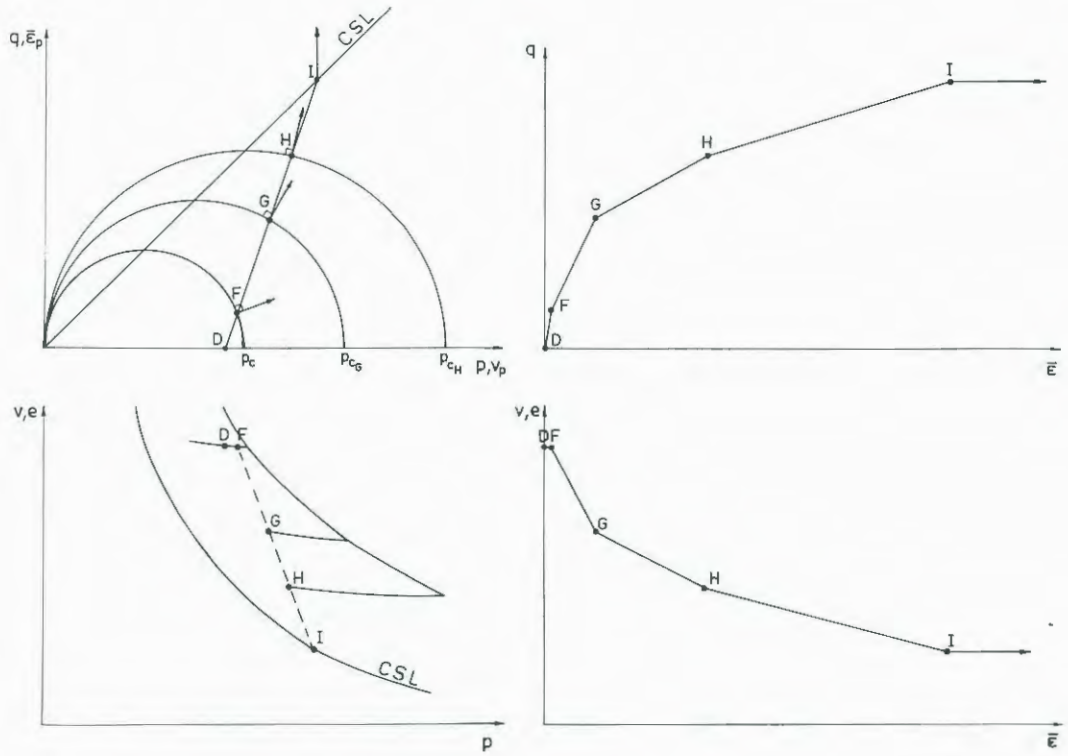

Fig. 62. Prediction of strains according to Critical State Theory. Example B.

The material remains elastic until point F on the yield curve is reached.

The elastic volume change $v_{(D-F)}$ is calculated from the curve for elastic deformations. The distortional strain $\bar{\varepsilon}_{(D-F)}$ becomes $\Delta q_{(D-F)}/3G$.

At point F the material flows and the volume will decrease until point I on the critical state line is reached.

For prediction of the strains during this process points G and H are selected.

At point G the material has reached a new equivalent isotropic preconsolidation pressure p_{eG}. The void

ratio at point G is found on the curve for elastic volume changes for p_{eG} and the volumetric strain is calculated. The distortional strain $\bar{\varepsilon}_{(F-G)}$ is the sum of the plastic distortional strain $\bar{\varepsilon}_{p(F-G)}$ calculated from the flow rule at point F and the elastic distortional strain $\bar{\varepsilon}_{e(F-G)} = \Delta q_{(F-G)}/3G_{(F-G)}$.

In the same way the strains from G to H and from H to I are calculated.

At point I the critical state is reached and the material continues to flow at constant volume.

5. LIMITATIONS OF THE CRITICAL STATE THEORY

As has been shown the critical state theory models soil behaviour taking into account compressibility, effect of preconsolidation, swelling and recompression, dilatancy and friction angle at constant volume. The predicted stress-strain relations resemble those actually measured and the model can be considered a very good tool for the general understanding of soil behaviour.

However, later research at Cambridge (Wroth & Wood, 1975) and elsewhere has shown that the model heavily overpredicts dilatancy for clays in the supercritical stress range.

The failure criterion $q = M \cdot p$ is similar to extended von Mises criteria (Bishop, 1971) but the Mohr-Coulomb criterion is generally accepted as a failure criterion for clays. The difference becomes great when the intermediate principal stress increases. The model assumes isotropic soil while almost all natural clays are anisotropic.

The yield surface has the same shape independent of the combination of isotropic and deviatoric stresses which caused the preconsolidation effect.

These limitations seriously reduce the practical usefulness of the model.

6. YIELDING AND FLOW IN NATURAL CLAYS

In 1975 two reports were presented concerning yield stresses for plastic Drammen clay in Norway. Berre (1975) presented results from drained triaxial tests along different stress paths and the stresses for which yield occurred. Ramanatha Iyer (1975) reported drained triaxial tests on the same material but at very low effective stresses. These later tests were performed with stresses in the supercritical range so that yield and failure coincide. The yield stresses for Drammen clay are plotted in Fig. 63.

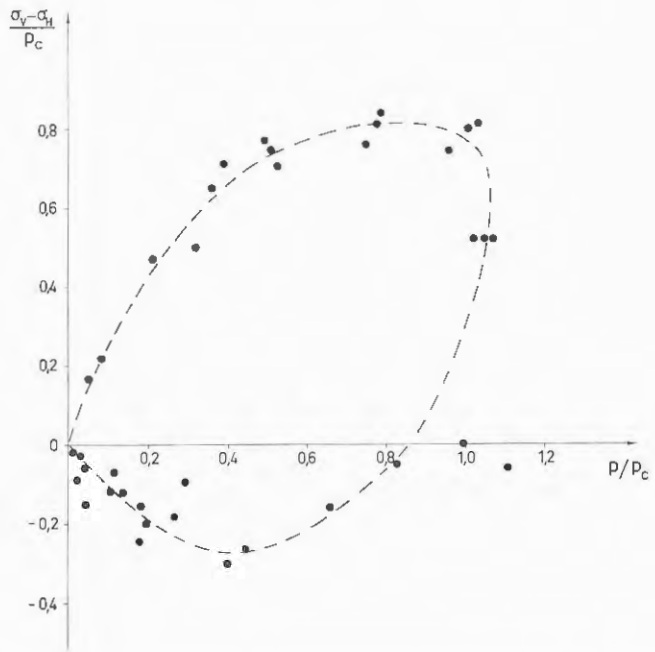

Fig. 63. Yield stresses in Drammen clay (from Berre (1975) and Ramanatha Iyer (1975)).

Unfortunately there is no standardized definition for yield. Berre has pointed out difficulties as some

tests have a distinct breaking point between elastic and plastic behaviour while the transition is more gradual for other tests.

The tests on Drammen clay show that the supercritical stress range is very small and that it is doubtful whether dilatancy can be used as an additional strength parameter for this clay. The yield surface is clearly anisotropic and Mohr-Coulomb's failure criterion seems to apply.

A Canadian Champlain sea clay from Ottawa was thoroughly investigated by Wong & Mitchell (1975), Fig. 64.

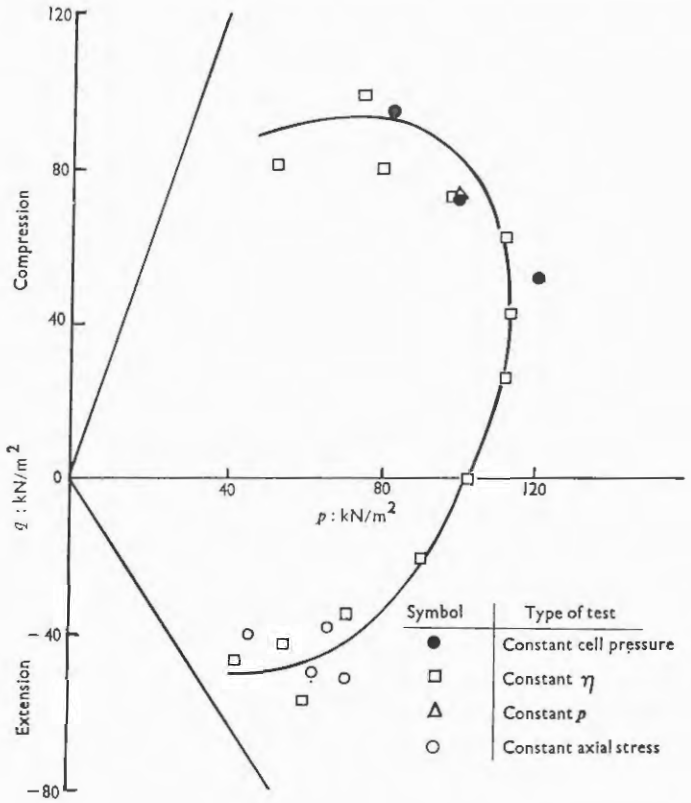

Fig. 64. Yield stresses for Ottawa clay (from Wong & Mitchell (1975)).

They also found that the yield surface was anisotropic. The Mohr-Coulomb failure criterion seemed to be the criterion most in agreement with the failure stresses. In this investigation the plastic flow was also studied, Fig. 65.

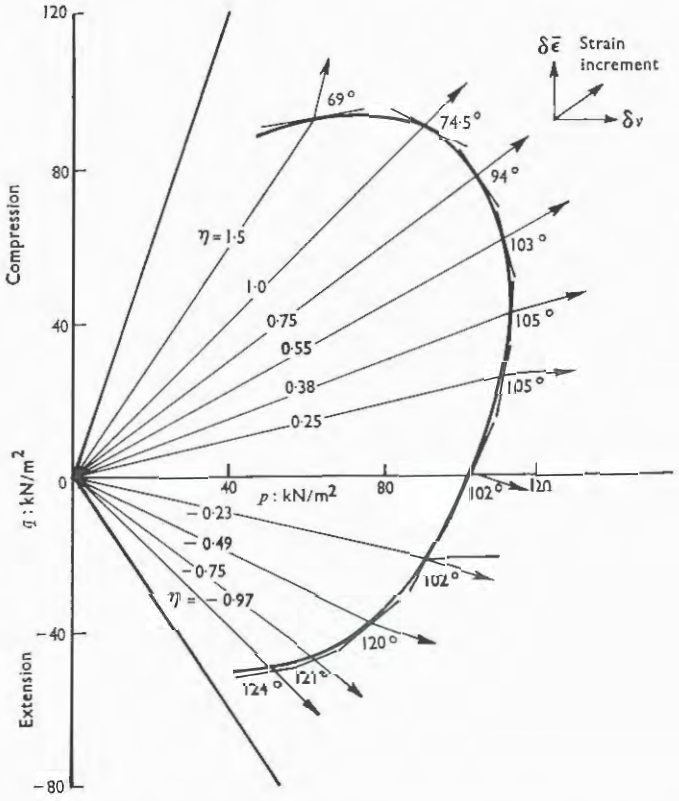

Fig. 65. Plastic flow in Ottawa clay compared to the normality rule (from Wong & Mitchell (1975)).

It was found that the normality rule was not applicable for this material and yield surface. Another result that neither dilatancy equations nor critical state theory accounts for is that shear deformations occur when the soil yields for an isotropic stress condition.

Tavenas & Leroueil (1977, 1979) have studied yield curves for clays from Quebec in triaxial compression testing. They suggested that the yield curve could be described as an ellipse centered around the K_{onc}-line, Fig. 66.

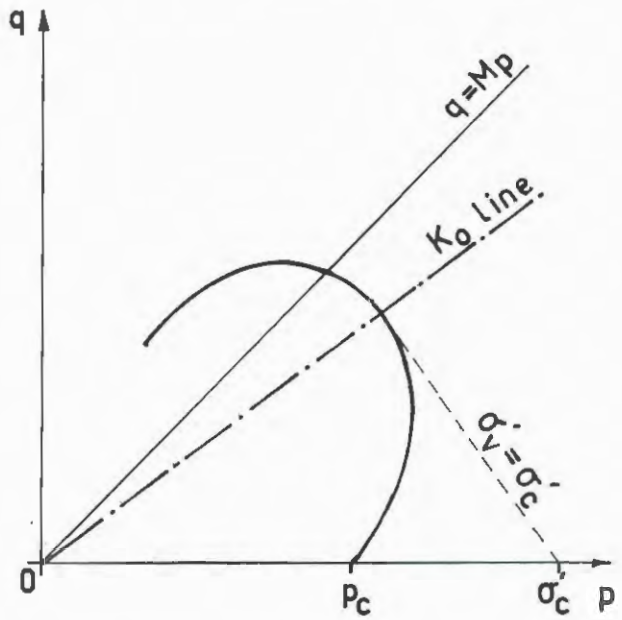

Fig. 66. Yield curve according to Leroueil & Tavenas (1981).

The top of the ellipse coincides with the line for vertical effective pressure equal to the vertical preconsolidation pressure.

At SGI Swedish clays were investigated for determination of the yield surface. A model where the yield surface was determined by the Mohr-Coulomb failure criterion and the preconsolidation pressure in the vertical and horizontal directions was presented (Larsson, 1977).

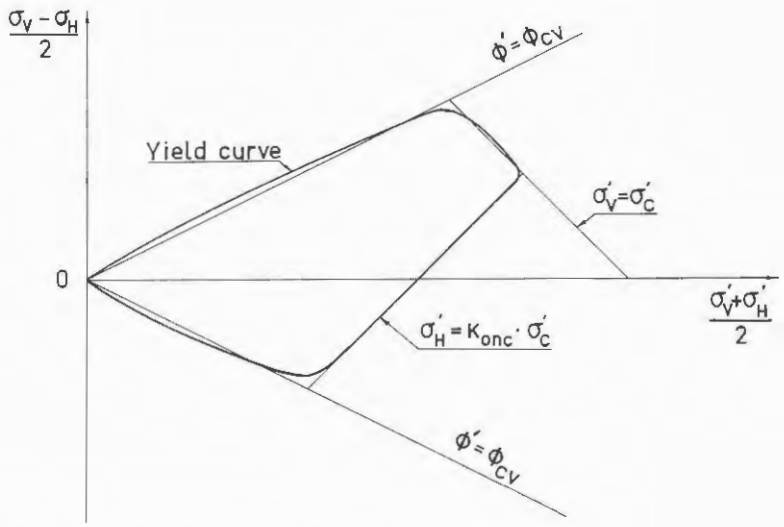

Fig. 67. Yield surface in the SGI model.

Fig. 67 is valid for cases where the vertical and horizontal stresses are principal stresses. This is the case in most triaxial and plane strain testing. The model yield surface in Fig. 67 consists of four straight lines with sharp corners. The real yield surface is somewhat rounded but corresponds essentially to the simple model. The model has later been compared to results from a number of clays and has consistently given compatible results (Larsson & Sällfors, 1981). A prediction on how the yield surface changes with stress rotation has also been made.

In Fig. 67 the q-p diagram has been abandoned as it is not suited for this yield criterion.

Studies on plastic flow by Lewin (1972, 1973) have shown that for clays which have been anisotropically consolidated and unloaded the normality rule is not applicable and the plastic flow is greatly dependent on the stress history. They also show that when a clay has been consolidated for an anisotropic stress condition shear deformations occur when the soil yields for an isotropic stress state.

Test results from triaxial compression tests on St Alban clay from Quebec confirm the results from Ottawa clay (Faveau-Brucy, 1977).

7. DRAINED TESTS ON BÄCKEBOL CLAY

7.1 Scope of the study

A comprehensive study has been carried out at SGI to investigate the yield surface and flow rules more closely and to compare and link the results from different tests. The study comprises the previously mentioned oedometer tests and triaxial tests, plane strain tests and direct shear tests. The bulk of the tests have been performed on Bäckebol clay. Test results from the Institute's consulting projects have been examined to check the general validity of the results on Bäckebol clay.

7.2 Bäckebol clay

The Bäckebol test field is situated in the Göta river valley on the western side of the river about 10 km north of Gothenburg. The ground surface is very flat in this area and the distance from the test field to the river is about 200 m. The area has been extensively investigated by the Geotechnical Department at Chalmers University and SGI and a number of research projects have been carried out here e.g. Fellenius (1971), Torstensson (1973), Sällfors (1975), Larsson (1975).

The geology and the geotechnical properties of the test area used by Chalmers University where the samples for the present study were taken has been described by Torstensson (1973), Sällfors (1975) and Larsson (1975). A brief summary is given here.

The clay is a marine clay. The ground surface has an elevation of 5 m in reference to the river and the

clay deposit is some 40 m deep. The groundwater level varies a little with season but is about 0.5 m below the ground surface. The uppermost metre consists of a dry crust followed by a grey clay with some shells. Down to 3 m root threads may occur. The organic content is less than 1%. The clay content ranges from 55 to 75%, Fig. 68. At the levels of particular interest, 3-6 m depth, it is 55 to 60%. Particles 2-20 µm in size amount to 35-40% and particles >20 µm to 5%. The clay is a Quaternary post-glacial sedimentary clay with illite as the predominant clay mineral. Silt particles are mainly quartz and feldspars (Pusch, 1973).

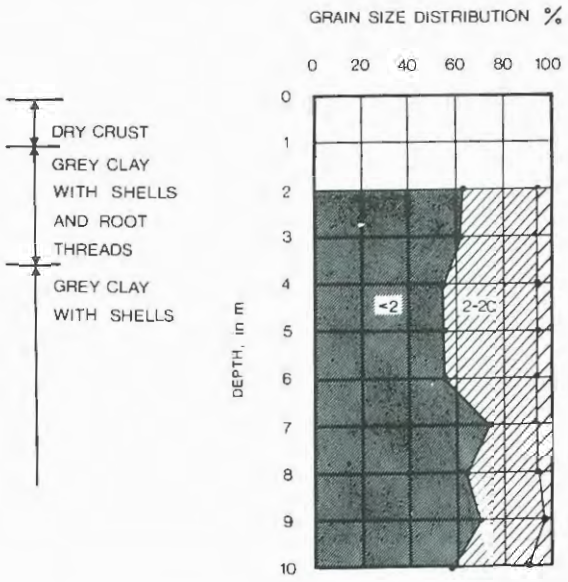

Fig. 68. Particle size distribution in Bäckebol clay. The figures in the graph indicate particle sizes in µm (from Sällfors (1975)).

Water contents and Atterberg limits together with density are shown in Fig. 69.

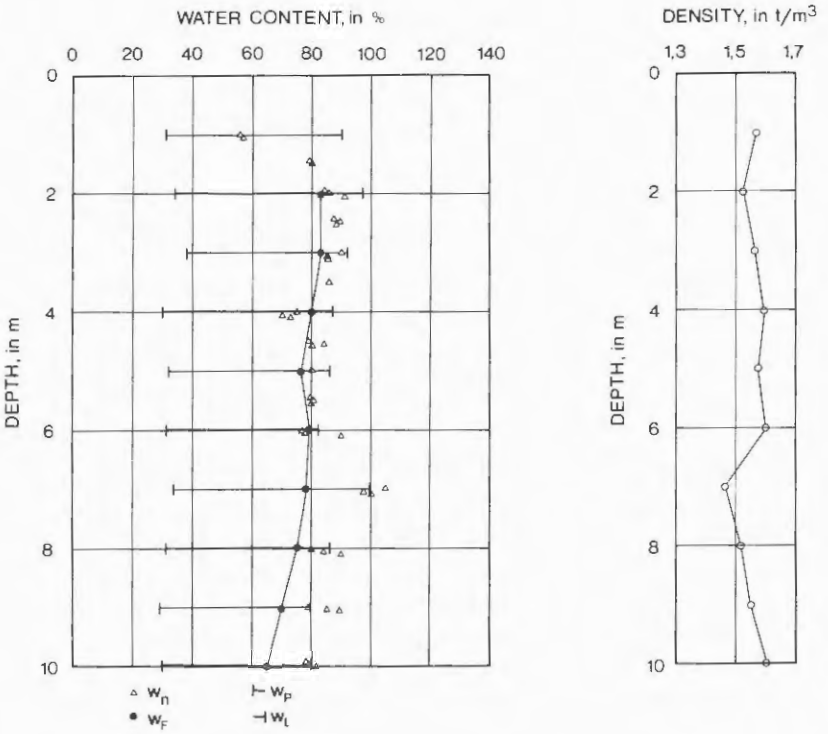

Fig. 69. Water contents and density for Bäckebol clay down to 10 m below ground surface.

The natural water content is almost equal to the liquid limit. At levels between 3 and 6 m they are 80-90% and the plasticity index is about 55%. From about 7 m depth the character of the clay differs slightly from the upper clay.

The undrained shear strengths and rate effects of this clay have been extensively investigated (Torstensson, 1973, Larsson, 1975). Vane tests and undrained triaxial compression tests and, more recently, undrained plane strain compression tests all show that at a standard testing rate a fairly constant mean value of 17 kPa for the strength between 2 and 7 m depth is obtained, Fig. 70.

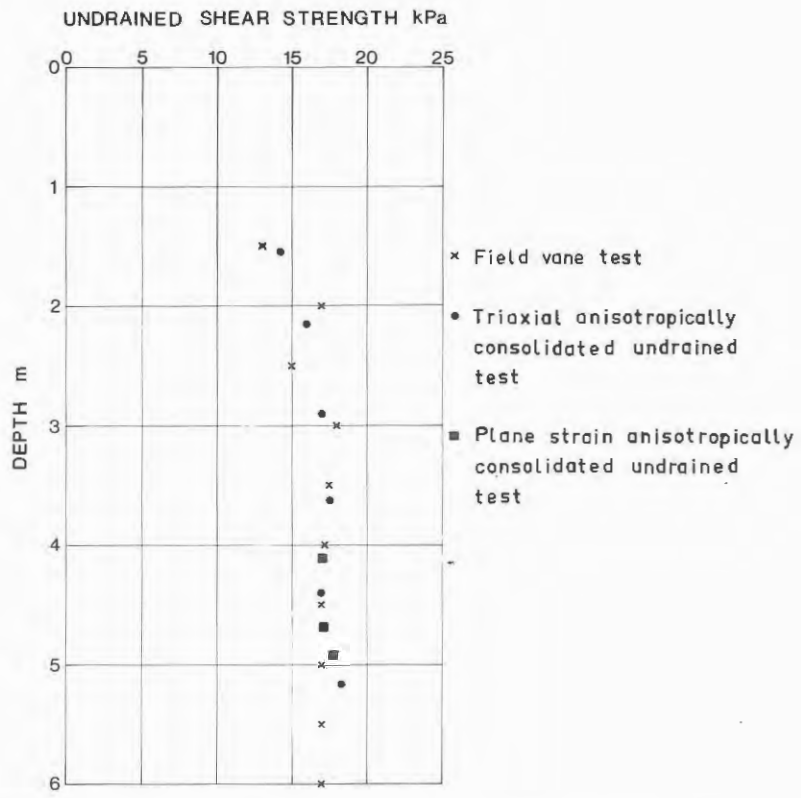

Fig. 70. Undrained shear strength in Bäckebol clay.

At about 7 m the undrained shear strength starts to increase with depth. The sensitivity of the upper clay is about 17.

The preconsolidation pressure has been investigated in the laboratory and in full-scale field tests (Sällfors, 1975), Fig. 71.

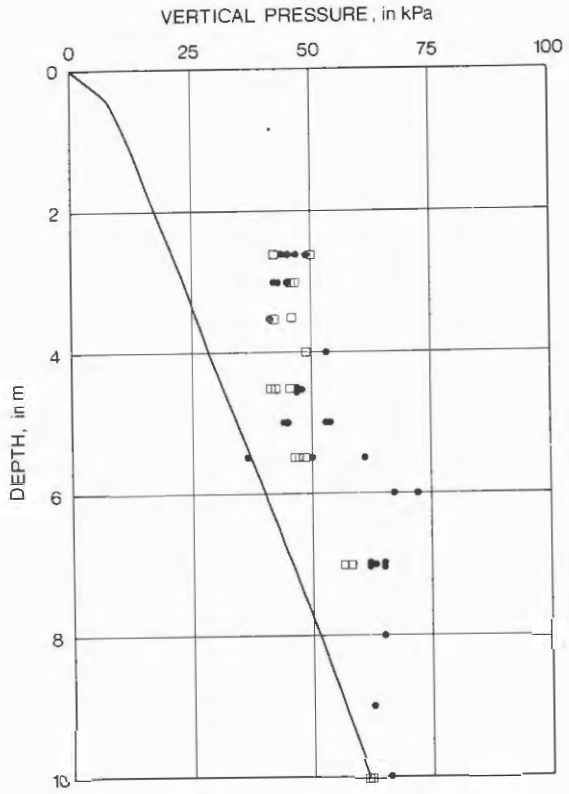

Fig. 71. Preconsolidation pressure in Bäckebol clay (from Sällfors (1975)).

• σ_c' determined from CRS-tests; □ σ_c' determined from full-scale field tests.

Solid curve: in situ vertical effective stress.

The investigation shows that the preconsolidation pressure is almost constant at 48 kPa in the upper clay down to about 6 m depth and then starts to increase.

The in situ effective horizontal stress has also been measured in a number of ways and a K_{onc} of about 0.7 was found (Larsson, 1975), Fig. 72. At depths between 4-6 m K_{onc} was found to be between 0.65 and 0.7.

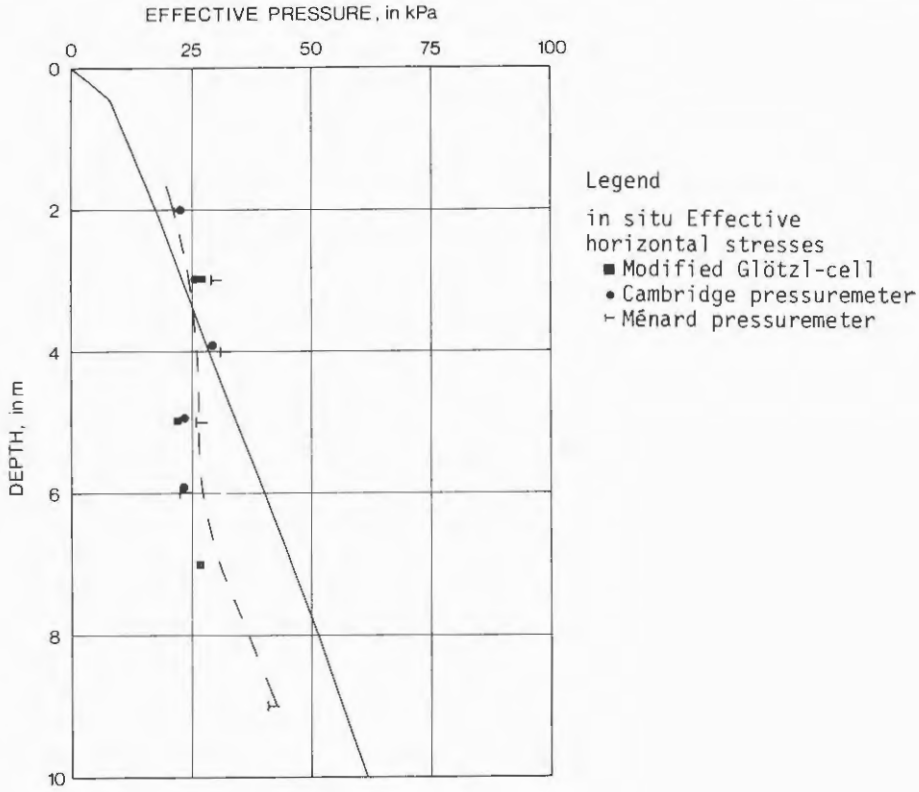

Fig. 72. Distribution of in situ effective stresses in Bäckebol clay. Solid curve: effective vertical pressure, broken curve: calculated horizontal pressure using $K_{onc} = 0.7$.

7.3 Test apparatus

7.3.1 Direct shear apparatus

In Sweden shear strength is often determined by direct shear tests in the SGI apparatus. The apparatus is a modified SGI oedometer with facilities for shearing the soil sample after consolidation. The sample has a diameter of 50 mm and the sample height after consolidation should be between 10 and 20 mm. Depending on the compression during consolidation the sample is consolidated in slightly different ways. The sample is placed on a fixed pedestal ϕ50 mm which has a filter stone on top and an internal drainage channel.

A top part which at this stage is fixed so that it can only move vertically is lowered onto the sample. This part also has a diameter of 50 mm, a filter stone and drainage channel. If the compression during consolidation is expected to be small the sample is surrounded by a rubber membrane. Thin metal rings are fitted outside the rubber membrane to keep the sample diameter constant during the test. There are small vertical clearances between the rings to prevent transmission of vertical forces by the rings. The rubber membrane is sealed against the pedestal and top part by clamps and drainage is provided by the filter stones and the drainage channels.

If the compression during consolidation is expected to be large the sample first has to be consolidated inside a confining ring where most of the compression is allowed to take place. The confining ring is then replaced by the rubber membrane and the metal rings before the final load is applied. This operation is carried out with the samples in place in the shear apparatus.

The apparatus is shown in Fig. 73.

The test is performed by first applying the vertical load to the sample and allowing it to consolidate.

After the consolidation the sample is sheared.

The bolts fixing the top part are removed and the ball bearing which transmits the vertical load allows the top part to move horizontally with a tolerable amount of friction. In shearing the top part is moved horizontally at a constant speed while the bottom pedestal is fixed. The sample thereby undergoes a fairly uniform angular distortion. During the test the horizontal shear stress, the horizontal displacement of the top part and the height of the sample are measured by

electronic transducers and automatically recorded. The vertical stress remains constant. Consolidation is usually allowed for 24 hours and the rate of shear is such that an angular distortion of the sample of 0.15 radians is obtained in another 24 hours.

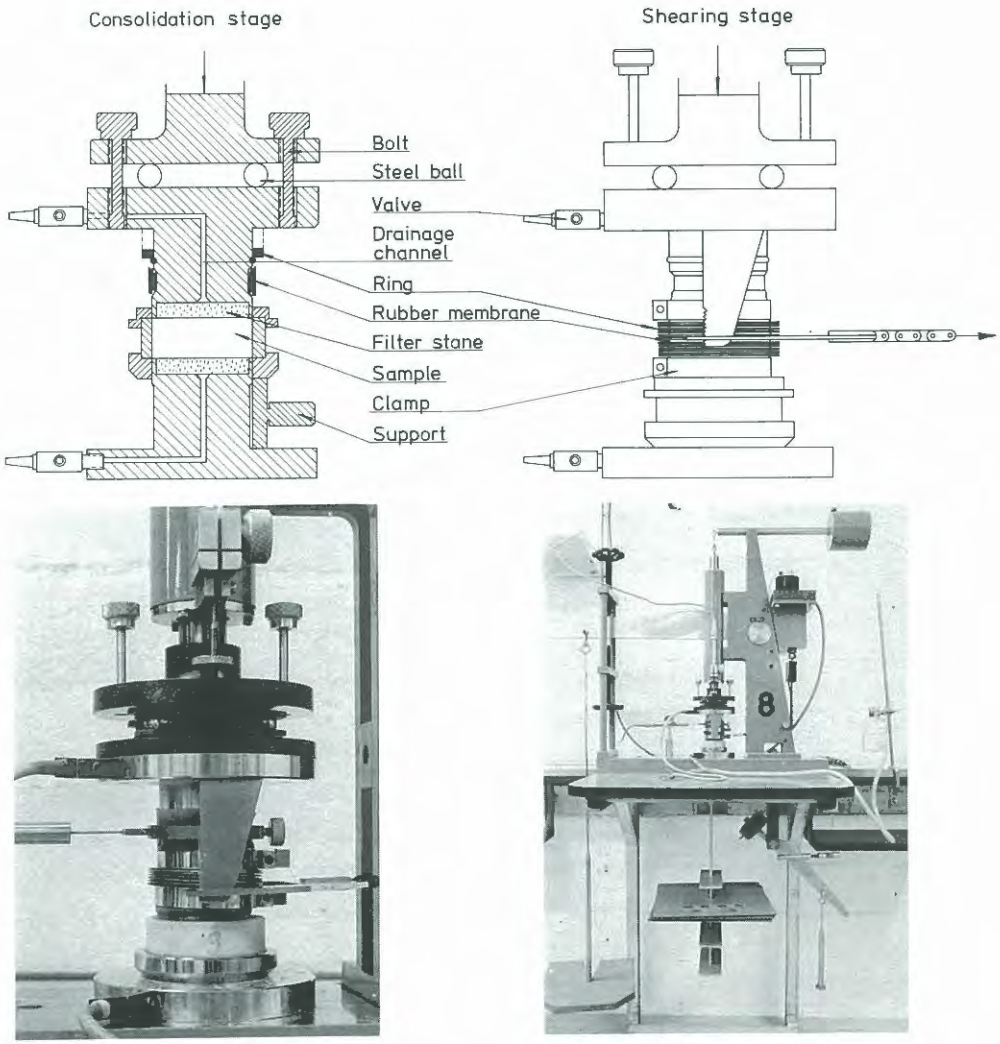

Fig. 73. The SGI shear apparatus.

7.3.2 Triaxial apparatus

Triaxial tests and apparatus are thoroughly described elsewhere e.g. Bishop and Henkel (1962), Andresen & Simons (1960), Berre (1979). Therefore only a brief description of some special equipment used at SGI will be described.

The triaxial cells differ somewhat depending on the type of test for which they are used.

The following types of tests were performed in the present study:

1. Compression tests with constant cell pressure
2. Extension tests with constant cell pressure
3. Compression tests with "constant" vertical stress and decreasing cell pressure
4. Extension tests with "constant" vertical stress and increasing cell pressure
5. Stepwise compression tests with constant vertical stress and decreasing cell pressure.

All the tests were performed on samples with a height of 100 mm and a diameter of 50 mm.

There is now advanced computer-regulated triaxial equipment which can perform all these tests but in this case the tests were performed with relatively simple equipment already on hand at SGI.

Compression and extension tests with constant cell pressure were performed in a modified Geonor triaxial apparatus of an older model. The modification consists of replacing the old pressure system with air pressure regulators and replacing the old measuring system with electronic transducers. The load cell measuring deviatoric stress is placed inside the cell to avoid friction errors, Fig. 74.

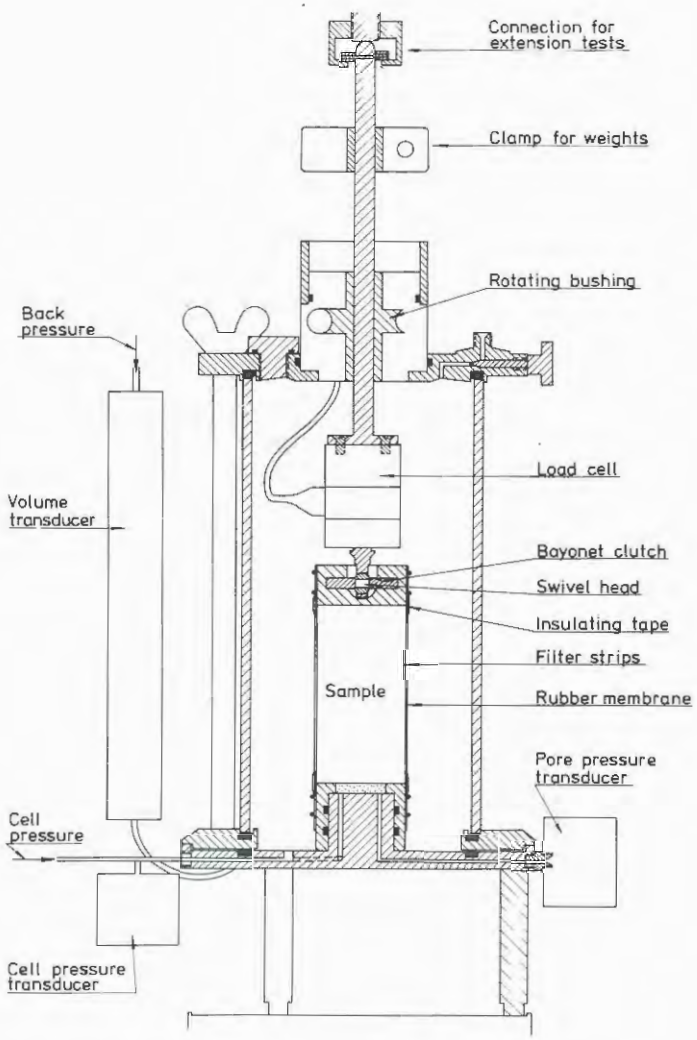

Fig. 74. Triaxial cell with internal load cell.

The cell fluid in which the load cell is submerged must be non-conducting. In most tests castor oil has been used but for some paraffin oil was used.

The top cap and the pedestal are made of polished perspex. To minimize end friction only the pedestal has a filter stone which covers half the cross-sectional area. In extension tests a top cap which can be connected to the load cell by a bayonet clutch

is used. In these tests a layer of insulating tape is applied at the joints between sample and top cap and sample and pedestal to prevent intrusion of the rubber membrane into the joints. Filter papers cut in spirals as recommended by Berre (1979) were used to provide drainage. The samples were allowed to consolidate for 1-2 days and were then deformed at a rate of 1% per day.

In the tests with "constant" vertical stress and varying cell pressure special cells originally designed for creep tests (Larsson, 1977) were used. In these cells a piston with the same diameter as the sample (50 mm) passes vertically through the top of the cell, Fig. 75.

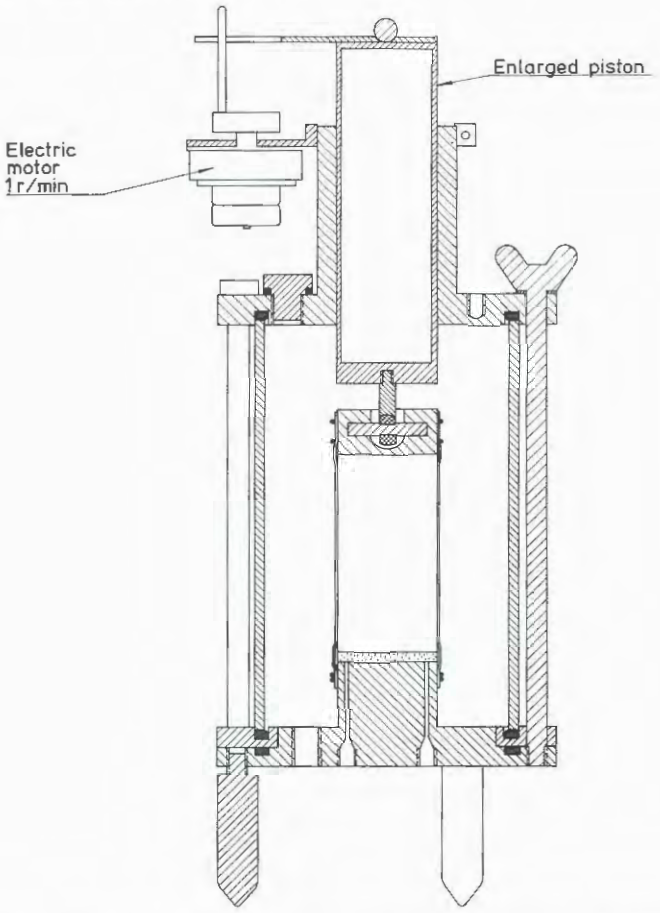

Fig. 75. Triaxial cell for "constant" vertical stress.

The piston is slowly rotated with an oscillating movement to prevent friction. The bayonet clutch between the top cap and the piston contains a swivel head to prevent application of torque to the sample. The vertical load remains almost constant throughout the test. As the deformations in a drained test become very large the vertical stress will not be constant but changes with changing sample area and rubber stresses. This drawback has been considered acceptable in this study. The cell pressure has been regulated by a motorized air pressure regulator which has been set to increase or decrease the pressure continuously at a rate of 1-2 kPa per day.

7.3.3 Plane strain apparatus

An apparatus was built at SGI in order to study the relevance of results from triaxial tests in the case of plane strain, Fig. 76.

The sample has a rectangular cross-section with a length of 126 mm and a width of 31 mm. The height of the sample is 65 mm. The dimensions were chosen to enable the use of ϕ100 mm rubber membranes. The top cap and the bottom pedestal have a gradual transition in cross-section from rectangular to circular with a constant circumference. At the circular cross-section the rubber membrane is sealed with O-rings. The end plates which prevent lateral deformation in the σ_2-direction are fixed on steel spindles specially made by the manufacturer of the ball-bearings. The load piston is a similar spindle and the bottom pedestal is also fixed on a special spindle. Load cells are fixed in the outer ends of the spindles. The upper load cell measures the deviatoric load applied to the sample. The two horizontal load cells measure the difference in σ_2 and σ_3 required to prevent any deformation in the σ_2 direction and the bottom load cell measures the reaction force to the applied force at the top to estimate frictional losses. To minimize

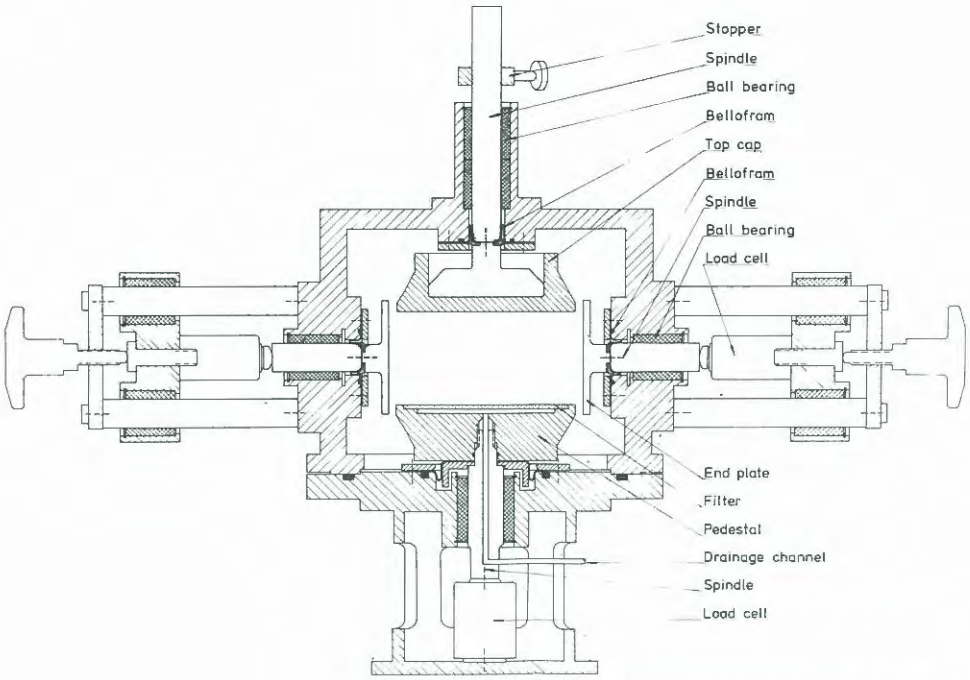

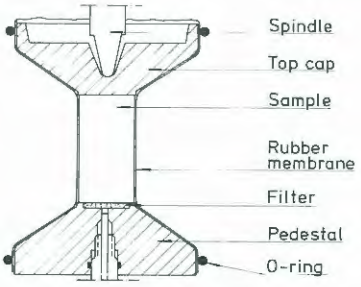

Cross section of sample

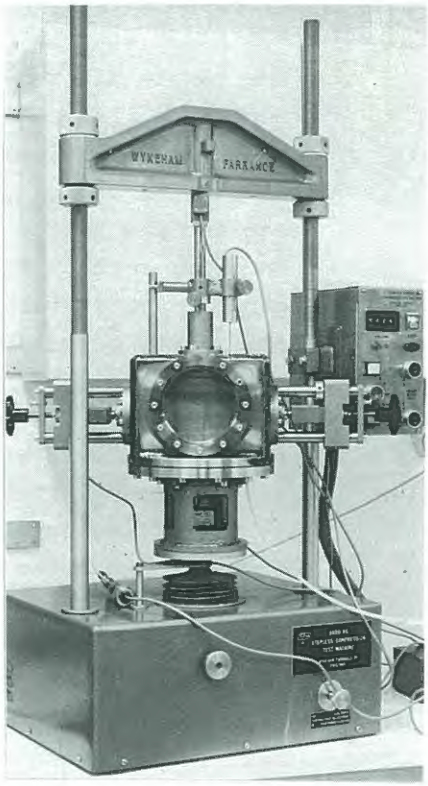

Fig. 76. SGI plane strain apparatus.

deformations in the measuring system the load cells are of the piezo-electric type. The spindles are sealed at the cell walls by belloframs. The top cap and the bottom pedestal are made of polished perspex. Drainage is provided by strips of filter paper on the sides of the sample and a filter stone in the pedestal. The filter stone covers part of the contact area and underneath it a channel leads through the bottom spindle out to the measuring and pressure systems. To minimize friction the ends of the sample in contact with the horizontal plates are greased with silicon grease and an extra strip of thin greased rubber membrane is applied on these surfaces. The difference in readings from top and bottom load cells was always less than five per cent and in calculations the average value has been used. Consolidation of the sample is allowed for two days. During the first day σ_2 equals σ_3 and the plates are then moved in and a small pressure is applied to ensure contact. The sample is slightly longer than the top cap and bottom pedestal to ensure that the plates come into contact with the sample and not with these parts.

The plane strain apparatus is placed in an ordinary press and the pressure systems are the same as for triaxial tests. Only compression tests are run and so far the cell pressure has been kept constant. The rate of compression is 1% a day. Tests have been performed on samples cut in the vertical and horizontal directions. The samples used in this apparatus have been taken with a ϕ200 mm sampler which was lent by the Norwegian Geotechnical Institute.

7.4 The test series

Direct shear tests were performed on samples which were consolidated for different vertical stresses. The consolidation stresses were chosen to enable a continuous study of how the strength and deformation

parameters vary with stress level. All the samples were taken at a depth of 4 m in Bäckebol.

The triaxial samples were consolidated for isotropic stresses in the lower stress range and anisotropic in the higher. The first assumption was that the preconsolidation pressure in the vertical direction was 50 kPa and that the K_{onc} value was 0.7 and thus the horizontal preconsolidation pressure 35 kPa. Samples were consolidated isotropically for 5, 10, 15, 20, 25 and 30 kPa and anisotropically for $\sigma_3' = \sigma_H'$ equal to 30 kPa and $\sigma_1' = \sigma_V'$ 35, 40 and 45 kPa. From these consolidation stresses the four different types of test: 1. σ_H' constant, σ_V' increasing, 2. σ_H' constant, σ_V' decreasing, 3. σ_V' "constant", σ_H' increasing and 4. σ_V' "constant", σ_V' decreasing were performed.

The test results showed that the first assumption on preconsolidation stresses had overestimated them somewhat. The vertical preconsolidation pressure was in fact about 48 kPa and the horizontal preconsolidation pressure about 32 kPa. Those samples which had been consolidated close to any of these stresses showed higher yield stresses than the other samples. This was attributed to a quasi-preconsolidation pressure built up due to creep deformations during consolidation. These tests were remade at somewhat lower consolidation stresses. A few of the tests with lowering of the cell pressure were made stepwise to study creep effects.

The plane strain tests were consolidated in a similar manner. Two test series were run; one with samples cut in the vertical direction and one with samples cut in the horizontal direction. The horizontal samples were cut so that in the test σ_1 and σ_2 were applied in previously horizontal directions and σ_3 in the previously vertical direction. The vertical samples were consolidated for the same stresses as

the triaxial tests and the horizontal samples for isotropic stresses up to 30 kPa only.

Compression tests were then performed on all samples.

In the triaxial and plane strain tests samples from 3.5 m to 5.5 m depth in Bäckebol were used.

7.5 Test results

7.5.1 Stress-strain curves and yield

Different types of stress-strain relations were obtained depending on whether the stresses in the samples were increasing or decreasing. When the stresses were increasing the shape of the stress-strain curve was dependent on the stress level and the relation between deviatoric and normal stresses. Typical stress-strain relations for tests with increasing major stress and constant minor stress are shown in Fig. 77.

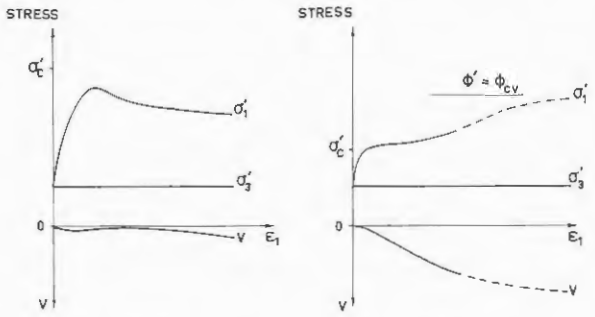

Fig. 77. Typical stress-strain relations in drained triaxial tests on clay from tests with increasing vertical stress.

The curve for major effective principal stress σ_1' versus major principal strain ε_1 rises at low stress levels up to near failure following a hyperbolic function. As the minor effective stress σ_3' is held constant the increase in major principal stress is

equal to the increase in deviatoric stress, $\Delta\sigma_1' = \Delta(\sigma_1-\sigma_3)$. The increase in σ_2' in plane strain tests is very small at the beginning of the test.

The strains increase rapidly just before failure and σ_1' decreases after failure in tests at low stress level. The volume of the sample decreases at the start of the test. At failure it has a tendency to increase (at very low stresses) or remain constant and at large shear strains it has a tendency to decrease.

At higher stress levels no failure is obtained. The σ_1'-ε_1 curve rises rapidly until a certain effective stress is reached. At that stress the curve makes a fairly sharp break after which its rise is much slower. The stress at which the curve breaks corresponds very well to the preconsolidation pressure when σ_1' is in the vertical direction and to $K_{onc} \cdot \sigma_c'$ when σ_1' is in the horizontal direction.

In anisotropically consolidated tests with increasing horizontal stress the break in the curve occurs at an effective horizontal stress of $K_{onc} \cdot \sigma_c'$ even if the vertical stress is still the major stress.

If the test is continued the major stress increases and approaches the value corresponding to mobilization of ϕ_{cv}. For soft clays this value is not reached within the limits of the standard test $\varepsilon_{1_{max}} \approx 0.15$. The volume of the sample decreases from the start of the test. The volume decrease increases in relation to the major principal strain at the strain corresponding to the break in the σ_1'-ε_1 curve. The volume decrease in relation to ε_1 thereafter slowly decreases with increasing ε_1.

Fig. 78 shows the stress-strain relations obtained in the tests with increasing stresses.

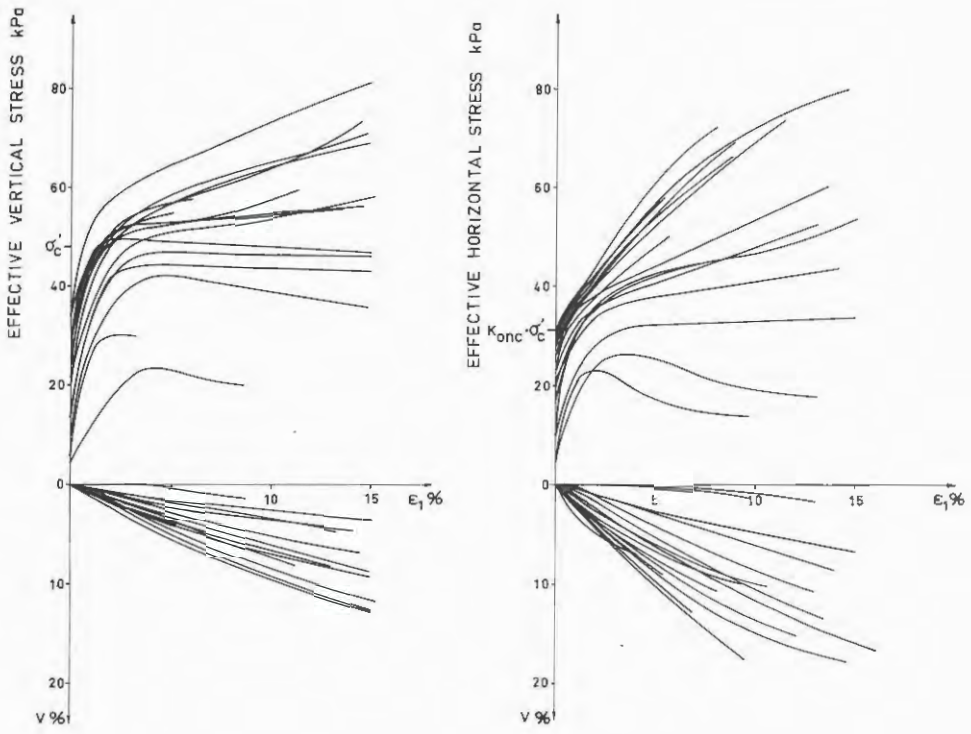

σ_1' in the vertical direction

σ_1' in horizontal direction

Fig. 78. Stress-strain relations from the tests on Bäckebol clay with increasing stress.

If the volume change is plotted against the major principal stress as in the oedometer test a curve with basically the same shape as the oedometer curve is obtained unless the sample fails. This is natural as the oedometer test is a special type of a drained triaxial test, Fig. 79.

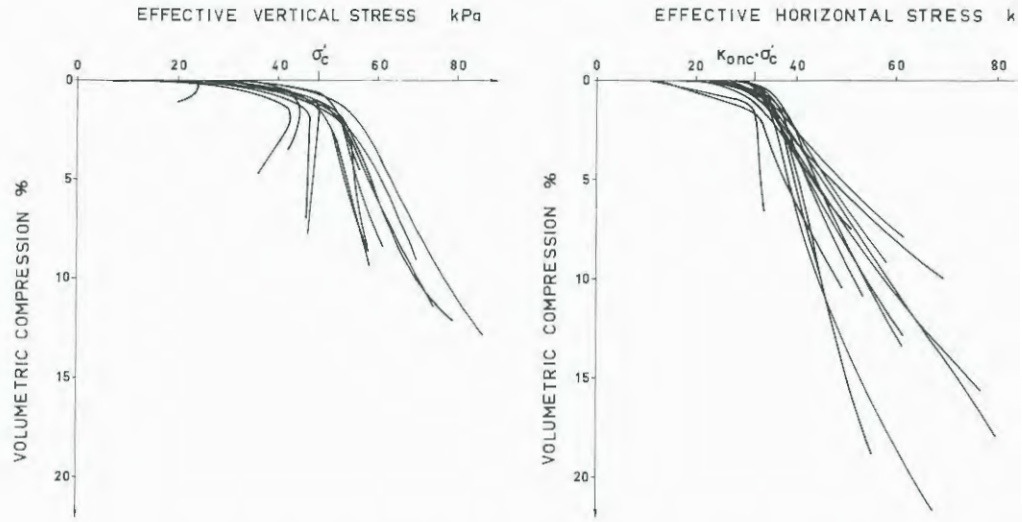

Fig. 79. Volume change versus major principal stress in tests on Bäckebol clay with increasing stresses.

These curves can be evaluated in the same way as the oedometer curve from CRS-tests and the preconsolidation pressure thus evaluated can be considered as the yield stress.

For the tests where failure was obtained the evaluation of yield becomes more subjective. It could either be taken as the stress at a certain major principal strain or the stress at which this strain increases faster than the hyperbolic relation from the start of the test. The latter type of evaluation has been chosen here and the evaluated yield stresses are close to the failure stresses.

In tests with decreasing stresses failure is always obtained. In this case the curve for the minor principal stress versus the major principal strain starts with a hyperbolic shape. As the major principal stress is held constant the change in minor principal stress is equal to the change in deviatoric stress, Fig. 80.

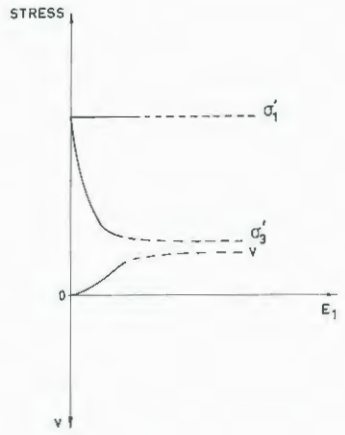

Fig. 80. Typical stress-strain relation in stress controlled tests with decreasing stress level.

ε_1 rapidly increases close to the failure stresses. The volume increases in these tests until failure is reached with the exception of tests where the constant stress is very close to the yield stress in this direction. In these tests a small volume decrease occurs as the deviatoric stress increases. The volume increase can be plotted against the decrease in minor stress and a swelling curve similar to the swelling curve from the oedometer is obtained. These tests could not be evaluated after failure. Most of them were stress-controlled so that the test was carried out as far as failure and in the strain-controlled extension tests the samples were compressed in the middle to an hour-glass shape.

The creep deformations could be studied in the tests with stepwise decrease of the minor principal stress. They confirmed the evaluation of yield at the point where ε_1 starts to increase faster than the hyperbolic relation for the first part. The creep rate increases at the same point and it is open to question whether the measured shear strength above this point can be considered as anything but a rate effect.

The stress-strain-volume relations have shown that yield occurs close to the failure stresses or at either of two limiting effective stresses depending on which stress is increased. The yield points are plotted in Fig. 81.

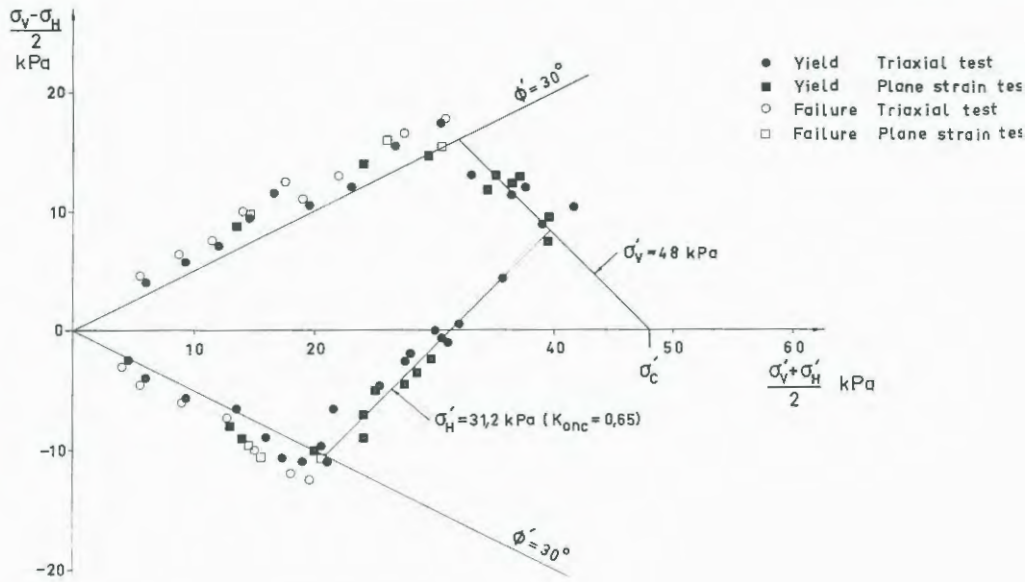

Fig. 81. Yield points for Bäckebol clay.

In Fig. 81 the measured failure stresses are also plotted and it can be seen that the differences between failure and yield in these tests is small. The yield surface suggested by Larsson 1977 is also inserted in the figure. This yield surface is based on the Mohr-Coulomb failure criterion with $\phi' = 30^0$ $c' = 0$ and a vertical preconsolidation pressure of 48 kPa. This preconsolidation pressure can be compared with the laboratory and field values in Fig. 71. The K_{onc} value is 0.65 and can be compared with the value of 0.65-0.7 from field and laboratory measurements, Fig. 72. The Mohr-Coulomb failure criterion with $\phi' = 30^0$ $c' = 0$ gives a safe prediction of the yield

surface in the lower stress region. The parameters $\phi' = 30^0$ and $c' = 2$ kPa correspond to the average of the results. In the investigation into rate effects on the strength parameters of Bäckebol clay (Larsson, 1975) it was found that in undrained tests the parameters $\phi' = 30^0$ and $c' = 2$ kPa correspond to a normal testing rate but the c' parameter became 0 at a very low rate.

The following studies of dilatancy will show that the apparent c' value is a result of an increase in ϕ' with decreasing stress level.

7.5.2 Compressibility

The compressibility of a soil is usually measured in oedometer tests. The oedometer test is a triaxial test with zero lateral strain which means that the minor principal stresses σ_2' and σ_3' are kept in the relation to σ_1' required to keep the sample diameter constant. As this relation is fairly constant during the test it closely corresponds to a constant q/p test. According to critical state theory the plastic compressive strains are the result of exceeding the yield surface. The ratio q/p governs the increase in equivalent isotropic preconsolidation pressure and thereby the plastic volumetric strains. Few data from natural clays with varying ratio q/p have been found in literature and in those available the points are few and the scatter great. Some data from constant q/p tests on two Canadian clays have been plotted in Fig. 82. The compressibility is expressed as a pseudo "Bulk modulus" (dp/dv) evaluated at the straight part of the p-v curve just after yield.

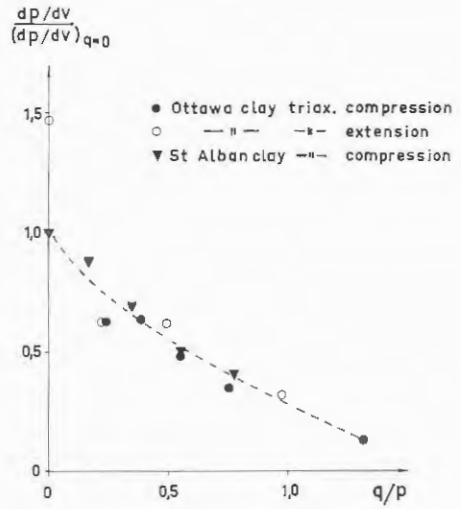

Fig. 82. Pseudo "Bulk modulus" for Canadian clays in constant q/p tests. (Wong (1971), Faveau-Brucy (1977).)

In Fig. 82 there seems to be a certain relation. In Fig. 83 however the results from the tests on Bäckebol clay are plotted, q/p is evaluated at the yield point.

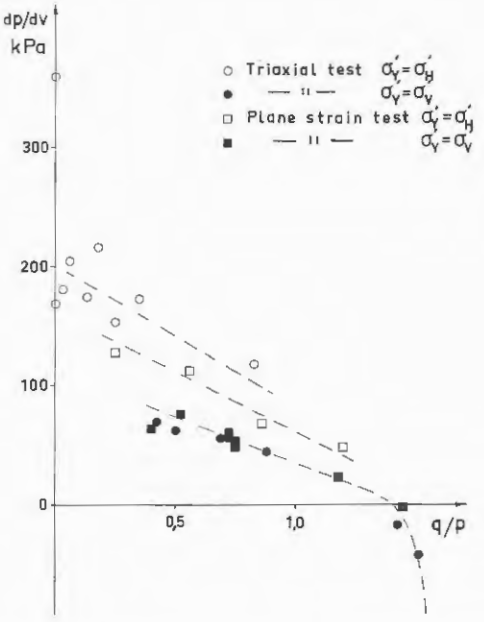

Fig. 83. Pseudo "Bulk modulus" for Bäckebol clay.

These results show a pronounced effect of the type of test on the results. The highest "bulk modulus" dp/dv is obtained in tests where yield is caused by exceeding the preconsolidation pressure in the horizontal direction. This corresponds to a higher oedometer modulus in tests on horizontal samples than on vertical samples. In tests where yield is caused by a horizontal stress the "bulk modulus" is highest in tests where the horizontal stresses are increased equally. For all tests the "bulk modulus" decreases with increasing ratio q/p.

In volumetric compression most of the deformations are sliding deformations between particles and a rearrangement of particles. The higher the shear stress is the easier this rearrangement is achieved while an isotropic stress increase hampers this process. A stress increase in two directions is also more restrictive for movements than a stress increase in a single direction.

Considering both this and the fact that an anisotropically consolidated natural clay has to have a fairly high shear stress to yield for a vertical pressure the compressibility can be expressed in a simpler way. If the tests are evaluated in the same way as CRS oedometer tests with the constant modulus of volumetric compression E_v equal to $\Delta\sigma'_y/\Delta v$ where σ'_y is the stress for which the clay yields and this modulus is plotted against q/p the relation in Fig. 84 is obtained. E_v in the CRS-test is equal to M_L.

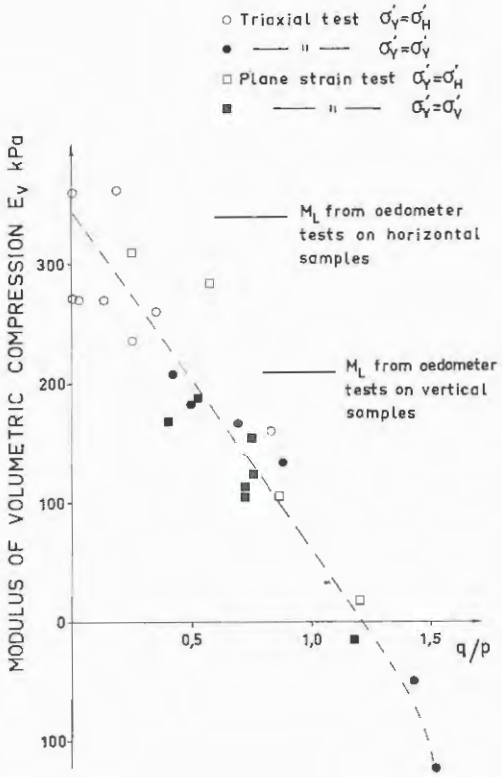

Fig. 84. Modulus of volumetric compression E_v for Bäckebol clay.

From this plot it appears that the compressive strains in the stress region where the modulus remains constant can be evaluated from $\Delta v = \frac{\Delta \sigma'_y}{E_v}$

where $E_v = Ev_{q=0} \cdot (1-q/1.2p)$

The tests on Canadian clays in Fig. 82 have been replotted in Fig. 85 as the modulus of volumetric compression versus q/p and show a similar relation.

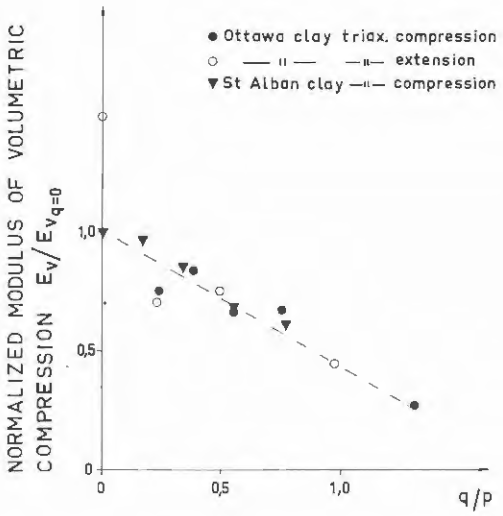

Fig. 85. Modulus of volumetric compression for two Canadian clays (from Wong (1972) and Faveau-Brucy (1977)).

7.5.3 Plastic flow

The plastic deformations have been studied in an attempt to find a simple flow rule. Considering the shape of the yield surface there can be no "normality rule" as in the critical state theory.

The dilatancy equations were used for the test results and instead of using them for a peak value they were used continuously thorughout the test. The equations used were:

to determine ϕ_f according to Rowe

$$\tan^2(45^0+\phi_f/2) = \frac{\sigma_1'}{\sigma_3'(1 - \frac{dv}{d\varepsilon_a})}$$

for compression tests and

$$\tan^2(45^0+\phi_f/2) = \frac{\sigma_1'(1 - \frac{dv}{d\varepsilon_a})}{\sigma_3'}$$

for extension tests

to determine ϕ_r with the Bishop type of equation

$$\sin \phi_r = \frac{\sigma_1' - \sigma_3' (1 - \frac{dv}{d\varepsilon_1})}{\sigma_1' + \sigma_3' (1 + \frac{dv}{d\varepsilon_1})}$$

to determine ϕ_p

$$\phi_p = \arcsin \frac{\sigma_1' - \sigma_3'}{\sigma_1' + \sigma_3'} + \arctan \frac{dv \tan \beta}{\frac{2d\varepsilon_1}{\cos \beta} - dv}$$

where $\beta = 45^0 + \phi_p/2$

The plane strain tests do not quite fulfil the assumptions for the last formula although this has also been used in these tests for purposes of comparison. The difference should be small.

An alternative formula suggested by Bishop & Eldin (1953) was also tested but the results were inconsistent.

In the tests ϕ_r and ϕ_p became constants after a certain deformation. In tests where yield occurred for vertical stresses the mobilized angle of friction at yield was 12^0 or more and ϕ_r and ϕ_p became constants at yield. In the tests where σ_V' was initially greater than σ_H' and the horizontal stress was increased ϕ_r and ϕ_p did not become constant until the shear stress direction was reversed. By then the volume could be reduced by as much as 12%. In tests where yield was caused by a horizontal stress greater than the vertical stress ϕ_r and ϕ_p became constants at yield.

In a highly compressible anisotropically consolidated material like natural soft clays a flow rule based on dilatancy equations cannot therefore be used for yield at fairly isotropic stresses. Nor can it be used

during the process of reversing the main principal stress direction from the direction it had during anisotropic consolidation to the opposite direction. For other cases however it seems applicable.

Even if ϕ_r and ϕ_p are constants during a test they vary with stress level.

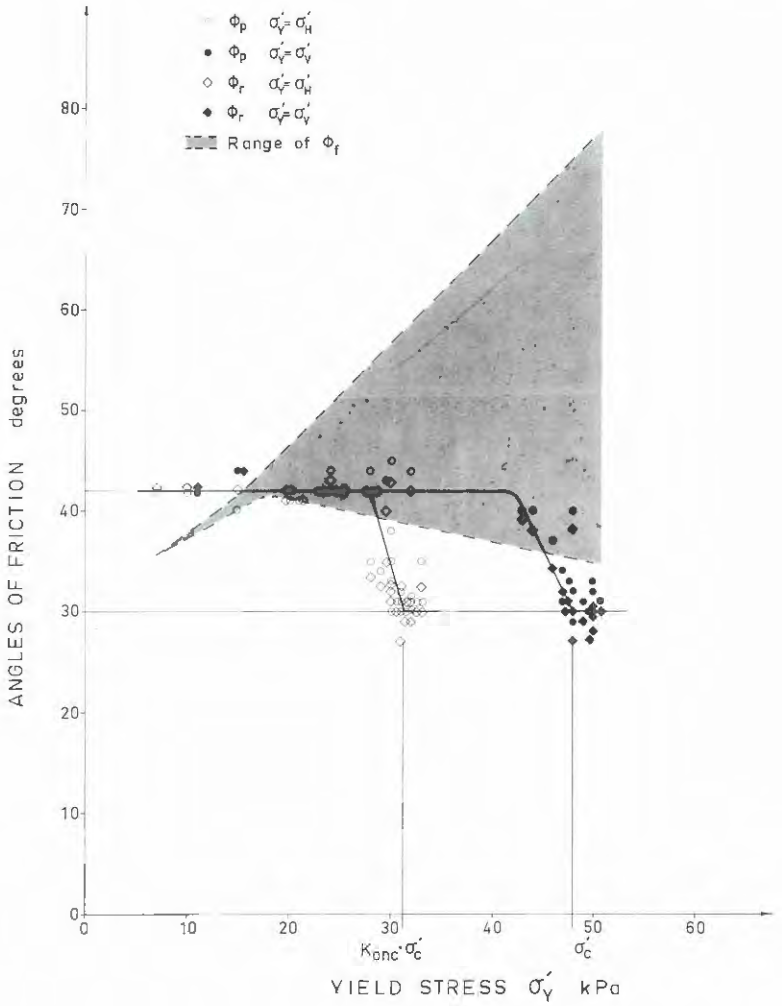

Fig. 86. ϕ_f, ϕ_r and ϕ_p at different yield stresses.

In Fig. 86 the evaluated values of ϕ_f, ϕ_r and ϕ_p are plotted against the effective stress for which they

yielded. For ϕ_r and ϕ_p there are two distinct levels. If the soil yields at a stress lower than the preconsolidation stress in the direction of the yield stress an almost constant value of 42^0 is obtained. If the soil yields because the preconsolidation pressure in the yield direction is exceeded ϕ_r and ϕ_p become an almost constant 30^0.

The evaluated value of ϕ_f is not a constant during the test. As can be seen in the figure the trend is consistent with ϕ_f increasing with the yield stress but the variation within one test is such that no flow rule can be based on it.

The sudden drop in ϕ_p and ϕ_r when the preconsolidation pressure is exceeded may be due to two interacting phenomena. As shown in Fig. 56 ϕ_r decreases with increasing porosity for a sand. In a sand an increasing porosity means an interacting compressibility. In a soft clay the exceeding of the preconsolidation pressure directly changes its character from a material close to critical density to a highly compressible material. If the structure of the clay is examined it will be found to be built up of particles and particle aggregates of very irregular shape. As long as the normal stresses are kept below the stresses for which the clay has consolidated these aggregates can be assumed to act as units. When the preconsolidation pressure is exceeded the aggregates start to crush and break down and the friction will be based on the shape of the single particles rather than the aggregates.

The trend of the value of ϕ_f also corresponds to the trend in Fig. 56.

An alternative flow rule has been suggested by Lewin, 1973. From a comprehensive study on triaxial tests he suggested that the test results should be plotted in

a triaxial stress plane (Henkel, 1960) where σ'_V is plotted versus $\sqrt{2}\sigma'_H$, Fig. 87.

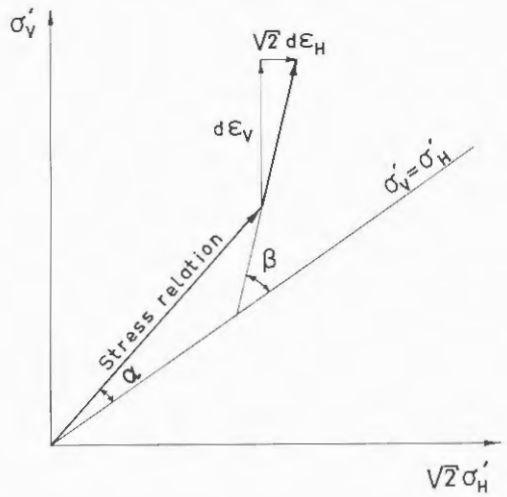

Fig. 87. Plot for evaluation of α and β.

The stress angle α is evaluated in this plot as the angle between the stress relation $\sigma'_V/\sqrt{2}\sigma'_H$ and the line for isotropic stresses.

$$\alpha = arctan \frac{\sigma'_V}{\sqrt{2}\sigma'_H} - arctan \frac{1}{\sqrt{2}}$$

α is roughly equal to the mobilized angle of friction ϕ'. The strain angle β is evaluated in the same way as

$$\beta = arctan \frac{d\varepsilon_V}{\sqrt{2}\, d\varepsilon_H} - arctan \frac{1}{\sqrt{2}}$$

If $\beta = 0$ the strains are isotropic and there is no shear strain. If $\beta = 90^0$ the volume remains constant and failure occurs.

The results from four drained triaxial test series are plotted in Fig. 88.

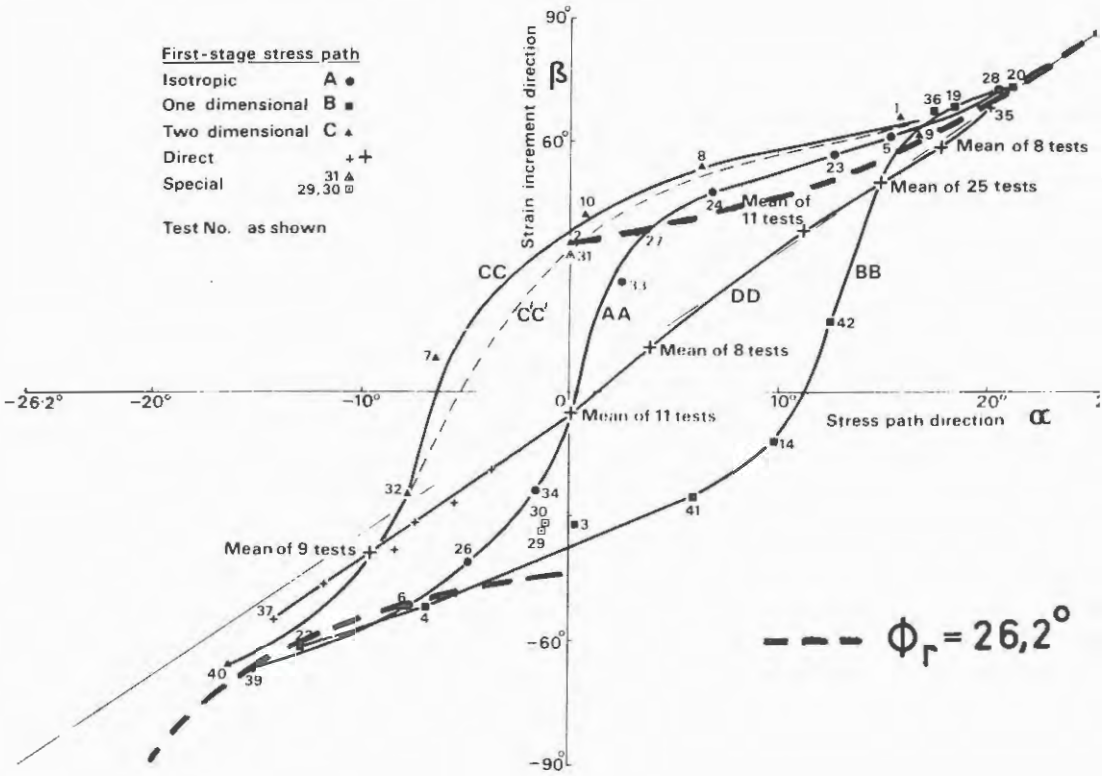

Fig. 88. α-β relationship from Lewin (1973).

The line *D-D* corresponds to a test series where the samples were not preconsolidated but the whole test was performed at the same stress ratio. The curve *A-A* corresponds to a test series where the samples were first consolidated isotropically and then brought to the stress relation α at constant isotropic stress. In the tests α was then kept constant. The curve *B-B* corresponds to a test series where the samples were first consolidated anisotropically under K_o conditions ($\varepsilon_H = 0$) and then brought to the stress condition α under constant isotropic stress. During the tests α was kept constant. Curve *C-C* finally corresponds to a test series where during the first stage of consolidation the horizontal stresses were increased and the vertical pressure adjusted to keep the sample

height constant. The samples were then brought to the stress rate α under constant isotropic stress and this was kept constant throughout the test.

As the second stage of consolidation with stress changes under constant isotropic stress involves consolidation and reshaping of the yield surface none of these lines corresponds to the most common field case. Curve *B-B* is closest to a clay which has consolidated under K_o-conditions and line *C-C* corresponds to an opposite extreme.

In Fig. 88 two lines corresponding to the dilatancy equation for ϕ_r have been inserted. It can be seen that for α greater than 10^0-14^0 the plastic flow closely follows that equation regardless of the previous type of consolidation. For lower shear stresses the plastic flow depends on the previous consolidation history. In this range however, Lewin has pointed out that the β relation changes and the soil loses its "memory" of previous stress history with increasing deformation.

The results from Bäckebol clay have been plotted in the same way and the curve is similar to curve *B-B* in Lewin's (1973) plot, Fig. 89.

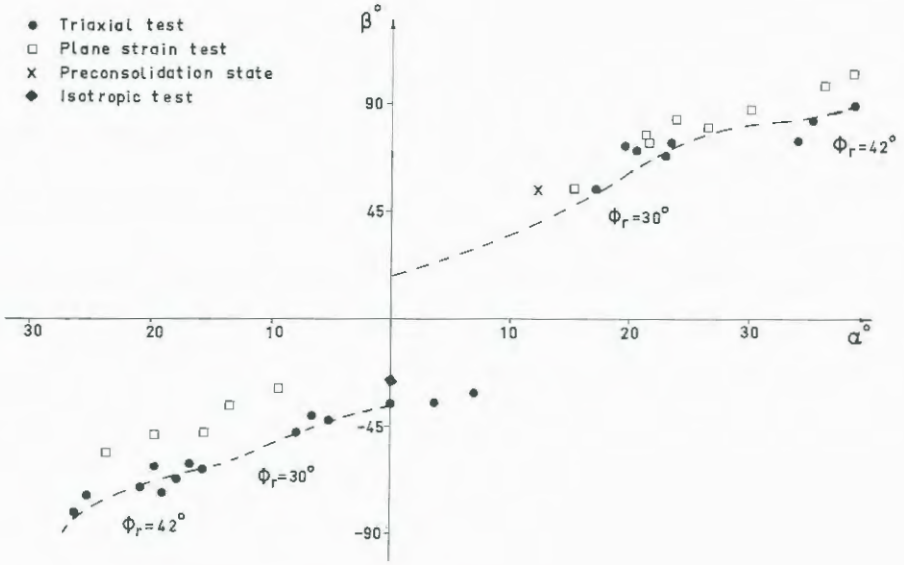

Fig. 89. α-β relation for Bäckebol clay.

The α-β relation predicted using dilatancy and ϕ_r is inserted in Fig. 89. The prediction is very good and seems to be valid for most of the passive side and for α values higher than 12° on the active side. 12° corresponds to the mobilized friction during previous consolidation with $K_{onc} = 0.65$.

It should be noted that in passive, plane strain tests the anisotropically consolidated clay flows as if it was more isotropically consolidated. In this special case the soil is isotropically consolidated in the σ_1 and σ_2 directions and anisotropically in the σ_1 and σ_3 directions. The plane strain tests differ slightly from the triaxial tests and should strictly not be plotted in the same plane, although the error in this case is very small.

Looking back at Lewin's (1973) test results it appears that:

Plastic flow can be predicted using dilatancy equations and ϕ_r' for anisotropically consolidated soils in active tests when the shear stress is equal to or greater than the shear stress during consolidation and in passive tests. Here "active" stands for tests where the major principal stress is in the same direction as the major consolidation stress. "Passive" stands for tests with the major stress in the opposite direction from the major consolidation stress. Dilatancy equations and ϕ_r can also be used for isotropically consolidated soils if the mobilized angle of friction is greater than 10^0, Fig. 90.

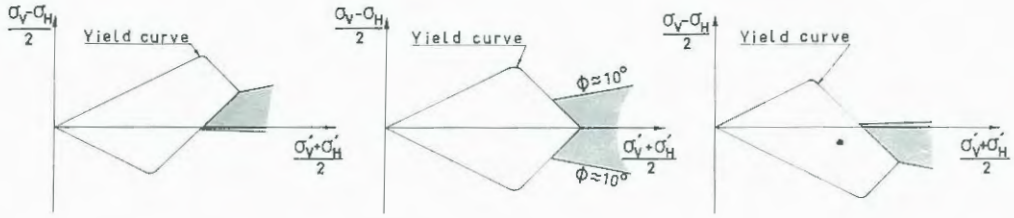

Fig. 90. Restrictions for the sole use of dilatancy equations and ϕ_r for predictions of strains in soft clay. In shaded areas the variation of compressibility with direction has to be considered.

In the stress regions where dilatancy equations are not valid the plastic strains are governed more by directional differences in compressibility due to the stress history.

7.5.4 Results from direct shear tests

The drained shear tests gave results following the standard pattern described by Larsson (1977). Some of the stress-strain curves are plotted in Fig. 91.

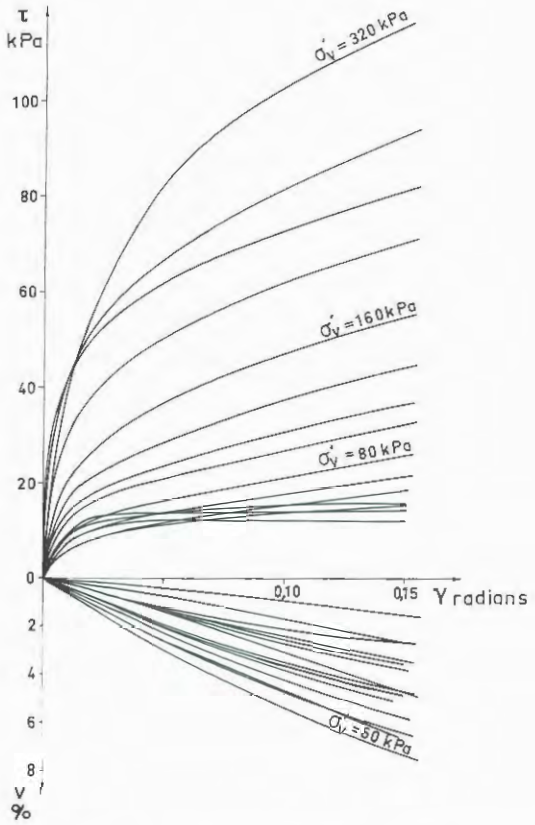

Fig. 91. Shear stress, angular distortion and volume change in drained direct shear tests on Bäckebol clay.

Shear failure is obtained only at very low vertical stresses. In Swedish practice failure is evaluated at the peak or at an angular distortion of 0.15 radians if no peak is obtained. The "shear strengths" thus evaluated are plotted in Fig. 92.

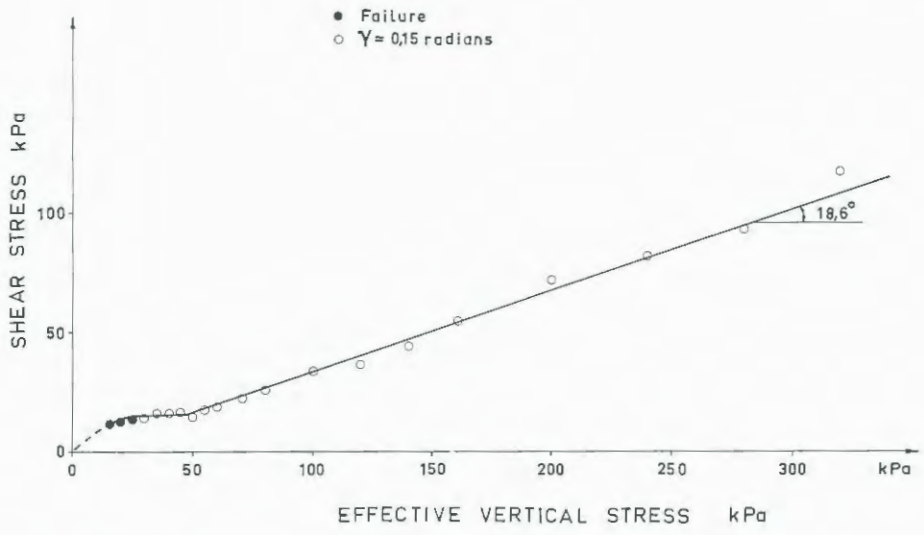

Fig. 92. "Shear strength" versus vertical stress in drained direct shear tests on Bäckebol clay.

The shear stress at 0.15 radians angular distortion is by no means a failure stress but should rather be seen as the shear stress that can be mobilized at "tolerable" deformations. As real failure at higher stresses occurs only after very large deformations in these clays some sort of limiting deformation criterion usually has to be applied for practical engineering cases. Real shear failures at moderate strains in direct shear only occur at vertical stresses well below the preconsolidation pressure, ($\sigma'_V \approx 0.5\ \sigma'_c$ is used as a rule of thumb).

When the tests are evaluated with respect to dilatancy it is found that after a small angular distortion of about 2 radians the shear process is entirely governed by the compressibility of the sample. The evaluated angles of friction ϕ_f, ϕ_r or ϕ_p become almost constant.

These angles are plotted in Fig. 93.

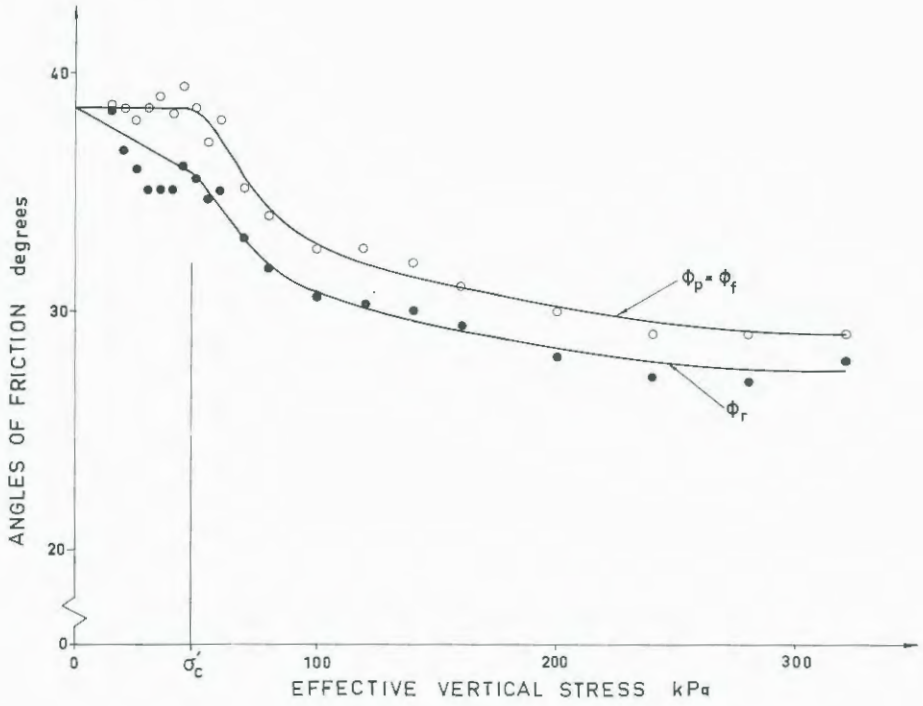

Fig. 93. ϕ_f, ϕ_r and ϕ_p from direct shear tests on Bäckebol clay.

The values for ϕ_p follow the same trend as for triaxial and plane strain tests with a ϕ_{pmax} of 38.5^0 and a ϕ_{pmin} of 30^0. The drop at the preconsolidation pressure is not as direct as in the other types of tests. ϕ_r has the same maximum 38.5^0 as ϕ_p at very low stresses where the soil does not change its volume. ϕ_r then gradually decreases and the break in the curve at the preconsolidation pressure is less pronounced than for other tests. ϕ_{rmin} becomes about 28^0.

In direct shear tests a consolidation of the samples for stresses close to the preconsolidation pressure will create a quasi-preconsolidation pressure. The effects of repeated loading and secondary compression will cause an excess settlement corresponding to a higher preconsolidation pressure. The breaks in the ϕ_p and ϕ_r versus σ'_V relations thus occur at pressures somewhat higher than the preconsolidation pressure.

Direct shear tests at vertical stresses close to the preconsolidation pressure are normally avoided for soft clays.

The ϕ_r-σ'_v relation probably shows best what happens in the sample. The vertical effective stress is the major principal stress only at the start of the test. As the shear stress is applied the principal stresses are rotated. An effective normal stress greater than σ'_v then acts in a direction where the preconsolidation pressure is less than in the vertical direction. The breakdown of the soil structure thus starts at a vertical pressure much lower than the preconsolidation pressure and is more gradual. An indication of this is also found in the volume changes during the tests. The volume changes at an angular distortion of 0.15 radians are plotted in Fig. 94.

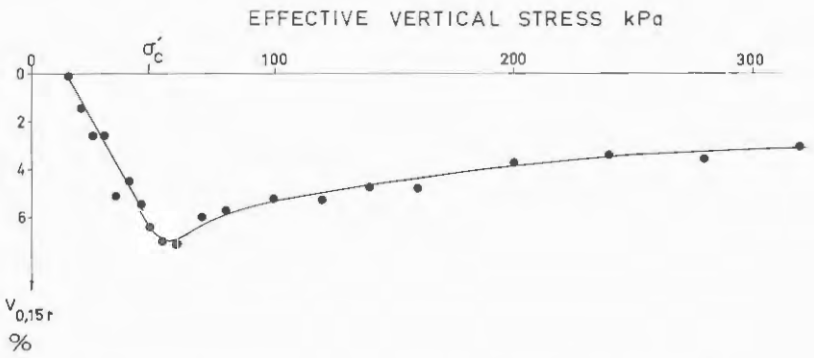

Fig. 94. Volume decrease at an angular distortion of 0.15 radians in drained direct shear tests on Bäckebol clay.

In Fig. 94 it can be seen how the volumetric compressions start at very low stresses and gradually increase to a maximum close to the preconsolidation pressure. At higher stresses the compressibility decreases in a way similar to that of the compressibility measured in the oedometer.

The "shear strength" curve in Fig. 92 is the net result of the changes of ϕ_r and compressibility with vertical pressure in this type of test. ϕ_r from direct shear tests is slightly less than ϕ_r from plane strain and triaxial tests. The difference is in the order of 2^0-3^0 which is in good agreement with the values presented by Rowe (1969).

8. RESIDUAL FRICTION IN CLAYS

The pattern with a value of ϕ_r in the order of 40^0 at very low stresses reducing to 30^0 for higher stresses has been found to be a rule for Swedish clays. As ϕ_r is assumed to be the friction at constant volume it should correspond to the effective angle of friction measured in undrained tests. Due to the pore pressure changes failure in undrained tests will occur at stresses close to the preconsolidation stress in the major stress direction. This angle has been measured for a great number of Scandinavian clays and has been found to be a fairly constant 30^0 (e.g. Berre & Bjerrum 1973, Larsson 1977, Börgesson 1981). A comprehensive study of the residual angle of resistance for a number of minerals and natural clays was reported by Kenney (1967). These studies showed that micaceous and illitic clays and natural Norwegian clays of this type have a residual friction angle of about 30^0, Fig. 95.

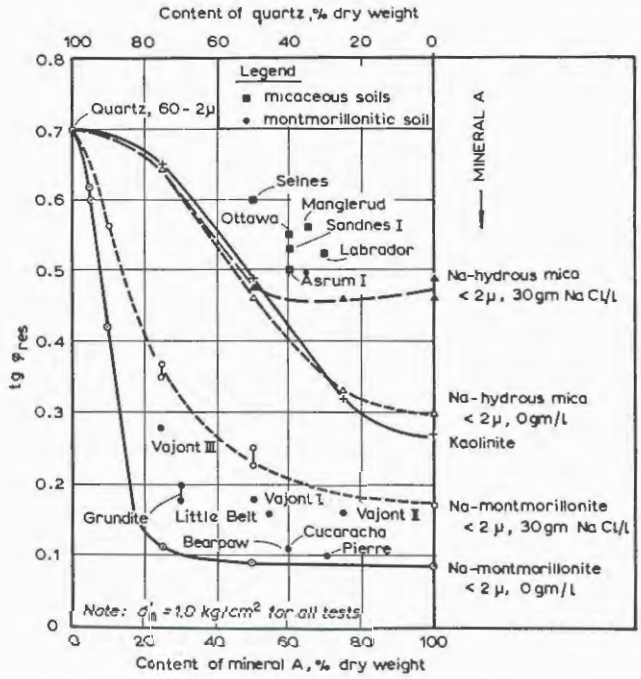

Fig. 95. Residual angle of friction. From Kenney (1967).

Most Swedish soft clays are of the same type. Kenney's (1967) results show that clays with different clay minerals may have considerably lower residual friction angles. Lower ϕ_r values have been noticed in the SGI laboratory in tests on clays from some other parts of the world.

9. DRAINED SHEAR STRENGTH IN SOFT CLAYS

Shear failure in soft clays occurs according to the Mohr-Coulomb criteria. Shear failure occurs at stresses close to the yield stresses in cases where previous consolidation stresses are not exceeded. In cases where the preconsolidation stresses are exceeded shear failure occurs only when the residual angle of friction is mobilized. Due to the compressibility of the soil this state is not reached until after very large deformations. For practical purposes some criterion

for permissible deformations has to be used. However, in this stress region the undrained shear strength is lower than the drained shear strength and is usually the governing factor. The drained parameters determine the volumetric strains and the associated shear strains.

The yield stresses at low effective stresses are found to be slightly above the stresses corresponding to $\phi' = 30^0$.

Close to the preconsolidation stresses yield occurs at $\phi' = 30^0$. The yield stresses are time-dependent. At effective normal stresses higher than 80% of the preconsolidation pressure in this direction there is secondary consolidation according to the oedometer tests. This level has been confirmed by undrained creep tests (Larsson, 1977). This secondary deformation is made easier and more pronounced by an increased shear stress level. The definition of yield thereby becomes a question of definition similar to the definition of the preconsolidation pressure if the volumetric strains are used as yield criterion. If axial strain is used as yield criterion the axial strains increase as the creep effects increase. The yield surfaces are often rounded off at the upper and lower corners which can partly be attributed to the secondary deformation. The radius of these "rounding-offs" depends on how much the shear stress levels affect the rate of secondary deformation, Fig. 96.

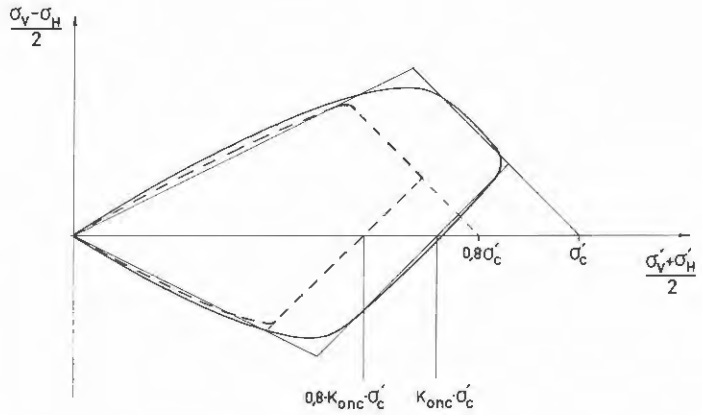

Fig. 96. Yield curves. Solid curve: yield at the pre-consolidation stresses and normal testing rate. Broken curve: yield if secondary consolidation and creep are considered.

At normal stresses lower than 0.8 σ_c' and high shear stresses there may be a slow creep and breakdown in the soil structure. In a large stress region the shear stresses are higher than the shear stresses during consolidation. Such a process at a mobilized angle of friction higher than 30^0 would with time lead to failure. The secondary consolidation effects at angles of mobilized friction lower than 30^0 lead only to somewhat larger deformations, not to shear failure. A friction angle of 30^0 can thus safely be used in calculations with drained shear strength in cases where previous maximum effective normal stresses are not exceeded in any direction.

When the previous maximum effective normal stresses are exceeded the limiting criterion usually becomes a deformation criterion. If the stress path in the field can be predicted the deformations may be predicted with knowledge of the yield surface, the soil compressibility and dilatancy equations using ϕ_p. If tests are performed to measure the deformations directly they must simulate the stress paths in the field as closely as possible. The method of running

drained triaxial compression tests consolidated isotropically for stresses higher than the preconsolidation pressure is not an appropriate method for tests on soft clays. From such tests a mobilized angle of friction ϕ' in the order of 16^0-20^0 has often been evaluated at an axial deformation of 10-15%. Considering that a natural normally consolidated clay with a typical K_{onc} value of 0.5 has a mobilized angle of friction of 20^0 in its natural state such test values have no pratical application.

In less compressible soils where a peak stress or residual state is reached during the test the method is useful in determining these parameters but not in determining deformations.

10. COMMENTS ON THE TESTS AND THE TEST RESULTS

The aim of the tests was to study yield and plastic drained deformations. The measuring system was therefore designed to have capacity for large strains rather than sensitivity for measuring minute changes. The starting points of the tests were selected to obtain an even spacing of the points on the yield surface using the simple test methods described. The deformations within the yield surface have therefore not been studied in detail and the test procedure during consolidation would have to be altered to achieve practically useful results. A few observations could be made however. In tests with increasing stresses the volumetric compression at stresses well below yield followed a fairly linear relation $\Delta v = M\Delta\sigma_1'$ as in the oedometer. In tests with decreasing stresses the samples swelled similar to swelling in the oedometer.

The deformation in the principal strain direction ε_1 followed a hyperbolic function up to yield.

In the plane strain tests the intermediate stress σ_2' increased slowly up to yield. The stress state at yield was thus not very far from the triaxial case. At yield σ_2' started to change and after some further deformation it stabilized to a constant relation to σ_1'; $\sigma_2'/\sigma_1' = 0.57$.

The tests which later proved to have been consolidated for stresses too close to the yield stresses showed that yielding for one principal stress expands the yield surface in that direction but not in the other direction, Fig. 97.

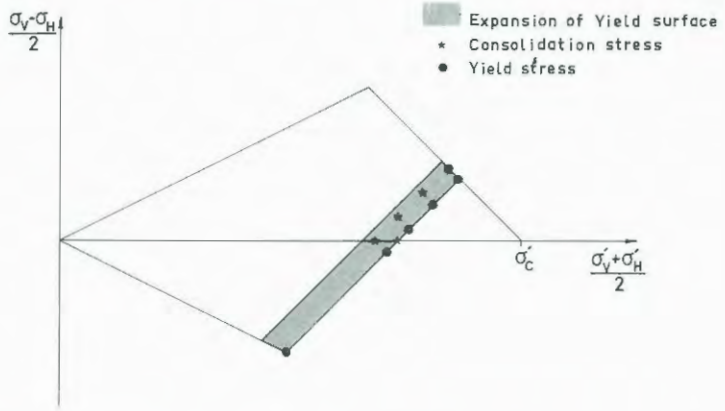

Fig. 97. Increase in yield surface due to yield for a horizontal stress increase.

The shaded area in Fig. 97 shows the increase in yield surface which resulted from the too high horizontal consolidation stresses. The preconsolidation pressures are the soil's "memory" of previous stress history which is changed and modified with new plastic strains. Large plastic strains will therefore destroy the old memory and impose a new structure adapted to the new stress situation. The yield surface may shrink in one direction or even both, although the material decreases in volume.

REFERENCES

Andreasson, L. (1973), Kompressibilitet hos friktionsjord. Laboratoriestudium. Statens institut för byggnadsforskning, Stockholm, Rapport R36:1973./ Thesis, Chalmers University of Technology, Gothenburg 1973.

Andresen, A. and Simons, N.E. (1960), Norwegian Triaxial Equipment and Technique. ASCE Research Conference on Shear Strength of Cohesive Soils, Boulder, Colorado, June 1960.

Berre, T. (1972), Sammenheng mellom tid, deformasjoner och spenninger for normalkonsoliderte marine leirer. Proc. Nordic Conf. on Soil Mech., Trondheim 1972.

Berre, T. and Bjerrum, L. (1973), Shear Strength of Normally Consolidated Clays. Proc. 8th Int. Conf. Soil Mech. and Found. Eng., Vol. 1, pp. 39-49, Moscow 1973.

Berre, T. (1975), Bruk av triaxial- og direkte skjaerforsök till lösning av geotekniske problemer. Nordiska Geoteknikermötet i Kopenhamn 1975.

Berre, T. (1979), Triaxial Testing at the Norwegian Geotechnical Institute. Report, Norwegian Geotechnical Institute, Oslo 1979.

Bishop, A.W. and Eldin, A.K.G. (1953), The effect of stress history on the relation between ϕ and porosity in sand. 3rd International Conference on Soil Mechanics and Foundation Engineering, Zürich 1953, Vol. 1, pp. 100-105.

Bishop, A.W. (1954), Correspondence on a paper by A.D.M. Penman. Geotechnique, Vol. 4, No. 1, pp. 43-45.

Bishop, A.W. and Henkel, D.J. (1962). The Measurement of Soil Properties in the Triaxial Test. 2nd edition, London, Arnold, 1962.

Bishop, A.W. (1971), Shear strength parameters for undisturbed and remoulded soil specimens. Proceedings, Roscoe Memorial Symposium, Cambridge 1971.

Bjerrum, L. (1967), Seventh Rankine Lecture: Engineering Geology of Norwegian Normally-Consolidated Marine Clays as Related to Settlements of Buildings. Geotechnique, Vol. 17, No. 2, pp. 81-118.

Bjerrum, L. (1972), The effect of Rate of Loading on the p_c-value Observed in Consolidation Tests of Soft Clays. Written Contribution to the Discussion in Session III. Proceedings, ASCE, Spec. Conf., Vol. 3, pp. 167-168, Purdue, Indiana.

Bjerrum, L. (1973), Problems of Soil Mechanics and Construction on Soft Clays and Structurally Unstable Soils. General Report, 8th International Conference on Soil Mechanics and Foundation Engineering, Moscow 1973, Proceedings, Vol. 3, pp. 111-159.

Burmeister, D.M. (1951), The Application of Controlled Test Methods in Consolidation Testing. Symp. on Consolidation Testing of Soils, ASTM, Spec. Tech. Publ., No. 126, p. 83, Philadelphia, Pennsylvania.

Börgesson, L.B. (1981), Shear strength of inorganic silty soils. 10th International Conference on Soil Mechanics and Foundation Engineering, Proceedings, Stockholm 1981.

Börgesson, L.B. (1981), Mechanical Properties of inorganic Silt. Thesis, University of Luleå 1981.

Casagrande, A. (1936), The determination of the Preconsolidation Load and its Practical Significance. 1st International Conference on Soil Mechanics and Foundation Engineering, Vol. 3, p. 60, Cambridge, Massachusetts, 1936.

Crawford, C.B. (1964), Interpretation of the Consolidation Test. Journal of the Soil Mechanics and Foundation Engineering Division, ASCE, Vol. 90, No. SM5, pp. 87-109.

Crawford, C.B. (1965), The Resistance of Soil Structure to Consolidation. Canadian Geotechnical Journal, Vol. 2, No. 2, pp. 90-97.

Faveau-Brucy, F. (1977), Effets du passage en l'état normalement consolidé sur l'état limite d'une argile naturelle. Thesis, Université Laval, Quebec, 1977.

Fellenius, B. (1971), Negative Skin Friction on Long Piles Driven in Clay. Swedish Geotechnical Institute, Proceeding, No. 25.

Hansbo, S. (1975), Jordmateriallära, Almqvist & Wiksell, Stockholm.

Hanssen J. Brinch (1966), Stress-strain relationship for sand. Bulletin No. 20, Danish Geotechnical Institute, Copenhagen.

Hartlén, J. (1974), Skånska moränlerors hållfasthets- och bärighetsegenskaper. Thesis, Chalmers University of Technology, Gothenburg 1974.

Helenelund, K.V. (1951), Om konsolidering och sättning av belastade marklager. Diss. Järnvägsstyrelsens Geotekniska Sektion, Meddelande 3, Helsingfors 1951.

Henkel, D.J. (1960), The relationship between the effective stresses and water content in saturated clays. Geotechnique, Vol. 10, 1960, pp. 41-54.

Högberg, E. (1972), Vattenhaltens inverkan på densitet och kompressibilitet hos packade jordar. Report R8:1972, Statens institut för byggnadsforskning, Stockholm.

Janbu, N. (1963), Soil compressibility as determined by oedometer and triaxial tests. 3rd European Conference on Soil Mechanics and Foundation Engineering, Vol. 1, Wiesbaden 1963.

Janbu, N. (1970), Grunnlag i geoteknikk. Tapir forlag, Trondheim 1970.

Janbu, N., Tokheim, O. and Senneset, K. (1981), Consolidation Tests With Continuous Loading. Proceedings, 10th International Conference on Soil Mechanics and Foundation Engineering, Stockholm 1981.

Kallstenius, T. (1963), Studies on Clay Samples Taken with Standard Piston Sampler. Proceedings, No. 21, Swedish Geotechnical Institute, Stockholm 1963.

Karlsson, R. and Viberg, L. (1978), Snabba ödometerförsök. Report No. 5, Swedish Geotechnical Institute, Linköping 1978.

Karlsson, R., Consistency Limits. Report in preparation, Swedish Geotechnical Institute, Linköping.

Kenney, T.C. (1967), The Influence of Mineral Composition on the Residual Strength of Natural Soils. Proceedings of the Geotechnical Conference, Oslo 1967, Vol. 1.

Larsson, R. (1975), Measurement and Calculation of Horizontal Stresses in Clay. Chalmers University of Technology, Gothenburg 1975.

Larsson, R. (1975), The effect of rate of loading on the shear strength parameters of a high-plastic marine clay. Chalmers University of Technology, Gothenburg 1975.

Larsson, R. (1977), Basic behaviour of Scandinavian soft clays. Report No. 4, Swedish Geotechnical Institute, Linköping 1977.

Larsson, R. and Sällfors, G. (1981), Beräkningar av sättningar i lera. Väg- och vattenbyggaren, No. 3-1981, pp. 39-42.

Larsson, R. and Sällfors, G. (1981), Hypothetical Yield Envelope at Stress Rotation. 10th International Conference on Soil Mechanics and Foundation Engineering, Proceedings, Stockholm 1981.

Leonards, G.A. (1972), Written Contribution to the Discussion in Session III. Proceedings, ASCE, Spec. Conf., Vol. 3, pp. 169-173, Purdue, Indiana.

Leonards, G.A. (1975), Personal communication.

Leroueil, S. (1977), Quelques considerations sur le comportement des argiles sensibles. Thesis, Université Laval, Quebec 1977.

Leroueil, S., LeBihan, J.P. and Tavenas, F. (1980), An approach for the determination of the preconsolidation pressure in sensitive clays. Canadian Geotechnical Journal, Vol. 17, No. 3, August 1980.

Leroueil, S. (1981), Personal communication.

Lewin, P.I. (1972), Three-dimensional anisotropic consolidation of clay and the relationship between plane strain and triaxial test data. RILEM, Symposium deformation and rupture of solids subjected to multiaxial stresses, Cannes 1972.

Lewin, P.I. (1973), The influence of stress history on the plastic potential. Symposium on the role of plasticity in soil mechanics, Cambridge 1973.

Lindblom, U. (1972), Kompressionsegenskaper hos traktorutbredda sprängstensfyllningar, med särskild hänsyn till sättningar hos grundplattor. Thesis, Chalmers University of Technology, Gothenburg 1972.

Lo, K.Y. (1963), Secondary Compression of Clays. Publication No. 53, Norwegian Geotechnical Institute, Oslo 1963.

Lowe III, J. and Obrician, V. (1969), Controlled Gradient Consolidation Test. Journal of the Soil Mechanics and Foundation Engineering Division, ASCE, Vol. 95, No. SM1.

Magnan, J.P., Baghery, S., Brucy, M. and Tavenas, F. (1979), Etude numerique de la consolidation unidimensionelle en tenant compte des variations de la perméabilité et de la compressibilité du sol, du fluage et de la non-saturation. Laboratoires des Ponts et Chaussées, Bulletin de Liaison, 1979, No. 103, pp. 83-94.

Mesri, G. (1973), Coefficient of Secondary Compression. ASCE, Journal of the Soil Mechanics and Foundation Engineering Division, Vol. 99, No. SM1, Jan. 1973.

Mesri, G. and Rokhsar, A. (1974), Theory of Consolidation for Clays. ASCE, Journal of the Soil Mechanics and Foundation Engineering Division, Vol. 100, No. GT8, Aug. 1974.

Mesri, G. and Godlewski, P.M. (1977), Time- and Stress-Compressibility Interrelationship. ASCE, Journal of the Soil Mechanics and Foundation Engineering Division, Vol. 103, No. GT5, May 1977.

Mesri, G., Ullrich, C.R. and Choi, Y.K. (1978), The rate of swelling of overconsolidated clays subjected to unloading. Geotechnique, Vol. 28, No. 3, Sept. 1978.

Newland, P.I. and Allely, B.H. (1957), Volume changes in drained triaxial tests on granular materials. Geotechnique, Vol. 7, No. 1, 1957.

Odhe, J. (1951), Grundbaumechanik. Hütte Bd III, Berlin 1951.

Pusch, R. (1973), Influence of Organic Matter on the Geotechnical Properties of Clays. Document D11:1973, Statens institut för byggnadsforskning, Stockholm 1973.

Ramanatha Iyer, T.S. (1975), The Behaviour of Drammen Plastic Clay under Low Effective Stresses. Canadian Geotechnical Journal, Vol. 12, No. 1, Febr. 1975.

Reynolds, O. (1885), On the dilatancy of media composed of rigid particles in contact. Phil. Mag. 20, pp. 469-481.

Roscoe, K.H., Schofield, A.N. and Wroth, C.P. (1958), On the yielding of soils. Geotechnique, Vol. 8, No. 1, 1958.

Roscoe, K.H. and Schofield, A. (1963), Mechanical Behaviour of an Idealized "Wet-Clay". Proceedings, 3rd European Conference on Soil Mechanics and Foundation Engineering, Vol. 1, pp. 47-54, Wiesbaden 1963.

Roscoe, K.H. and Burland, J.B. (1968), On the generalized stress-strain behaviour of 'wet' clay. Engineering plasticity. Conference in Cambridge, March 1968.

Rowe, P.W. (1962), The stress-dilatancy relation for static equilibrium of an assembly of particles in contact. Royal Society Academy, Proceedings 269:500-527.

Rowe, P.W., Barden, L. and Lee, I.K. (1964), Energy components during the triaxial cell and direct shear tests. Geotechnique, Vol. 14, No. 3, Sept. 1964.

Rowe, P.W. and Barden, L. (1966), A new consolidation cell. Geotechnique, Vol. 16, No. 2, pp. 162-170.

Rowe, P.W. (1969), The relation between the shear strength of sands in triaxial compression, plane strain and direct shear. Geotechnique, Vol. 19, No. 1, March 1969.

Schmertman, J.M. (1953), Estimating the True Consolidation Behaviour of Clay from Laboratory Test Results. ASCE, Journal of the Soil Mechanics and Foundation Engineering Division, Vol. 79, Separate No. 311, p. 26.

Schofield, A.N. and Wroth, P. (1968), Critical State Soil Mechanics. McGraw-Hill, London 1968.

Skempton, A.W. and Bishop, A.W. (1950), Measurement of shear strength of soils. Discussion by A.W. Bishop, Geotechnique, Vol. 2, No. 2.

Skinner, A.E. (1969), A note on the influence of inter-particle friction on the shearing strength of a random assembly of spherical particles. Geotechnique, Vol. 19, pp. 150-157.

Smith, R.E. and Wahls, H.E. (1969), Consolidation Under Constant Rate of Strain. ASCE, Journal of the Soil Mechanics and Foundation Engineering Division, Vol. 95, No. SM2, pp. 519-539.

Šuklje, L. (1957), The Analysis of the Consolidation Process by the Isotache Method. Proceedings, 4th International Conference on Soil Mechanics and Foundation Engineering, London, Vol. 1, pp. 200-206, Vol. 3, pp. 107-109.

Šuklje, L. and Kovačič, I. (1979), Consolidation of Drained Multi-layer Viscous Soils. Acta Geotechnica 74-76, University of Ljubljana 1979.

Sällfors, G. (1975), Preconsolidation Pressure of Soft High-Plastic Clays. Thesis, Chalmers University of Technology, Gothenburg 1975.

Tavenas, F. and Leroueil, S. (1977), Effects of stresses and time on yielding of clays. Proceedings, 9th International Conference on Soil Mechanics and Foundation Engineering, Tokyo, Vol. 1, pp. 319-326.

Tavenas, F. and Leroueil, S. (1979), Clay behaviour and the selection of design parameters. European Conference on Soil Mechanics and Foundation Engineering, Brighton 1979, Vol. 1.

Taylor, D.W. (1948), Fundamentals of Soil Mechanics. John Wiley & Sons, New York 1948.

Terzaghi, K. (1943), Theoretical Soil Mechanics. John Wiley & Sons, New York 1943.

Terzaghi, K. and Peck, R.B. (1948), Soil mechanics in engineering practice. John Wiley & Sons, New York 1948.

Tokheim, O. and Janbu, N. (1976), A continuous consolidation test. The Norwegian Institute of Technology, Trondheim 1976.

Torstensson, B-A. (1973), Kohesionspålar i lös lera. En fältstudie. Thesis, Report R38:1973, Statens institut för byggnadsforskning, Stockholm.

Virgin, Å. (1918), Markytans höjdförändringar hos lösa jordlager. Teknisk Tidskrift, VoV., Vol. 48, H.6., Stockholm.

Wong, P.K.K. (1972), Strength and stress-strain relations of a sensitive clay. Thesis, Queens University, Kingston, Ontario.

Wong, P.K.K. and Mitchell, R.J. (1975), Yielding and plastic flow of sensitive cemented clay. Geotechnique, Vol. 25, No. 4, pp. 763-782.

Wroth, P. and Wood, D. (1975), Course on Critical State Soil Mechanics at Chalmers University of Technology, Gothenburg 1975.

Kompendium i geoteknik 1946. Meddelande No. 1, Swedish Geotechnical Institute, Stockholm 1946.

Kompendium i geoteknik 1959. Meddelande No. 5, Swedish Geotechnical Institute, Stockholm 1959.

Kompendium i geoteknik 1972. Meddelande No. 10, Swedish Geotechnical Institute, Stockholm 1972.

STATENS GEOTEKNISKA INSTITUT
Swedish Geotechnical Institute
S-581 01 Linköping
Tel: 013/11 51 00

Serien "Rapport" ersätter våra tidigare serier: "Proceedings (27 nr), "Särtryck och Preliminära rapporter" (60 nr) samt "Meddelanden" (10 nr).

The series "Report" supersedes the previous series: "Proceedings" (27 Nos), "Reprints and Preliminary Reports" (60 Nos) and "Meddelanden" (10 Nos).

RAPPORT/REPORT

No.		År	Pris kr (Sw.crs)
1.	Grundvattensänkning till följd av tunnelsprängning. *P. Ahlberg, T. Lundgren*	1977	50:-
2.	Påhängskrafter på långa betongpålar. *L. Bjerin*	1977	50:-
3.	Methods for reducing undrained shear strength of soft clay. *K.V. Helenelund*	1977	30:-
4.	Basic behaviour of Scandinavian soft clays. *R. Larsson*	1977	40:-
5.	Snabba ödometerförsök. *R. Karlsson, L. Viberg*	1978	25:-
6.	Skredriskbedömningar med hjälp av elektromagnetisk fältstyrkemätning - provning av ny metod. *J. Inganäs*	1978	40:-
7.	Förebyggande av sättningar i ledningsgravar - en förstudie. *U. Bergdahl, R. Fogelström* *K.-G. Larsson, P. Liljekvist*	1979	40:-
8.	Grundläggningskostnadernas fördelning. *B. Carlsson*	1979	25:-
9.	Horisontalarmerade fyllningar på lös jord. *Johan Belfrage*	1981	50:-

RAPPORT/REPORT

No.		År	Pris kr (Sw.crs)
10.	Tuveskredet 1977-11-30. Inlägg om skredets orsaker.	1981	50:-
11a.	Tuveskredet geoteknik	1981	
11b.	Tuveskredet geologi	1981	
11c.	Tuveskredet geohydrologi	1981	
12.	Drained behaviour of Swedish clays. *R. Larsson*	1981	50:-

STATENS GEOTEKNISKA INSTITUT
Besöksadr.: Olaus Magnus väg 35, LINKÖPING
Postadr.: 581 01 LINKÖPING, tel 013-11 51 00